



HAL
open science

Deconstructing Noncovalent Kelch-like ECH-Associated Protein 1 (Keap1) Inhibitors into Fragments to Reconstruct New Potent Compounds

Jakob S Pallesen, Dilip Narayanan, Kim T Tran, Sara M Ø Solbak, Giuseppe Marseglia, Louis M E Sørensen, Lars J Høj, Federico Munafò, Rosa M C Carmona, Anthony D Garcia, et al.

► To cite this version:

Jakob S Pallesen, Dilip Narayanan, Kim T Tran, Sara M Ø Solbak, Giuseppe Marseglia, et al.. Deconstructing Noncovalent Kelch-like ECH-Associated Protein 1 (Keap1) Inhibitors into Fragments to Reconstruct New Potent Compounds. *Journal of Medicinal Chemistry*, 2021, 64 (8), pp.4623-4661. 10.1021/acs.jmedchem.0c02094 . hal-03223155

HAL Id: hal-03223155

<https://hal.science/hal-03223155>

Submitted on 15 Nov 2021

HAL is a multi-disciplinary open access archive for the deposit and dissemination of scientific research documents, whether they are published or not. The documents may come from teaching and research institutions in France or abroad, or from public or private research centers.

L'archive ouverte pluridisciplinaire **HAL**, est destinée au dépôt et à la diffusion de documents scientifiques de niveau recherche, publiés ou non, émanant des établissements d'enseignement et de recherche français ou étrangers, des laboratoires publics ou privés.

Deconstructing Non-Covalent Kelch-like ECH-Associated Protein 1 (Keap1)

Inhibitors into Fragments to Reconstruct New Potent Compounds

Jakob S. Pallesen,[†] Dilip Narayanan,[†] Kim T. Tran,[†] Sara M. Ø. Solbak,[†] Giuseppe Marseglia,^{†,‡} Louis M. E. Sørensen,[†] Lars J. Høj,^{†,‡} Federico Munafò,^{†,‡} Rosa M. C. Carmona,[†] Anthony D. Garcia,^{†,‡,§} Haritha L. Desu,[§] Roberta Brambilla,^{§,^} Tommy N. Johansen,[†] Grzegorz M. Popowicz,^{‡,¶} Michael Sattler,^{‡,¶} Michael Gajhede,[†] Anders Bach^{†,*}

[†]Department of Drug Design and Pharmacology, Faculty of Health and Medical Sciences, University of Copenhagen, Universitetsparken 2, DK-2100 Copenhagen, Denmark

[‡]Food and Drug Department, University of Parma, Parco Area delle Scienze 27/a, 43124 Parma, Italy

[§]École Nationale Supérieure de Chimie de Rennes, 11 Allée de Beaulieu, CS 50837, Rennes Cedex 7 35708, France

[¶]The Miami Project to Cure Paralysis, Dept. Neurological Surgery, University of Miami Miller School of Medicine, Miami, FL 33136, USA

[^]Department of Neurobiology Research, Institute of Molecular Medicine, and BRIDGE - Brain Research Interdisciplinary Guided Excellence, Department of Clinical Research, University of Southern Denmark, DK-5000 Odense, Denmark

[¶]Institute of Structural Biology, Helmholtz Zentrum München, 85764 Neuherberg, Germany

[‡]Biomolecular NMR and Center for Integrated Protein Science Munich at Department of Chemistry, Technical University of Munich, 85747 Garching, Germany

ABSTRACT

Targeting the protein-protein interaction (PPI) between nuclear factor erythroid 2-related factor 2 (Nrf2) and Kelch-like ECH-associated protein 1 (Keap1) is a potential therapeutic strategy to control diseases involving oxidative stress. Here, six classes of known small-molecule Keap1–Nrf2 PPI inhibitors were dissected into 77 fragments in a fragment-based deconstruction reconstruction (FBDR) study and tested in four orthogonal assays. This gave 17 fragment hits of which six were shown by X-ray crystallography to bind in the Keap1 Kelch binding pocket. Two hits were merged into compound **8** with a 220–380-fold stronger affinity ($K_i = 16 \mu\text{M}$) relative to the parent fragments. Systematic optimization resulted in several novel analogues with K_i values of 0.04–0.5 μM , binding modes determined by X-ray crystallography, and enhanced microsomal stability. This demonstrates how FBDR can be used to find new fragment hits, elucidate important ligand-protein interactions, and identify new potent inhibitors of the Keap1-Nrf2 PPI.

INTRODUCTION

Living systems are exposed to reactive oxygen species (ROS) and electrophiles from cellular energy metabolism and outside sources. To prevent damaging oxidative stress and maintain redox homeostasis, the production and elimination of ROS is generally tightly regulated. However, uncontrolled production of ROS plays a major role in inflammatory diseases, cancer, stroke, and neurodegenerative disorders.¹⁻³

The nuclear factor erythroid 2-related factor 2 (Nrf2) transcription factor is a principal regulator of the cellular defense system against oxidative stress, mediating the transcription of detoxification and antioxidant enzymes including superoxide dismutase (SOD), catalase, glutathione peroxidase (GPx), thioredoxin, heme oxygenase 1 (HO-1), ferritin, glutathione reductase, NAD(P)H dehydrogenase (quinone) 1 (NQO1), and glutathione S-transferase (GST).⁴⁻⁶ Under basal conditions, the cytosolic repressor protein, Kelch-like ECH-associated protein 1 (Keap1), keeps the cellular concentration of Nrf2 low by associating with the Nrf2-ECH homology 2 (Neh2) domain of Nrf2, promoting its polyubiquitination and thus proteasomal degradation.^{5, 7} Keap1 consists of three domains: A Broad complex, Tramtrack, and Bric-à-brac (BTB) domain, an Intervening Region (IVR), and a Kelch domain. The C-terminal Kelch domain is the recognition module for Nrf2, as a Keap1 homodimer, via its two Kelch domains, binds a high-affinity ETGE-motif and a low-affinity DLG-motif at the Neh2 domain of Nrf2.⁸⁻¹⁰ Keap1 functions as an adaptor for Cullin 3 (Cul3), which catalyzes the polyubiquitination of Nrf2 thereby controlling its cellular levels.⁹⁻¹² Importantly, increased levels of reactive oxidants or electrophiles modify specific sensor cysteine residues on the IVR and/or BTB domains of Keap1, leading to conformational changes of the Keap1–Nrf2–Cul3 complex and prevention of Nrf2 polyubiquitination.^{9, 13, 14} The accumulated Nrf2 is then translocated to the nucleus, where it increases expression of cytoprotective enzymes through activation of the antioxidant response elements (AREs).^{15, 16} Accordingly, Nrf2 activation has been found to protect neurons in cell and animal models of central nervous system (CNS) diseases, such as ischemic and hemorrhagic

stroke, traumatic brain injury, and neurodegenerative disorders,^{15, 17-19} and in conditions such as chronic obstructive pulmonary disease (COPD),²⁰ metabolic kidney, liver conditions,^{15, 21, 22} and some cancer types.²¹ Thus, targeting the protein-protein interaction (PPI) between the Neh2 domain of Nrf2 and the Kelch domain of Keap1 has been proposed as a potential therapeutic strategy to counterbalance oxidative stress.

To date, several classes of small-molecule inhibitors have been designed to non-covalently inhibit the PPI of the Keap1 Kelch domain and the Nrf2 Neh2 motifs,^{20, 23-33} including several recently developed compounds.³⁴⁻⁴⁵ However, the Neh2-binding pocket of the Keap1 Kelch domain is large (550–780 Å) and contains multiple arginine residues, thus representing a challenging target for drug development.¹⁴ This is reflected in the reported Keap1–Nrf2 PPI inhibitors, which generally have high molecular weights and contain carboxylic acids leading to poor cell and CNS permeability. Also, many of the compounds are either low-potent ($K_d/K_i > 1 \mu\text{M}$) or have suboptimal drug-related properties, such as low solubility, low metabolic stability, mutagenic properties, or low bioavailability and high clearance.^{14, 20, 28, 33, 46}

Fragment-based drug discovery (FBDD) has been effective in developing potent drug-like PPI inhibitors.^{47, 48} The core principal of FBDD is to start from small non-complex molecules known as fragments and carefully optimize the hits by either growing, linking, or merging, to improve the binding activity while maintaining high ligand efficiency (LE)⁴⁹ and promising physiochemical properties. This approach has been applied to Keap1 by screening a diverse library of approximately 330 fragments by X-ray crystallography followed by optimization of fragment hits into a nanomolar-affinity compound.^{20, 46} An alternative strategy, which is pursued herein, is to apply the fragment-based deconstruction-reconstruction (FBDR) approach. Here, known inhibitors are dissected or deconstructed into fragments whereby a target-biased library of fragments is made.^{47, 50-53} This often results in higher hit-rates, as the fragments are predisposed to bind the target, and can reveal which parts of the ligands are most essential for binding. Also, if structural data are obtained for the protein-fragment

complexes, this can identify the corresponding protein pocket hot spots. The deconstructed fragment hits can then be optimized to larger molecules with potential improved properties. Combining the facts that several small-molecule Keap1–Nrf2 inhibitors have been reported and that FBDD has successfully been applied to develop Keap1-Nrf2 inhibitors, we set out to explore if FBDR could be used to identify novel lead compounds for the Keap1–Nrf2 PPI.

For this FBDR study, we selected six classes of known small-molecule Keap1–Nrf2 PPI inhibitors and dissected them into fragments guided by the rule of three (Ro3)^{54, 55} thereby obtaining a deconstruction library of 77 fragments. The fragments were tested in four orthogonal assays—fluorescence polarization (FP), thermal shift assay (TSA), saturation-transfer difference (STD) NMR, and surface plasmon resonance (SPR). This was followed by selection of the most promising fragment hits and X-ray crystallographic characterization of their binding to the Keap1 Kelch domain. This allowed the merging of two fragment hits (**1m** and **4c**) into a novel lead compound (**8**) with a 220–380-fold stronger binding relative to parent fragments. Further structure-activity relationship (SAR) studies resulted in 31 compounds with improved binding affinity – several with nanomolar affinities and/or binding modes characterized by X-ray crystallography. Thus, with this study, we show that FBDR can be a fruitful approach for finding new and useful fragment hits, and for making new potent inhibitors of pharmacologically relevant targets, including challenging ones as the Keap1-Nrf2 PPI.

RESULTS AND DISCUSSION

Deconstruction of Known Small-Molecule Keap1–Nrf2 PPI Inhibitors into Fragments. Among 19 small-molecules representing the known classes of Keap1–Nrf2 inhibitors, we previously confirmed the binding activity of nine compounds in FP, TSA, and SPR, while the remaining were found not to bind the Keap1 Kelch

domain.³³ Here, six classes (**A–F**) of Keap1 inhibitors were included for deconstruction into fragments containing the following chemical cores (**Figure 1**): (**A**) 1,4-Diaminonaphthalene,^{24, 26} (**B**) 1,2,3,4-tetrahydroisoquinoline,²³ (**C**) 3-phenylpropanoic acid,²⁰ (**D**) 1-phenylpyrazole,³¹ (**E**) 1,4-diphenyl-1,2,3-triazole,⁵⁶ and (**F**) 1-(1,3,4-oxadiazol-2-yl)urea.^{57, 58} Classes **A–D** represent the most active Keap1–Nrf2 inhibitors with confirmed strong binding ($K_i = 1–560$ nM) to the Keap1 Kelch domain and cellular activity.³³ In addition, class **E** was included due to pronounced activity in our NQO1 induction cell assay, although the parent compound (1-(3-Iodophenyl)-4-(3-nitrophenyl)-1H-1,2,3-triazole)⁵⁶ was not active in the binding assays.³³ The compound leading to class **F** fragments did not show activity in our binding assays either,³³ but we included it herein as two crystal structures (based on soaking and co-crystallization, respectively) of the parent compound in complex with the Keap1 Kelch domain have been reported (although showing different binding modes).⁵⁸ The fragments were generally designed to comply with Ro3, including six very small (MW < 100 Da) fragments, but four larger fragments exceeding the Ro3 (MW > 300 Da) were also included.⁵⁵ The designed fragments were checked by the FAF-Drugs4 filtering tool⁵⁹ for potential problematic structural features. Deconstruction of class **A** inhibitors resulted in 24 fragments (**1a–x**), class **B** in 18 (**2a–r**), class **C** in 15 (**3a–o**), class **D** in four (**4a–d**), class **E** in 10 (**5a–j**), and class **F** in six fragments (**6a–f**), which provided the deconstruction library of 77 fragments (**Table S1** and **Figure 1**). The number of derived fragments depended on the possible deconstruction opportunities as well as the number and diversity of reported analogues within each class. Thirty fragments were available in-house and 47 were synthesized in 1–7 steps according to standard chemical procedures.

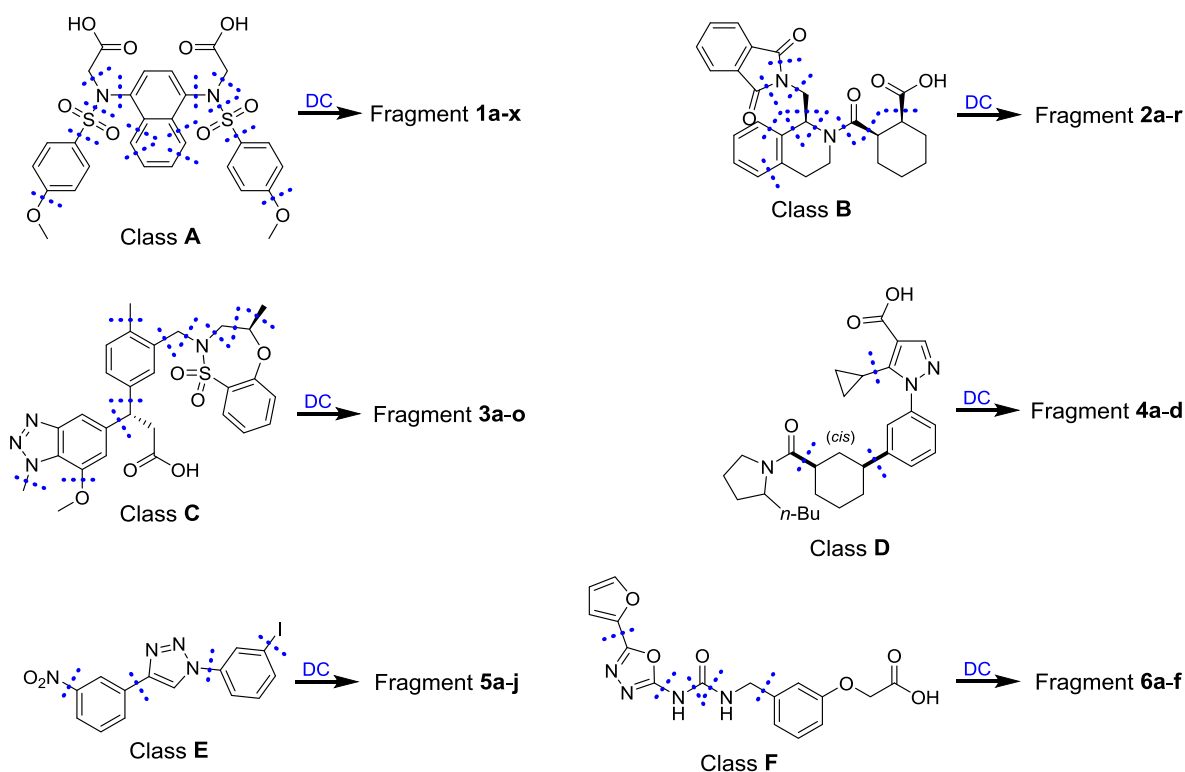


Figure 1. Deconstruction (DC) of the six classes (A–F) of Keap1–Nrf2 inhibitors into the related deconstructed fragments (1a–x, 2a–r, 3a–o, 4a–d, 5a–j, and 6a–f).

Fragment Screening by FP, TSA, STD NMR, and SPR. The 77 fragments were screened in four orthogonal assays—FP, TSA, STD NMR, and SPR—for their ability to bind to the Keap1 Kelch domain and/or inhibit the Keap1-Nrf2 PPI, followed by a series of hit validation steps. An FP inhibition assay was applied using Cy5 as a fluorophore attached *N*-terminally to a 9-mer peptide-moiety of Nrf2 with the sequence H-LDEETGEFL-NH₂.³³ In contrast to fluorescein-labeled probes, readouts with red-shifted fluorophores such as Cy5 are more resistant to fluorescence interferences from compounds.^{33, 60, 61} The fragments were initially tested in dose-response experiments (0.25–8 mM) in 8% DMSO. Fragments demonstrating >5% inhibition were characterized as primary hits. Furthermore, stable total fluorescence intensity (FLINT) values across the dose-response curve

were an additional hit criterion to discard false positives related to fluorescence interference such as auto-fluorescence or chemical quenching of probe.⁶⁰ Thereby, 23 fragments were defined as primary hits giving an initial hit-rate of 30%. Hereafter, the hits were validated in three FP counter assays—dose-response experiments using a FAM-labeled probe (FAM-LDEETGEFL-NH₂), dose-response experiments in the presence of 0.01% Triton-X to exclude aggregation-based promiscuous inhibitors,⁶² and dose-response experiments without addition of Keap1 to remove false-positives due to fluorescence inner-filter effects.^{24, 60, 61, 63-67} These counter assays reduced the number of hits to 13 giving a validated hit-rate of 17% (**Figure 2A** and **Table S2**).

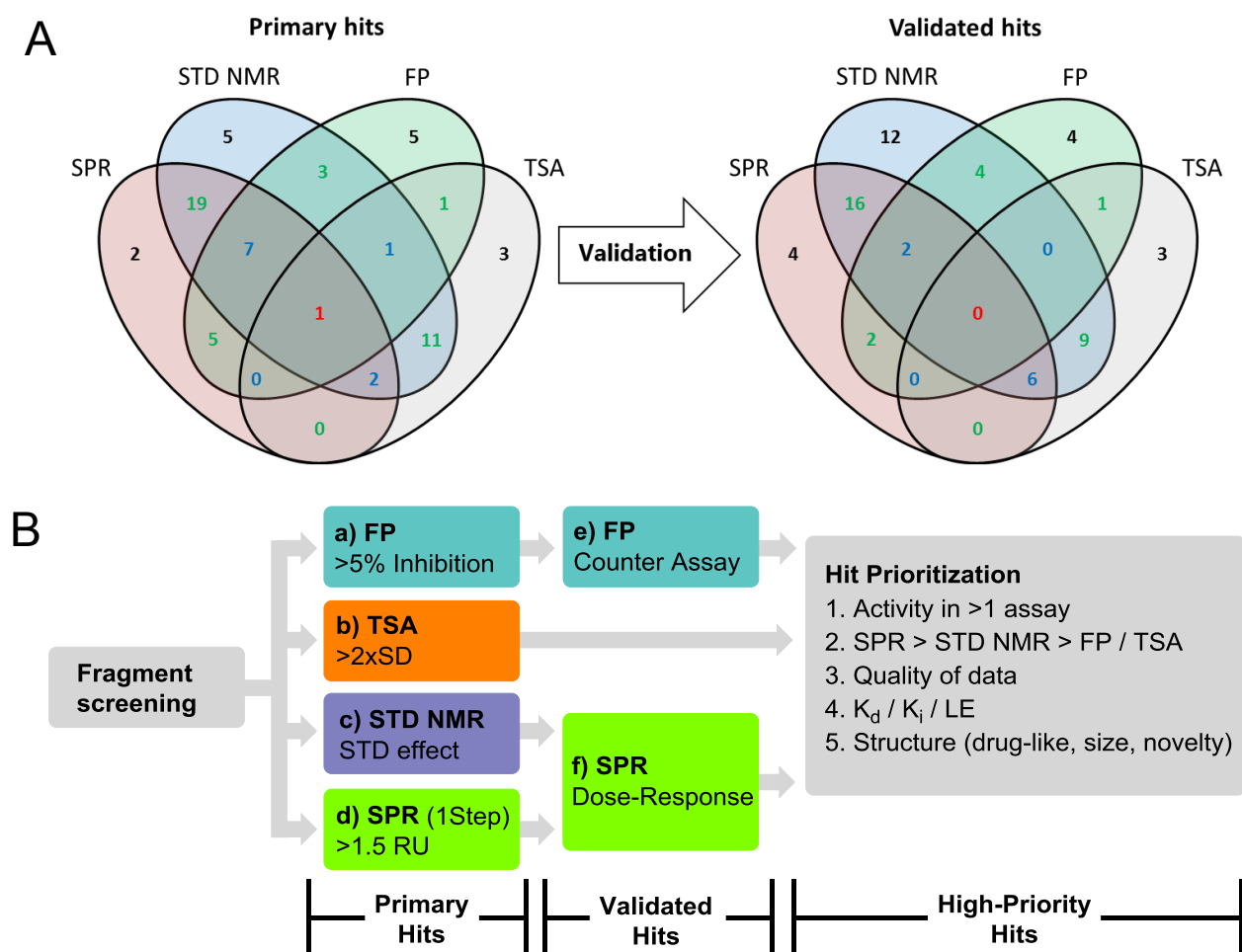


Figure 2. A) Venn-diagrams of the hits of the fragment screening before and after SPR validation. Red numbers; hits in four assays. Blue numbers; hits in three assays. Green numbers; hits in 2 assays. Black numbers; hits in one assay. B) The screening cascade including hit criteria and prioritizing parameters.

In TSA, the fragments were screened in dose-response tests of 0.5–8 mM in 0.5–8% DMSO. Fragments showing an increased ΔT_m larger than two standard deviations of the DMSO control, equaling ~ 0.2 °C, at any concentration were characterized as primary hits. This gave 19 fragments hits (hit-rate of 25%) (**Figure 2A** and **Table S2**).

In STD NMR, the fragments were screened at 1 mM with 3% DMSO- d_6 . Fragments with at least one signal in the ^1H -NMR spectrum displaying an STD% >1% were defined as primary hits. The STD NMR screening gave a high hit-rate of 64% (49 primary hits). Hits were clustered into fragments with STD% >10%, STD% ranging from 4–10%, and STD% of 1–4% (**Figure 2A** and **Table S2**). A poor correlation between the STD NMR amplification factor and affinity has been reported,⁶⁸ and thus we also included fragments having a low STD%.

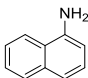
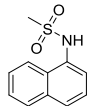
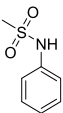
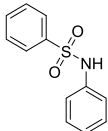
The primary SPR screen was performed by gradient OneStep injections^{69, 70} of the fragments up to 0.5 mM in a 4% DMSO buffer over covalently immobilized Keap1 Kelch at the biosensor chip surface. Thirty-six fragments demonstrating a MW normalized response level higher than 1.5 RU were coined primary hits, corresponding to a hit-rate of 47% (**Figure 2A** and **Table S2**).

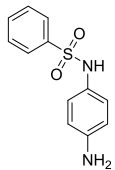
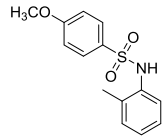
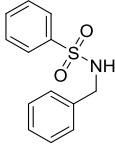
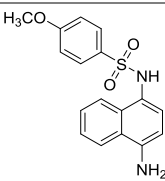
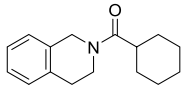
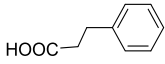
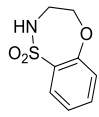
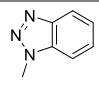
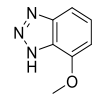
To guide hit prioritization, an SPR dose-response experiment was performed by multi-cycle injections of 0.125–1 mM of the primary STD and SPR hits. An additional six fragments were tested, which were not conclusively assessed by STD NMR due to solubility issues or direct magnetic saturation. A total of 30 fragments showed concentration-dependent and fragment-like response for two or more injections and were thereby considered

SPR validated hits. Among these, 22 were primary SPR hits (validated hit-rate of 29%). Of the 49 STD NMR hits, 24 were here validated by SPR (validated hit-rate of 31%), and so were three out of the six fragments not assessable by STD NMR (**Figure 2A**). Of the 24 SPR validated STD hits, two were also active in FP and six in TSA, but none in both FP and TSA (**Figure 2A** and **Table S2**).

The validated hits were prioritized based on the criteria specified in **Figure 2B**, resulting in 17 high-priority hits (**Table 1**). All 17 fragments were SPR hits and 15 of these were also STD NMR hits (the two remaining SPR hits could not be assessed by STD NMR). Among these, eight of them originate from class **A** inhibitors, one from class **B**, five from class **C**, one from class **D**, two from class **E**, and none from class **F** inhibitors.

Table 1. Binding Data (FP, TSA, STD NMR, and SPR) of High-Priority Fragment Hits.^{a-b}

Fragment#	Structure	FP (K_i /mM)	TSA (ΔT_m /°C@mM)	SPR (K_d /mM)	STD NMR (STD%@1mM)
1a		-	-	1.2 ± 0.3	9%
1b		-	-	0.70 ± 0.1	4%
1f		-	$0.35^\circ\text{C}@1\text{mM}$	3.7 ± 0.2	10%
1m		-	-	1.1 ± 0.3	9%

1n		-	-	0.96 ± 0.2	5%
1r		-	-	2.0 ± 0.8	6%
1s		-	-	1.2 ± 0.1	7%
1w		> 4	-	1.0 ± 0.2	ND
2s		-	-	0.42 ± 0.1	4%
3c		-	$0.1^\circ\text{C}@1\text{mM}$	3.2 ± 0.7	5%
3g		-	-	2.3 ± 0.5	14%
3j		-	-	3.9 ± 1	11%
3l		3.1 ± 0.7	-	1.4 ± 0.6	12%

3o		0.1 ± 0.1	-	0.22 ± 0.1	8%
4c		3.5 ± 0.7	-	1.1 ± 0.4	ND
5e		-	$0.16^\circ\text{C}@1\text{mM}$	0.99 ± 0.3	6%
5i		-	-	1.5 ± 0.4	9%

^aFP K_i values are shown as mean \pm SEM based on two to three individual measurements using the Cy5-probe; TSA ΔT_m values are shown at effective concentrations determined during the dose-response screening; SPR K_d values are shown as mean \pm SEM based on at least three dose-response measurements using steady-state affinity analysis of SPR sensorgrams (R_{max} was fixed to the value of a control compound when fitting); STD NMR effects are shown as the highest obtained STD% value obtained for a given signal during screening.

^b '-': No activity; ND: Not determined (due to direct saturation of ligand signal in STD NMR or solubility issues).

In general, high validated hit-rates of 17–31% were observed, as one would expect from a target-biased fragment library based on known inhibitors. Notably, eight fragments were hits in three assays, 32 in two assays, and 23 in one assay, while none were active in all four assays (**Figure 2A** and **Table S2**). This relatively low assay overlap could reflect the different sensitivities of the techniques, small variations in experimental conditions (DMSO %, buffers, temperature), and fragment concentrations. Also, their fundamental different read-out principles result in different types of false positives and negatives,⁷¹ e.g. aggregation can form a false

positive SPR signal,⁷² STD NMR can result in false negatives due to direct irradiation of the fragment,⁷¹ fluorescence interferences from compounds can cause false positives in FP, and fluorescence quenching by the fragments could lead to false negatives in TSA.⁷³ A low number of overlapping hits has also been observed in other fragment screening studies using similar assay technologies.^{74, 75} That said, there was a substantial overlap between STD NMR and SPR hits (**Figure 2A**), and activity in these assays were emphasized in our prioritization.

X-ray Crystallography of Fragment Hits. The binding poses of the high-priority hits were assessed by X-ray crystallography by soaking the fragments at 5–10 mM into crystals of mouse Keap1 Kelch domain in 5–10% DMSO.²⁰ Co-crystal structures of seven of the high-priority hits were obtained with good resolutions: **1f** (2.15 Å), **3c** (2.0 Å), **3g** (2.2 Å), **3j** (2.1 Å), **3l** (1.38 Å), **4c** (1.98 Å), and **5e** (2.3 Å). For **3l** and **4c**, well-defined electron-densities allowed an unambiguous placement of the ligands within the Neh2-binding site of the Kelch domain (**Figure 3A**). For **1f**, **3c**, **3g**, and **3j**, electron-densities proving that the fragments bind in the pocket were resolved. However, these electron-densities were not completely covering the modeled ligand structures at standard $2F_o - F_c$ crystallographic maps contoured at 1σ levels and thus some uncertainty is associated with determination of the binding modes (**Figure S1**). Fragment **5e** was found binding outside the pocket on the side of the Keap1 Kelch domain (*data not shown*), correlating with the fact that it was not an FP hit. On the other hand, **1f**, **3c**, **3g**, and **3j** were found in the Keap1 Kelch binding pocket despite not being FP hits either. This probably reflects that the FP assay is not sensitive enough to detect these weak binders.

The binding pocket has been divided into five interconnected subpockets, denoted P1–P5, where P1 and P2 contain mostly polar and basic residues (Arg483, Ser508, Arg380, Asn382, and Asn414), while the P5 contains a hydrophobic aromatic triad made up of Tyr572, Phe577, and Tyr334 (**Figure 3A**).²⁶ Both **4c** and **3c** bind in P1,

where their carboxylic acids interact with Arg415 and/or Arg483 via charge-assisted H-bonds (**Figure 3A** and **Figure S1B**). The sulfonamide of **1f** forms an H-bond with Ser602 in P2/P5 and the benzene ring of **1f** is placed at the aromatic triad of Tyr334, Tyr572, and Phe577 (**Figure S1A**). A similar binding of the rigidified sulfonamide **3g** is observed (**Figure S1C**). Finally, the benzotriazoles of **3i** and **3j** are both located in P4 (**Figure 1** and **Figure S1D**, respectively). The X-ray crystal structures of our fragments thus suggest subpockets P1, P4, and P5 to be hot spots of the Keap1 Kelch binding pocket, i.e. important contributors to binding energy, as has also previously been found by X-ray crystallographic fragment screening.²⁰ In comparison, P1 and P2 have been suggested to be the most important subpockets for binding of Nrf2,²⁶ while another study found three fragments binding in P1 and P4 after soaking 11 fragment hits.⁷⁶ The latter study also provided a computational analysis suggesting additional hot spots outside the canonical P1-5 subpockets.

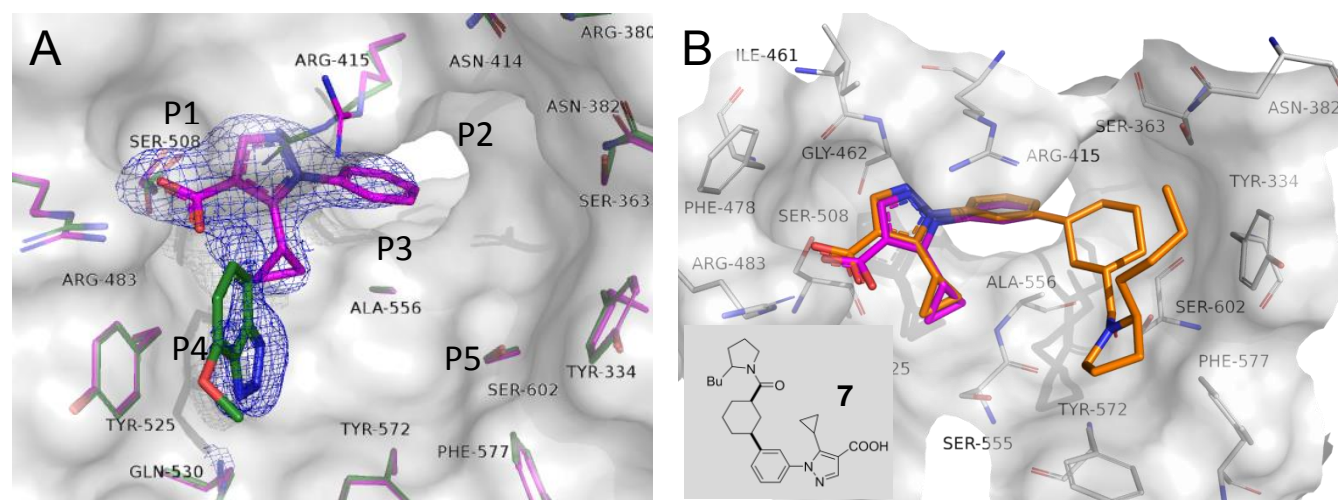
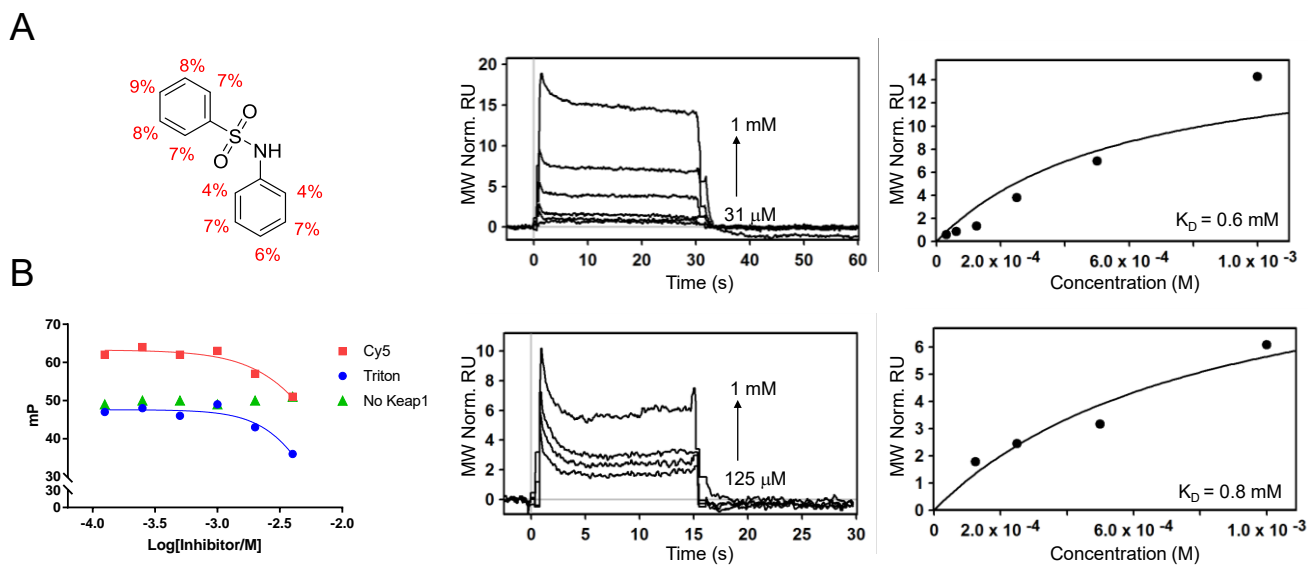


Figure 3. A) X-ray crystal structure of **3i** (green) (PDB ID: 6ZEW) and **4c** (purple) (PDB ID: 6ZEX) in complex with the Keap1 Kelch domain (the two structures are superimposed for illustrative purposes). Standard $2F_o - F_c$ electron density map carved around the fragments at 1.6 Å (blue) contoured at 1σ are shown. B) X-ray crystal structure of **4c** (purple) and the known class **D** inhibitor compound **7** (orange) in complex with the Keap1 Kelch domain (PDB ID: 6ZEX).

Furthermore, we solved the X-ray crystal structure of the original class **D** inhibitor 1-(3-((*cis*)-3-(2-butylpyrrolidine-1-carbonyl)cyclohexyl)phenyl)-5-cyclopropyl-1*H*-pyrazole-4-carboxylic acid (compound **7**),³¹ which we have previously synthesized and tested,³³ but whose binding mode to Keap1 Kelch has not been revealed before. Interestingly, the derived fragment **4c** retained the same binding mode as the known inhibitor (**Figure 3B**). Similarly, the sulfonamide-containing fragments **1f** and **3g** seem to recapitulate the binding modes seen for the larger known ligands they were derived from (**Figure S1** versus PDB ID 4IQK and 5FNU, respectively). These fragments therefore seem to bind to anchor points of the Keap1 Kelch pocket, i.e. particular important hot spots that dominate the free energy of binding.⁷⁷ In contrast, the binding poses of **3c**, **3j**, and **3l** were not conserved relative to the original ligand (PDB ID 5FNU), a common situation of FBDR,⁷⁸ indicating that these fragments will not serve as useful starting points generating larger compounds as their binding poses are likely to be altered throughout optimization.⁷⁷

Merging of Fragment Hits. In parallel with our efforts of obtaining X-ray crystal structures, molecular dockings of the fragments were also performed to guide optimization. Here, fragment **1m**, a high priority hit showing relatively high affinity in SPR and high STD NMR effects (**Table 1** and **Figure 4A**), was hypothesized to bind at the right-hand side in the Neh2 binding pocket (P2, P3, and P5) according to our docking model (**Figure 5A**). Specifically, it protrudes its aniline core into the area between Arg415 and Ala556 and places its benzenesulfonyl moiety optimal for hydrogen bonding with Ser602 and Ser363 and π - π stacking with Tyr334. When superimposing the docking pose of **1m** with the X-ray structures of the other sulfonamide-containing fragments—**1f** and **3g** (**Figure S1**) and **1e** (PDB ID: 5FZN)²⁰—a good overlap between the sulfonamide groups was observed (**Figure S2**) thus supporting the docking result.



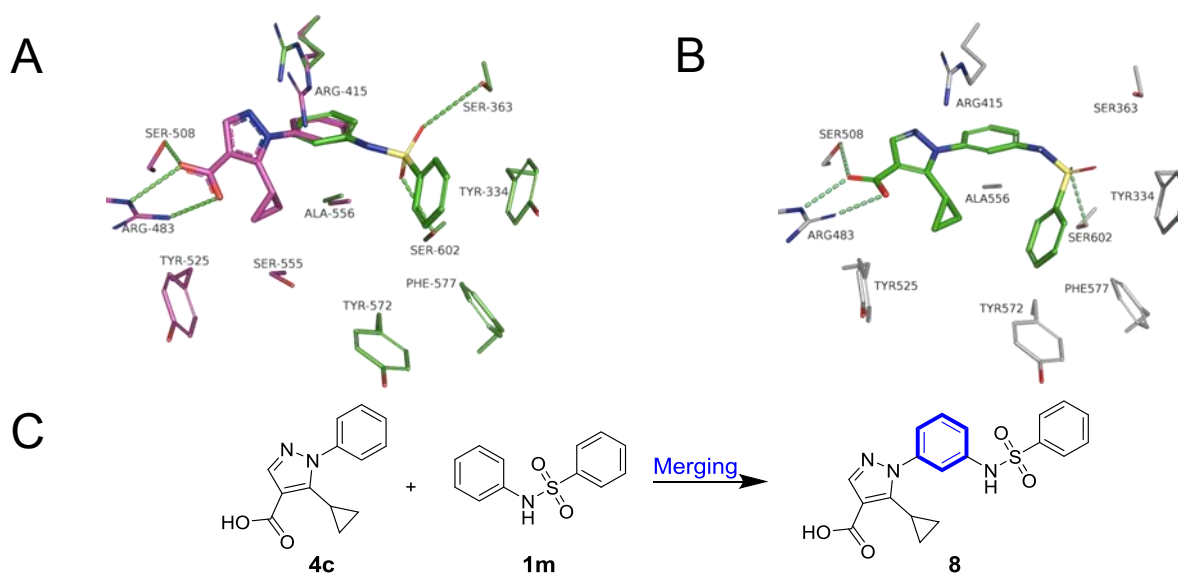


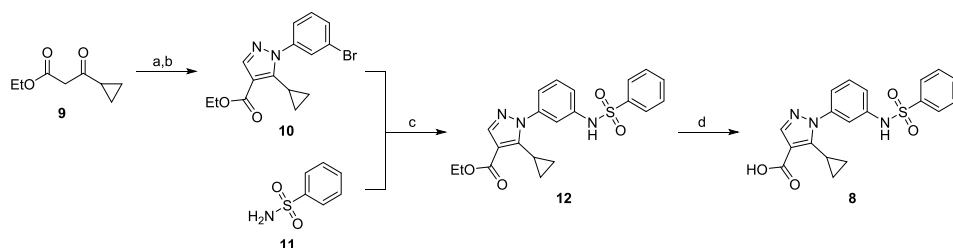
Figure 5. A) Binding mode of **1m** (as determined by docking; ligand and amino acid side chains in green) and **4c** (as determined by X-ray crystallography; ligand and amino acid side chains in purple) in the Keap1 Kelch domain. B) Docking of the **1m/4c** merged analogue (compound **8**). C) Conceptual scheme for the merging of **1m** and **4c** to design **8**.

Importantly, we noticed that the aromatic cores of **1m** and **4c** overlap as seen when superimposing the docking pose of **1m** and our X-ray crystal structure of **4c** (Figure 5A). Fragment **4c** was also a high priority hit showing activity in FP and SPR (Table 1 and Figure 4B). Thus, the superimposition indicates that merging the two cores with a *meta*-relationship would be feasible, as supported by docking, giving rise to the design of lead compound **8** (Figure 5B–C).

Compound **8** was made in 3 steps with the first step being an initial *de novo* pyrazole synthesis, consisting of a condensation of 1,3-ketoaldehyde, prepared *in situ*, with aryl hydrazine to efficiently give the aryl bromide intermediate.³² Subsequent Ullmann-type coupling with benzenesulfonamide and deprotection afforded **8** (Scheme 1). Evaluation by SPR showed **8** to exhibit a 380-fold stronger binding to the Keap1 Kelch domain,

displaying a $K_d = 2.9 \mu\text{M}$ (**Figure 6A–B**), compared to the two fragments **1m** and **4c** (both showing $K_d = 1.1 \text{ mM}$; **Table 1**). In the FP inhibition assay, **8** efficiently displaced the Nrf2 peptide probe with a K_i value of $15.6 \mu\text{M}$ (**Figure 6C**), corresponding to a 220-fold improvement relative to parent fragment **4c** (**Table 1**). Further, based on the FP K_i values (**Table 1**), LE was improved for **8** compared to **4c** (0.24 vs 0.20 kcal/mol, respectively) suggesting that compound **8** maintains or even improves the size-dependent binding efficiency of the original fragments. To further confirm that **8** binds in the Neh2 binding pocket and to verify its hypothesized binding mode, a 1.8 \AA X-ray crystal structure of the compound in complex with the Kelch domain was obtained (**Figure 6D**). This revealed the expected pose (**Figure 5B**), in which the central benzene is placed in P3 and acts as a linker between the pyrazole moiety probing the left-hand side (P1) of the pocket and the benzenesulfonamide moiety which occupies the right-hand side (P5) (**Figure 6D**).

Scheme 1. Synthesis of the merged lead compound **8**.



^a Reagents and conditions: (a) DMF-dimethyl acetal, 15 min, MW, 130 °C; (b) 3-Bromophenylhydrazine hydrochloride, TEA, EtOH, RT, 24 h, 85%; (c) CuI, K₂CO₃, *N,N*-dimethylglycine, DMF, 48 h, 160 °C, quantitative; (d) Aq. NaOH, EtOH, RT, 30 h, 17%.

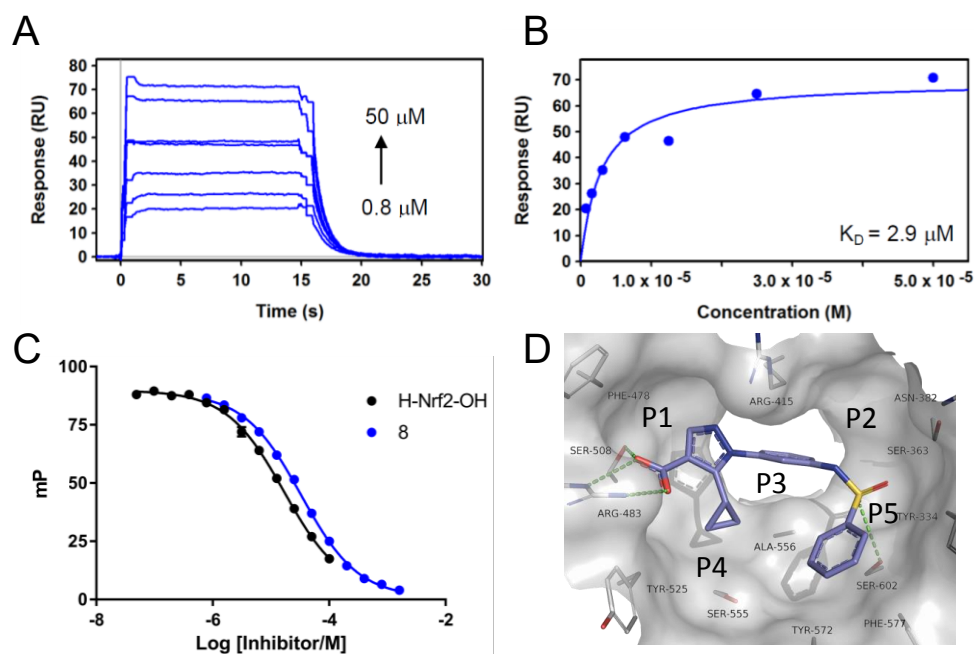


Figure 6. Binding of the merged compound **8** to the Keap1 Kelch domain. (A) SPR sensorgrams of **8** injected in two-fold serial dilutions ranging from 0.8 to 50 μM over immobilized Keap1 Kelch. (B) Plots of equilibrium binding responses from sensorgrams in A) against the injected concentrations of compound **8**. (C) Concentration response curves from the competitive FP assay of **8** using the Cy5-Nrf2 probe. The 9meric Nrf2 peptide H-Nrf2-OH (H-LDEETGEFL-OH) was used as a positive control. (D) X-ray crystal structure of **8** (blue) (PDB ID: 6ZEY) in complex with the Keap1 Kelch domain.

Initial Structure-Activity Relationship Study of Lead Compound 8. The lead optimization of **8** was guided by a combination of ligand-based and computer-aided drug design based on the X-ray crystal structure of **8** (**Figure 6D**). Five series (I–V) and two single structural modifications (VI–VII) (**Figure 7**), involving 35 compounds, were designed and synthesized. Growing from the *meta*-position of the aniline core (series I) could potentially facilitate interactions to the deeper parts of the central and narrow channel of the Keap1 Kelch domain, which

a computational analysis has suggested to be a hitherto unexploited hot spot area.⁷⁶ Growing from the nitrogen at the sulfonamide (series **II**) was expected to result in important interactions to the amino acids in P2, and modifications and/or elongation of the 5-cyclopropyl substituent (series **III**) were designed to facilitate binding in P4. The electrostatic demands of the sulfonyl ring in P5 were probed in series **IV** to target the three aromatic residues (Tyr334, Tyr572, and Phe577). The carboxy substituent of **8** engages with the donor duo of Arg483 and Ser508 in P1, a canonical binding mode seen for most potent known Keap1-Nrf2 inhibitors;¹⁴ here, various carboxylic acid bioisosteres were explored (series **V**). Also, introducing more flexibility around the sulfonamide was attempted by spacing the aryl ring and the nitrogen with a methylene (**VI**), and the pyrazole core was exchanged with the more electron-rich triazole (**VII**), which could also open up for more synthetic possibilities. The resulting compounds from series **I–VII**, compounds **8a–ai**, were synthesized according to the procedures described in the Supporting Information (**Scheme S1–7**).

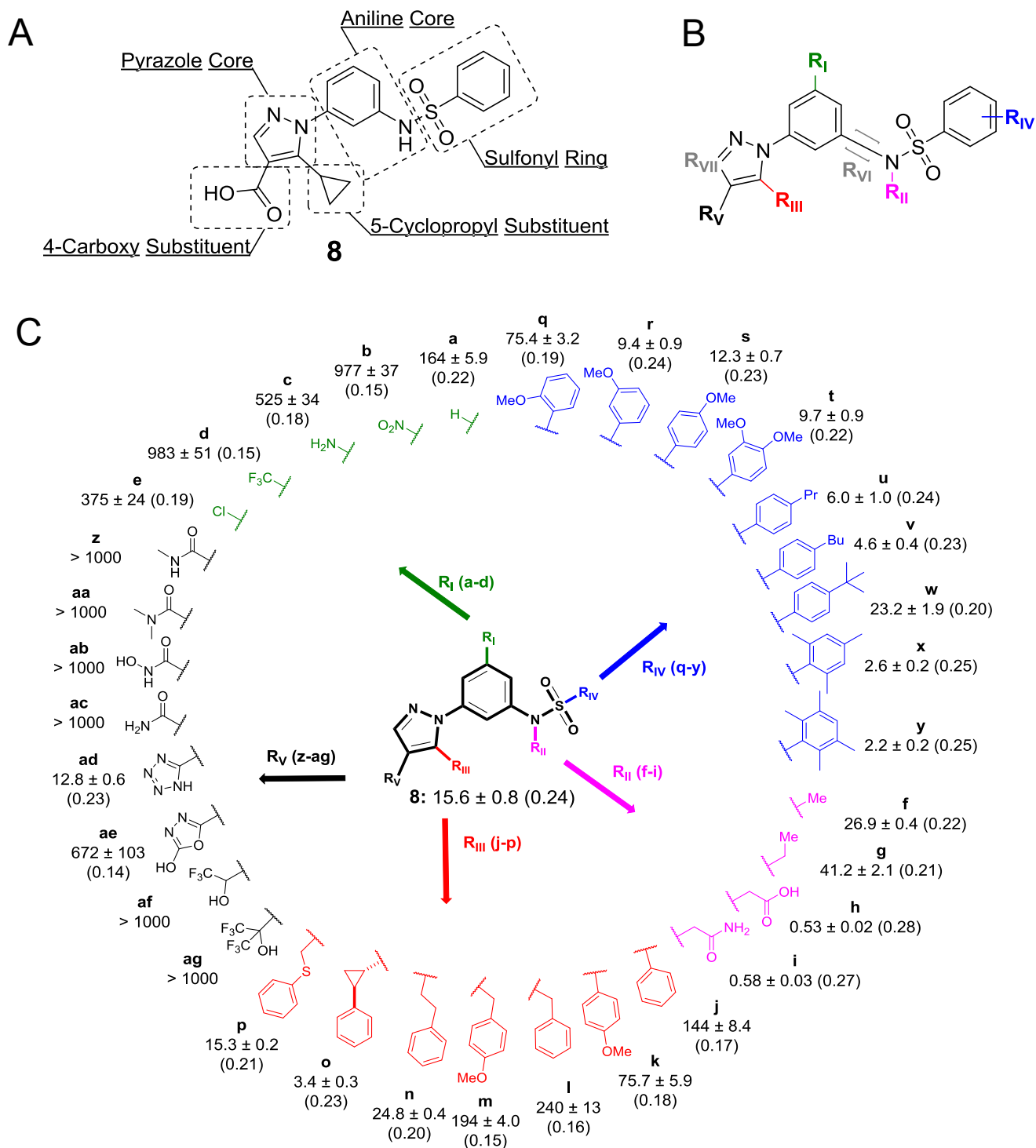


Figure 7. A) Substructure analysis of **8**. B) SAR study of **8** with representation of series I–V and the two single modifications VI–VII. C) The five series of analogues. I: Green, II: Pink, III: Red, IV: Blue, and V: Black. Binding

activities from the competition FP assay are shown as K_i values in μM ($n \geq 3$). LE values are shown in parenthesis. The analogues have only been modified at one position at a time. Compound **8a–e** do not contain a cyclopropyl group as compound **8** and the remaining analogues do.

The analogues were tested for binding affinity to the Keap1 Kelch domain by FP (**Figure 7C**). Growing from the *meta*-position of the aniline core (series I) was unfortunately not favorable. To facilitate synthesis, the 5-cyclopropyl moiety was omitted from the series I analogues (**8a–e**) (**Scheme S1**). Removal of the cyclopropyl group of **8** gave **8a** with a 11-fold increase in K_i relative to **8**, and adding the smaller substitutions in the *meta*-position resulted in a further 2.3–6-fold increase in K_i values of **8b–e** compared to **8a** (**Figure 7C**). To understand this, we solved the X-ray crystal structures of **8a–e** (**Figure S3**), which revealed that **8** and **8a** bind with the same binding mode, but that analogues **8b–d** are extruded from the binding pocket. The binding pose of the chlorine-substituted **8e** was also affected relative to **8a**, but to a lesser extent potentially reflecting its minor 2.3-fold decrease in affinity (**Figure S3**). Based on these results, it did not appear feasible to grow further into the central channel from the *meta*-position of the aryl core.

Guided by molecular docking, the sulfonamide of **8** was alkylated to probe the P2 subpocket (series II). Analogues with non-polar substituents—methyl (**8f**) and ethyl (**8g**)—resulted in a slight loss of affinity, whereas the polar substituents—carboxylic acid (**8h**) and amide (**8i**)—both led to ~30-fold stronger binding and higher LE values relative to compound **8** (**Figure 7C**). As expected, the X-ray crystal structures of **8h** revealed hydrogen bonding between the carboxylic acid of **8h** and polar groups (Asn414 and Arg415) in P2 (**Figure 8A**).

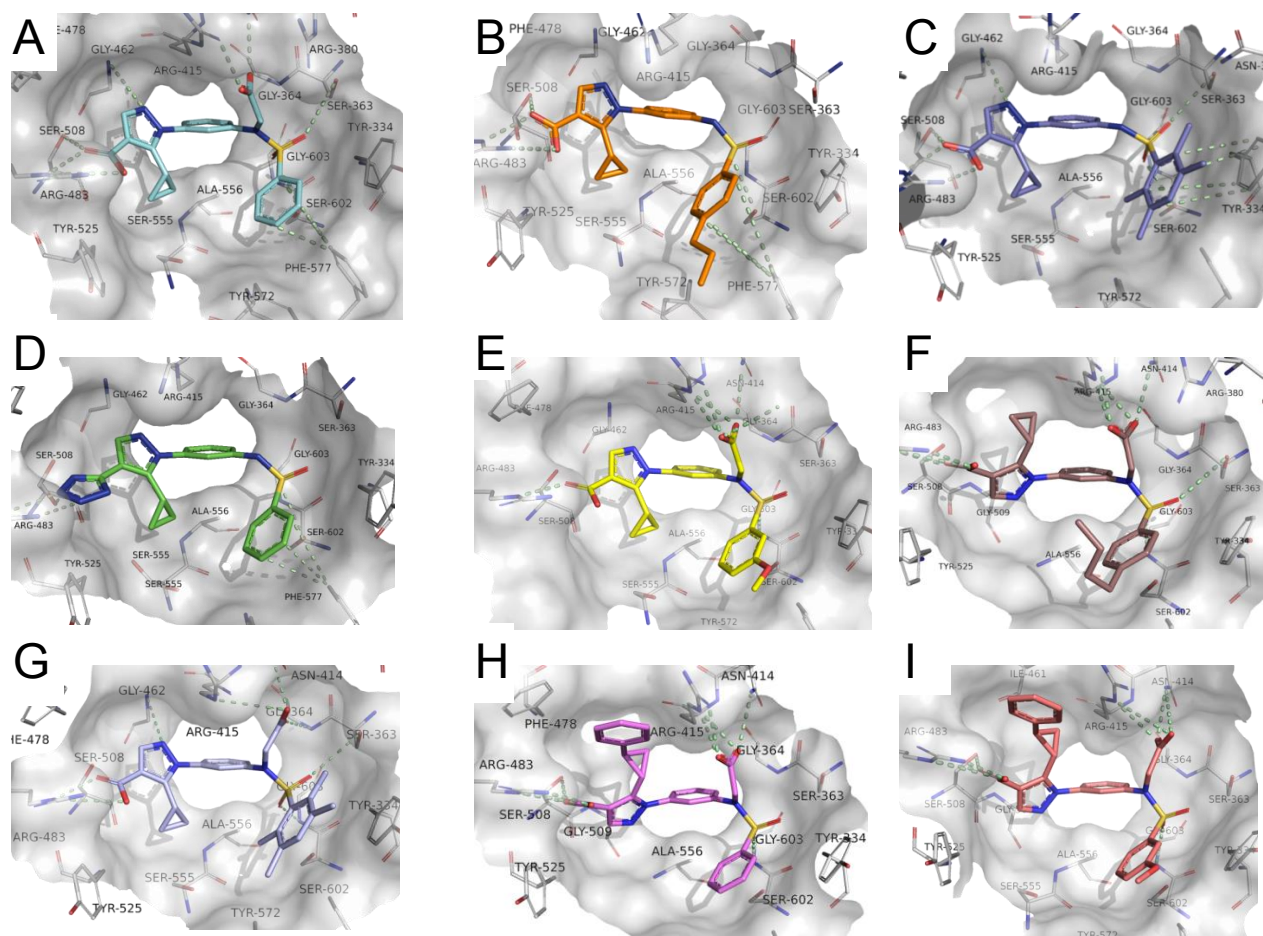


Figure 8. A) 1.74 Å X-ray crystal structure of **8h** (PDB ID: 6ZF1). B) 2.20 Å X-ray crystal structure of **8u** (PDB ID: 6ZF2). C) 1.59 Å X-ray crystal structure of **8y** (PDB ID: 6ZF0). D) 1.28 Å X-ray crystal structure of **8ad** (PDB ID: 6ZF3). E) 1.37 Å X-ray crystal structure of **77e** (PDB ID: 6ZF7). F) 1.29 Å X-ray crystal structure of **77g** (PDB ID: 6ZF5). G) 1.21 Å X-ray crystal structure of **77i** (PDB ID: 6ZF4). H) 1.37 Å X-ray crystal structure of **77n** (PDB ID: 6ZF6). I) 1.75 Å X-ray crystal structure of **77o** (PDB ID: 6ZF8).

Several benzyl moieties were substituted at the 5-position of the pyrazole core of **8** in place of the cyclopropyl (series **III**) in an attempt to reach subpocket P4 and possibly form π - π interactions with Tyr525. The FP data show that a two-carbon linker system between the pyrazole and the benzene ring as in compound **8n–p** is

required to improve or preserve the affinity for this series. Changing the linker system to a *trans*-cyclopropyl enhanced the binding activity five-fold (**8o** vs. **8**), giving a K_i of 3.4 μ M (**Figure 7C**).

A range of functional groups with differing electron donating capacities and bulkiness were substituted on the sulfonyl ring to explore its electrostatic and steric demands (series **IV**). The 4-*tert*-butyl-substituted analogue (**8w**) was only slightly weaker than **8**, whereas the 4-methoxy-substituted analogue (**8s**) has slightly enhanced binding, potentially due to an electrostatic effect. Affinity is affected by the substitution pattern as observed for the methoxy-substituted analogues (**8q–t**), where *meta*- and *para*-substitution enhance the affinity but the *ortho*-substitution decreases affinity by 5-fold. Substitutions with 4-propyl (**8u**), 4-*n*-butyl (**8v**), 2,4,6-tri-methyl (**8x**), or 2,3,5,6-tetra-methyl (**8y**) increased the affinity 3–7-fold and retained or slightly increased the LE compared to **8**. The binding modes of **8u** and **8y** were solved by X-ray crystallography and were found to be similar to each other and to that of **8**; for the 2,3,5,6-tetramethylbenzene of **8y** a π - π stacking with Tyr334 was observed, potentially correlating with its higher affinity relative to **8u** (**Figure 8B–C**).

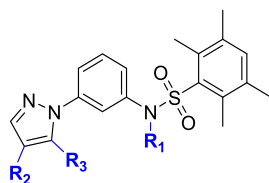
The carboxylic acid bioisostere series (**8z–ag**) resulted in mostly inactive compounds, except for the tetrazole analogue (**8ad**), which demonstrated the same affinity towards the Keap1 Kelch domain in FP as **8** (**Figure 7C**) and was able to retain the same binding mode as seen by X-ray crystallography (**Figure 8D**). The tetrazole is the most acidic bioisostere among the tested ones, which probably explains the retained binding activity.

Finally, introducing a methylene to provide a more flexible scaffold (**8ah**) or exchanging the pyrazole core with a triazole (**8ai**) reduced the affinity 3–5-fold compared to **8** (*data not shown*).

Optimization to High-Affinity Compounds. The most favorable modifications of compound **8** were combined into 18 target compounds (**77a–r**) (**Scheme S8–11**) in order to either optimize the physicochemical properties

(Table 2; compound **77a–d**) or with the focus of enhancing binding affinity (Table 3; compounds **77e–r**) compared to **8**. The compounds were synthesized by combining the chemistry applied for analogues **8a–ai** with minor adjustments; e.g. TBDMS was used as a protecting group of the carboxylic acid to ease the later deprotection step (**77c** and **77d**), and formation of the amide was done directly from the carboxylic acid via EDC-mediated coupling with ammonium chloride (**77d**).

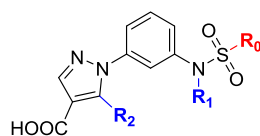
Table 2. Combined Structure-Activity Relationship (SAR) Study of 8.^a



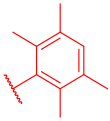
Cmpd	R1	R2	R3	FP K_i / μM	LE
8y	-H	-COOH		2.2 ± 0.2	0.25
77a	-CH ₂ COOH			0.66 ± 0.03	0.23
77b	-CH ₂ CONH ₂			1.5 ± 0.2	0.21
77c	-CH ₂ CONH ₂	-COOH		1.4 ± 0.1	0.23
77d	-CH ₂ CONH ₂	-COOH		0.37 ± 0.01	0.21

^aFP K_i values are shown as mean \pm SEM based on ≥ 3 individual measurements using the Cy5-probe. LE values are shown in parenthesis.

Table 3. Combined Structure-Activity Relationship (SAR) Study of 8.^a



R_0	$R_1 = H$	$R_1 = CH_2COOH$	$R_1 = H$	$R_1 = CH_2COOH$
	$R_2 =$	$R_2 =$	$R_2 =$	$R_2 =$
	8^b 15.6 ± 0.8 μM (0.24)	8h^b 0.53 ± 0.02 μM (0.28)	8o 3.4 ± 0.3 μM (0.23)	77n^b 0.13 ± 0.02 μM (0.25)
	8r 9.4 ± 0.9 μM (0.24)	77e^b 0.17 ± 0.02 μM (0.28)	77j 1.9 ± 0.2 μM (0.22)	77o^b 0.040 ± 0.006 μM (0.26)
	8u^b 6.0 ± 1 μM (0.24)	77f 0.34 ± 0.04 μM (0.26)	77k 2.7 ± 0.2 μM (0.21)	77p 0.079 ± +.001 μM (0.24)
	8v 4.6 ± 0.4 μM (0.23)	77g^b 0.40 ± 0.07 μM (0.25)	-	-
	8x 2.6 ± 0.2 μM	77h 0.63 ± 0.1 μM	77l 1.5 ± 0.2 μM	77q 0.098 ± 0.02 μM

	(0.25)	(0.25)	(0.22)	(0.24)
	8y^b	77i^b	77m	77r
	2.2 ± 0.2 μM	0.73 ± 0.07 μM	1.1 ± 0.06 μM	0.21 ± 0.02 μM
	(0.25)	(0.24)	(0.22)	(0.22)

^aFP K_i values are shown as mean ± SEM based on ≥3 individual measurements using the Cy5-probe. LE values are shown in parenthesis.

^bX-ray structure available (Figure 8).

With compounds **77a–b**, it was demonstrated that the carboxylic acid interacting with P1 of the Keap1 Kelch domain could be replaced with a tetrazole and still provide low-micromolar to high-nanomolar affinities (K_i = 0.66–1.5 μM; **Table 2**). The neutral amide group on the sulfonamide as in **77b** here led to a 2-fold lower affinity compared to the corresponding acid group (**77a**)—in contrast to the corresponding and equipotent amide- and acid-containing compounds **8i** and **8h** (K_i = 0.53–0.58 μM; **Figure 7C**). Also, the affinity of **77c** was only slightly (1.6-fold) improved relative to **8y**, which was not expected as a large (27-fold) affinity-boost was observed when adding the amide group to the sulfonamide of **8** to get **8i** (**Figure 7C**). Still, replacing the cyclopropyl of **77c** with *trans*-cyclopropylbenzene gave **77d** binding with high affinity (K_i = 0.37 μM), although on the expense of a lower LE (**Table 2**).

Our results demonstrated that the individual affinity-improving structural changes (**Figure 7C**) could not be easily combined to obtain additive or even synergistic effects (**Table 2**). Thus, a combinatorial and systematic approach was applied instead (**Table 3**). Here, it was seen that independently of the substitution at the benzenesulfonamide moiety, addition of an aliphatic carboxylate chain at the sulfonamide nitrogen results in improved binding affinity (**8h** and **77e–i**; **Table 3**). However, for the methylated benzene compounds (**77h** and

77i) the binding affinities were only improved 4- and 3-fold, respectively, whereas for the four remaining compounds (**8h** and **77e–g**) a 12- to 55-fold improvement was observed leading to very potent compounds such as **77e**, **77f**, and **77g** ($K_i = 0.17, 0.34, \text{ and } 0.40 \mu\text{M}$, respectively; **Table 3**). The X-ray structure of **77e**, **77g**, and **77i** were solved and showed favorable interactions between the aliphatic carboxylate group and the Asn414/Arg415 residues in all cases (**Figure 8E–G**). Interestingly, for **77g**, containing the long *n*-butyl chain in the *para*-position of the benzenesulfonamide moiety, the cyclopropyl is pushed upwards from the direction of P4 to P1. This was in contrast to molecular docking, which suggested that the cyclopropyl would point downwards towards P4.

Changing the cyclopropyl to a *trans*-cyclopropylbenzene led 2- to 5-fold improved binding affinities for all the compounds (**8o** and **77j–m**; **Table 3**). Interestingly, the binding affinity is improved the most when combined with the smallest substituent at the benzenesulfonamide moiety (3-methoxy; **77j**), which could be due to a higher degree of flexibility as a result of less intramolecular clashing of the various groups.

Finally, combining the aliphatic carboxylate and the *trans*-cyclopropylbenzene gave four compounds with binding affinities below or around 100 nM (**77n–q**) and LE values similar or improved relative to the original compound **8** (**Table 3**). Compound **77o** was particularly potent with a K_i of 40 nM and an improved LE of 0.26. Compared to the compounds with cyclopropyl (**8h** and **77e–i**), **77n–r** with *trans*-cyclopropylbenzene groups were 3–6-fold more potent. The binding data also indicates that the effect of adding the aliphatic carboxylate is highest for non-, meta-, or para-substituted compounds (26–48 fold improvement in K_i for **77n**, **77o**, and **77p** relative to **8o**, **77j**, **77k**, respectively), compared to ortho-substituted compounds (5–15-fold improvement in K_i for **77q** and **77r** relative to **77l** and **77m**, respectively) (**Table 3**). Noticeably, the X-ray crystal structures of **77n** and **77o** revealed that the *trans*-cyclopropylbenzene had shifted upwards – from P4 towards a generally unexplored and more hydrophobic part of P1 (containing Phe478 and Ile461) (**Figure 8H–I**) – in contrast to

molecular docking, which suggested that the *trans*-cyclopropylbenzene would fit into P4 and interact with Tyr525. The two compounds were made as a mixture of two enantiomers, but in both cases, it was the 1*S*,2*S* stereoisomer that fitted into the respective electron densities. Considering the high affinities of **77n** and **77o** (K_i = 130 and 40 nM, respectively) this unique and apparently favorable binding mode, which also leaves the P4 subpocket free, could be exploited in further drug design of Keap1-Nrf2 PPI inhibitors.

Biological Stability. Stability under biological conditions is an important parameter in the early phases of drug discovery and can be a limiting factor for more advanced pharmacological studies. We therefore evaluated the stability of key compounds against mouse liver microsomes and in human blood plasma. We found that compounds **8**, **8h**, **8i**, **77a**, **77e**, **77i** and **77o** were completely metabolic stable in the measured time span (240 min), while **77j** was degraded slowly (half-life, $t_{1/2}$, ~ 210 min). In contrast, the known inhibitor, compound **7**, from which our compounds were derived, degraded fast ($t_{1/2}$ = 27 min) (**Figure 9**). In blood plasma, the tested compounds were completely stable (**Figure 9**).

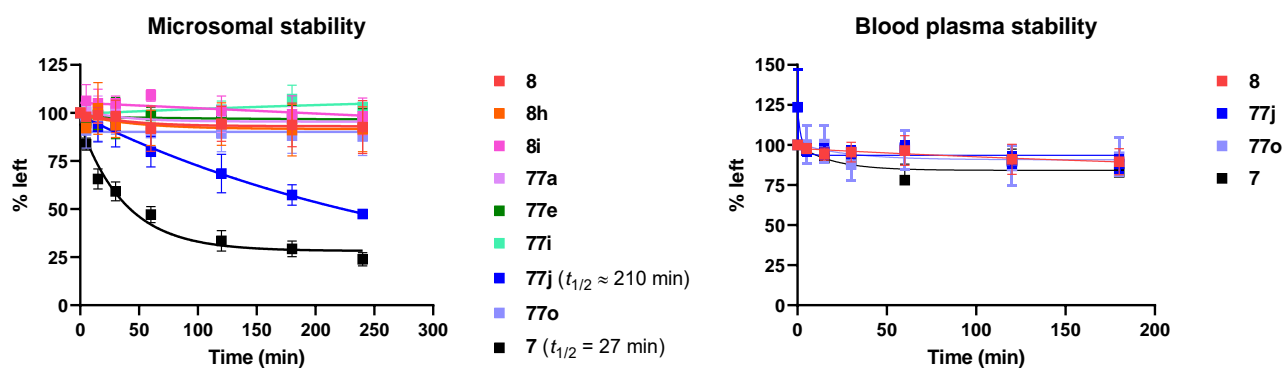


Figure 9. Stability of key compounds when incubated with mouse liver microsomes and human blood plasma. Data are shown as mean \pm standard error of the mean (SEM) of 2–4 individual experiments.

Membrane Permeability. To evaluate if our compounds could be used as potential cell active chemical probes we tested them in a parallel artificial membrane permeation assay (PAMPA). Unfortunately, all tested compounds (**8**, **8h-i**, **8z**, **8ad**, **77a**, **77e**, **77i**, **77j**, and **77o**) displayed very low permeabilities with less than 2% found in the acceptor compartment (**Table S4**). Noticeably, replacing the carboxylic acid of **8** with amide (**8z**) or tetrazole (**8ad**) did not significantly improve the permeability, as was the case for the larger tetrazole-containing analogue **77a** compared to **77i**. Also, the methoxy-substituted compounds (**77e**, **77j**, and **77o**) showed very low permeability independent of whether they had one or two carboxylic acids or benzene on the cyclopropyl part (**Table S4**). This poor membrane permeability was in contrast to **7**, which showed high permeability. Hence, even though **7** and our compounds share the structural motif corresponding to fragment **4c**, the physicochemical properties of our compounds are not favourable for membrane permeability. Compound **8** is smaller than **7** and both compounds contain one carboxylic acid moiety, thus these features do not seem to be determining for the permeability in this direct comparison. Instead, lipophilicity is much lower for **8** than **7** (CLogP: 2.4 and 4.6) and the topological polar surface area is much higher (tPSA: 99 and 73 Å²) (**Figure S4**), which can potentially explain the different capabilities to penetrate the PAMPA membrane. Likewise, **77o** has a higher tPSA than **7** (137 Å²), a slightly lower CLogP (3.9), and contains two carboxylic acid groups instead of one, which in combination could explain the lower permeability of **77o** relative to **7** (**Figure S4**).

Based on this, future optimization of **77o** and analogues should focus on balancing lipophilicity and polarity to improve the membrane permeability and thereby provide compounds more promising for cellular studies. A strategy could be to replace the sulphonamide group and perform a wider exploration of carboxylic acid bioisosteres, in addition to those studied here (**Figure 7**). Also, prodrug strategies that mask the carboxylic acid could be attempted.^{14, 42, 79}

CONCLUSION

This study demonstrates that FBDR can be used to develop new and potent inhibitors of the pharmacologically relevant Keap1–Nrf2 PPI. The approach of using a series of known small-molecules to design a deconstruction library of fragments, followed by reconstruction of the most promising hits and structure-based optimization has not previously been applied to the Keap1-Nrf2 PPI, and to the best of our knowledge this is the most extensive FBDR study reported in general. By generating a target biased library of 77 fragments followed by screening and validation using four orthogonal assays (FP, TSA, STD NMR, and SPR) we identified 17 well-characterized fragment hits against the Keap1 Kelch domain. Concurrently, we assessed the sensitivities and overlaps of hits between the assays, which revealed that SPR and STD NMR are superior in sensitivity and fragments that are active in SPR are generally also active in STD NMR, but less often active in FP and TSA. By analyzing the poses of seven fragment hits binding in the Keap1 Kelch domain by X-ray crystallography and comparing these with the binding modes of the original compounds, we identified the P1, P4, and P5 subpockets to represent hot spot areas, and P1 and P5 to be the most important anchor points for overall binding of the molecules. This unique structural insight allowed us to use structure-based drug design to select two promising fragment hits (**4c** and **1m**) and merge them into the novel compound **8** with enhanced affinity. Initial optimization, including bioisosteric replacements of the P1 binding carboxylic acid revealed that only the tetrazole group was also tolerated in this region. Substituents pointing towards the central channel were explored and SAR studies revealed the most favourable groups for targeting the P2, P4, and P5 subpockets. Further optimization guided by several X-ray structures and a systematic approach where we combined the most promising structural features resulted in particularly four compounds (**77n–q**) with high binding affinities (K_i values of 40–130 nM) and with the X-ray structures of **77n** and **77o** showing a novel binding mode

occupying the upper and hydrophobic part of P1. Also, our compounds were much more resistant to microsomal degradation compared to the original compound (**7**).

Overall, we demonstrate that FBDR can be an effective approach for finding new fragment hits and for making new potent inhibitors of the Keap1-Nrf2 PPI with improved properties, such as microsomal stability, and we thereby anticipate that FBDR can be a powerful strategy for other challenging drug targets. Although the current example of FBDR did unfortunately not lead to membrane permeable Keap1 inhibitors, we believe that the fragment hits, lead compounds, and structural insight provided herein can facilitate the development of compounds promising for cellular studies. Concretely, for this series, we suggest that future optimization focuses on balancing lipophilicity and polarity. Also, the carboxylic acid that interacts with the P1 arginine seems obligatory for obtaining high affinity, thus we propose to further explore bioisosteric replacements and prodrug strategies to mask the carboxylic acid and thereby provide biological active Keap1 inhibitors.

EXPERIMENTAL

Chemistry.

All chemicals used for synthesis were obtained from commercial suppliers and used without prior purification. ^1H NMR, ^{13}C NMR, and 2D-NMR spectra were recorded using either a 600 MHz Bruker Avance III HD instrument equipped with a cryogenically cooled 5 mm dual probe or a 400 MHz Bruker Avance III instrument equipped with a 5 mm broad band probe. Samples were dissolved in either DMSO- d_6 (VWR Chemicals, 99.80% D) or CDCl_3 (Cambridge Isotope Laboratories, Inc., 99.8% D) and analyzed at 300 K. TLC analyses were performed using TLC silica gel 60 F₂₅₄ aluminum plates (Merck). LC-MS mass spectra were obtained with an Agilent 6410 Triple Quadrupole Mass Spectrometer instrument using electron spray ionization (ESI) coupled to an Agilent 1200 HPLC system (ESI-LC-MS) with a C18 reverse phase column (Zorbax Eclipse XBD-C18, 4.6 mm × 50 mm), autosampler and diode array detector, using a linear gradient of the binary solvent system of buffer A (milliQ H₂O:MeCN:formic acid, 95:5:0.1 v/v%) to buffer B (milliQ H₂O:MeCN:formic acid, 5:95:0.043 v/v%) with a flow rate of 1 mL/min. During ESI-LC-MS analysis, evaporative light scattering (ELS) traces were obtained with a Sedere Sedex 85 Light Scattering Detector. Normal phase column chromatography was carried out using prepacked RediSep Rf silica flash cartridges on a CombiFlash[®] Rf+ apparatus. Preparative reverse phase HPLC was performed using an Agilent 1200 series HPLC preparative system with an Agilent Zorbax 300-SB-C18 column (21.2 × 250 mm). Microwave-assisted synthesis was carried out using a Biotage[®] Initiator+ apparatus. Hydrogenation reactions were performed on a H-Cube mini plus continuous hydrogenation apparatus (ThalesNano) using disposable catalyst cartridges preloaded with the required heterogeneous catalyst. All final compounds showed ≥95% purity by NMR and LC-MS. Exact concentrations of DMSO stocks for assay testing were determined by qHNMR, as previously described.³³

Synthesis of 1a–6f (The deconstruction fragment library)

Thirty fragments (1a, 1e, 1f, 1i, 1s, 2a-c, 2e, 2g, 2j, 2k, 2n, 2p, 3a-c, 3i, 3j, 4b, 5a-e, 6a-d, 6f) were available in-house. The remaining 47 fragments were synthesized as described below.

General procedure A: Conventional *N*-sulfonylation. A flask was charged with the aryl amine (1.0 equiv., 2.5 mmol), pyridine (1.5 equiv.), DCM (0.5 M) and then the sulfonyl chloride (1.1–1.2 equiv.). The mixture was stirred at RT for 3–21 h until complete conversion (as determined by TLC). The mixture was then added water (4 mL/mmol) and the aqueous phase extracted with DCM (3 x 2 mL/mmol). The combined organic phases were dried over Na₂SO₄ and concentrated in vacuo. Purification by flash column chromatography afforded the pure sulfonamides.

General procedure B: MW-assisted *N*-sulfonylation. A microwave vial was charged with the aryl amine (1.0 equiv., 1.0–5.0 mmol), pyridine (2.0 equiv.), DCM (0.2–1.0 M) and then the benzenesulfonyl chloride (1.0–2.0 equiv.). The vial was capped and subjected to microwave irradiation at 50 °C for 5–20 min until complete conversion (as determined by TLC). The mixture was then added 2 M HCl (10 mL/mmol), extracted with DCM (2–3 times with 10 mL/mmol), and the combined organic phases dried over Na₂SO₄ and concentrated in vacuo. Purification by flash column chromatography afforded the pure sulfonamides.

General procedure C: Pd-catalyzed nitro group reduction. A flask was charged with the nitro compound (1.0 equiv., 0.5 mmol) and MeOH or THF (0.1–1.0 M). The flask was evacuated and back-filled with nitrogen, and this was repeated twice more. Then 5 % Pd/C (30 w/w%) was added. The flask was evacuated and back-filled with nitrogen, and this was repeated twice more. Then the flask was evacuated and back-filled with hydrogen (balloon). The mixture was stirred under hydrogen at RT until complete conversion (as determined by TLC). The mixture was then filtered through a bed of celite, the bed further washed with DCM and the combined filtrated concentrated in vacuo.

General Procedure D: Selective O-Alkylation. A stirred solution of 2-amino-3-nitrophenol (68) (1.0 equiv.) in DMF (5–10 mL) was treated with potassium carbonate (1.2 equiv.) and alkylating agent (1.2 equiv.). After 18 h the mixture was poured into water. If no precipitation, the reaction mixture was extracted with EtOAc (25 mL) and washed with water (3 x 25 mL). The combined organic layer was dried over Na₂SO₄, concentrated in vacuo, and purified by flash column chromatography (Hep:EtOAc).

General Procedure E: Reduction of Aromatic Nitro Group. To a solution of the nitroaniline (1.0 equiv.) in EtOH (20–35 mL) SnCl₂·2H₂O (4.0 equiv.) was added. Then the reaction mixture was stirred at 75 °C for 1–3 h and the solvent was adjusted to pH = 14 using 40% NaOH. The reaction mixture was extracted with EtOAc (3 x 25 mL). The combined organic layer was dried over Na₂SO₄, concentrated in vacuo, and purified by flash column chromatography (Hep:EtOAc).

General Procedure F: Triazole Formation. To the 1,2-diamine (1.0 equiv.) in 10% H₂SO₄ (10–15 mL) at 0 °C, NaNO₂ (1.4 equiv.) was added in smaller portions over 20 min. After that the reaction was stirred for 30 min. The residue was diluted with water (35 mL) and washed with EtOAc (2 x 30 mL), washed with brine (30 mL), dried over Na₂SO₄, was concentrated in vacuo, and purified by flash column chromatography (Hep:EtOAc).

***N*-(Naphthalen-1-yl)methanesulfonamide (1b).** The general procedure A was followed starting from 1-aminonaphthalene (0.36 g, 2.50 mmol) and mesyl chloride (0.21 mL, 2.75 mmol). Complete conversion was seen after 3 h, and purification afforded **1b** as a white powder (0.28 g, 1.25 mmol, 50 %). ¹H NMR (400 MHz, DMSO-d₆) δ 9.71 (s, 1H), 8.29 – 8.23 (m, 1H), 7.98 – 7.92 (m, 1H), 7.89 – 7.82 (m, 1H), 7.62 – 7.48 (m, 4H), 3.02 (s, 3H). ¹³C NMR (101 MHz, DMSO-d₆) δ 133.97, 132.91, 129.51, 127.99, 126.60, 126.26, 125.67, 123.33, 123.19, 39.89. LC-MS (ESI): m/z 220.6 [M-1]⁻, t_R = 4.02 min, purity > 95% (UV).

***N*-(Naphthalen-1-yl)benzenesulfonamide (1c).** The general procedure A was followed starting from 1-aminonaphthalene (0.36 g, 2.50 mmol) and benzenesulfonyl chloride (0.36 mL, 2.75 mmol). Complete conversion was seen after 3 h, and purification afforded **1c** as a white solid (0.54 g, 3.70 mmol, 69 %). ¹H NMR (400 MHz, DMSO-d₆) δ 10.23 (s, 1H), 8.00 (dd, J = 8.5, 1.2 Hz, 1H), 7.88 (dd, J = 8.0, 1.3 Hz, 1H), 7.78 (dd, J = 8.4, 1.1 Hz, 1H), 7.75 – 7.64 (m, 2H), 7.64 – 7.55 (m, 1H), 7.55 – 7.35 (m, 5H), 7.16 (dd, J = 7.4, 1.2 Hz, 1H). ¹³C NMR (101 MHz, DMSO-d₆) δ 140.02, 133.82, 132.67, 132.29, 129.34, 129.08, 127.89, 126.69, 126.62, 126.14, 125.96, 125.42, 123.19, 123.01. LC-MS (ESI): m/z 283.1 [M-1]⁻, t_R = 5.10 min, purity > 95% (UV).

Naphthalen-1-ylglycine (1d). To a solution of 1-aminonaphthalene (0.29 g, 2.00 mmol) in MeOH (25.0 mL) cooled to 0 °C were added NaOAc (0.33 g, 4.00 mmol), glacial acetic acid (0.46 mL, 8.00 mmol), glyoxylic acid monohydrate (0.28 g, 3.00 mmol) and NaCNBH₃ (0.13 g, 2.00 mmol). The solution was slowly allowed to reach RT over 4 h. Upon complete conversion, the mixture was filtered through a plug of celite and the filtrate concentrated in vacuo. Purification by preparative HPLC afforded **1d** as a green-grey crystalline solid (0.054 g, 0.27 mmol, 13 %). ¹H NMR (400 MHz, DMSO-d₆) δ 8.15 – 8.08 (m, 1H), 7.81 – 7.74 (m, 1H), 7.43 (m, 2H), 7.30 – 7.23 (m, 1H), 7.14 (d, J = 8.1 Hz, 1H), 6.35 (dd, J = 7.6, 1.0 Hz, 1H), 3.98 (s, 2H). ¹³C NMR (101 MHz, DMSO-d₆) δ 172.57, 143.53, 133.95, 127.96, 126.61, 125.63, 124.14, 122.90, 121.35, 115.95, 103.04, 44.89. LC-MS (ESI): m/z 200.6 [M-1]⁻, t_R = 4.06 min, purity > 95% (UV).

N-(o-Tolyl)methanesulfonamide (1g). The general procedure A was followed starting from o-toluidine (0.27 mL, 2.50 mmol) and mesyl chloride (0.21 mL, 2.75 mmol). Complete conversion was seen after 3 h, and purification afforded **1g** as a white solid (0.35 g, 1.90 mmol, 76 %). ¹H NMR (400 MHz, DMSO-d₆) δ 9.02 (s, 1H), 7.31 – 7.11 (m, 4H), 2.97 (s, 3H), 2.31 (s, 3H). ¹³C NMR (101 MHz, DMSO-d₆) δ 135.47, 134.00, 130.81, 126.46, 126.21, 126.07, 40.06, 18.05. LC-MS (ESI): m/z 184.4 [M-1]⁻, t_R = 3.43 min, purity > 95% (UV).

N-(2,3-Dimethylphenyl)methanesulfonamide (1h). The general procedure A was followed starting from 2,3-dimethylaniline (0.31 mL, 2.50 mmol) and mesyl chloride (0.21 mL, 2.75 mmol). Complete conversion was seen after 21 h, and purification afforded **1h** as a white solid (0.45 g, 2.20 mmol, 90 %). ¹H NMR (400 MHz, DMSO-d₆) δ 9.00 (s, 1H), 7.14 – 7.05 (m, 3H), 2.93 (s, 3H), 2.25 (s, 3H), 2.20 (s, 3H). ¹³C NMR (101 MHz, DMSO-d₆) δ 137.67, 135.19, 133.64, 127.99, 125.59, 124.67, 39.81, 20.20, 14.45. LC-MS (ESI): m/z 198.6 [M-1]⁻, t_R = 3.79 min, purity > 95% (UV).

***N*-(4-Aminophenyl)methanesulfonamide (1j).** The compound was synthesized in two steps. For step 1, the general procedure A was followed starting from 4-nitroaniline (0.35 g, 2.50 mmol) and mesyl chloride (0.23 mL, 3.20 mmol). Complete conversion was seen after 48 h, and purification afforded *N*-(4-nitrophenyl)methanesulfonamide (**1j-I1**) as a yellow solid (0.22 g, 1.00 mmol, 42 %). ¹H NMR (400 MHz, DMSO-d₆) δ 10.72 (s, 1H), 8.29 – 8.15 (m, 2H), 7.44 – 7.31 (m, 2H). ¹³C NMR (101 MHz, DMSO-d₆) δ 144.93 , 142.18 , 125.45 , 117.50 , 39.64. LC-MS (ESI): m/z 215.6 [M-1]⁻, t_R = 3.48 min, purity > 95% (UV). For step 2, the general procedure C was followed starting from **1j-I1** (0.10 g, 0.46 mmol) in THF (10 mL). Complete conversion was seen after 4 h, and workup afforded **1j** as a buff-colored powder (0.085 g, 0.46 mmol, 99 %). ¹H NMR (400 MHz, DMSO-d₆) δ 8.89 (s, 1H), 6.93 – 6.85 (m, 2H), 6.55 – 6.47 (m, 2H), 5.01 (s, 2H), 2.80 (s, 3H). ¹³C NMR (101 MHz, DMSO-d₆) δ 146.66, 125.97, 124.78, 114.08, 38.16. Two other signals under DMSO-peak (HSQC). LC-MS (ESI): m/z 187.1 [M-1]⁻, t_R = 0.77 min, purity > 95% (UV).

4-Methoxybenzenesulfonamide (1k). A solution of 4-methoxybenzenesulfonyl chloride (1.00 g, 4.84 mmol) in acetone (2.0 mL) was added to 25% aqueous ammonia (9.68 mL), and the solution stirred at RT for 22 h. Upon complete conversion, the reaction mixture was quenched with 2 M HCl and extracted with EtOAc. The organic phase was dried over MgSO₄, filtered and concentrated in vacuo. Purification by flash chromatography afforded **1k** as a white solid (0.10 g, 0.53 mmol, 11 %). ¹H NMR (400 MHz, Chloroform-d) δ 7.84–7.74 (m, 2H), 6.67–6.87 (m, 2H), 4.60 (s, 2H), 3.81 (s, 3H). ¹³C NMR (101 MHz, Chloroform-d) δ 162.51, 136.94, 128.66, 114.26, 55.65.

((4-Methoxyphenyl)sulfonyl)glycine (1l). A solution of glycine (0.15 g, 2.00 mmol) and NaHCO₃ (0.42 g, 5.00 mmol) in water (3.0 mL) was heated at 80 °C till complete dissolution and then added 4-methoxybenzenesulfonyl chloride (0.41 g, 2.00 mmol). The mixture was stirred at 80 °C for 2 h. Upon complete conversion, the reaction mixture was neutralized to pH 1 with 2 M HCl, extracted with EtOAc (2 x 20 mL), and the combined organic phases concentrated in vacuo. Purification by preparative HPLC afforded **1l** as a white solid (0.040 g, 0.16 mmol, 8 %). ¹H NMR (400 MHz, DMSO-d₆) δ 12.63 (s, 1H), 7.84 (t, J = 6.1 Hz, 1H), 7.77 – 7.66 (m, 2H), 7.15 – 7.03 (m, 2H), 3.83 (s, 3H), 3.53 (d, J = 6.1 Hz, 2H). ¹³C NMR (101 MHz, DMSO-d₆) δ 170.20, 162.09, 132.28, 128.66, 114.16, 55.59, 43.74. LC-MS (ESI): m/z 244.0 [M-1]⁻, t_R = 2.30 min, purity > 95% (UV).

N-Phenylbenzenesulfonamide (1m). The general procedure B was followed starting from aniline (0.46 mL, 5.00 mmol) and benzenesulfonyl chloride (0.96 mL, 7.50 mmol). Complete conversion was seen after 10 min by TLC (R_f 0.56, hep:EtOAc 1:1), and purification afforded **1m** as a white solid (1.10 g, 4.70 mmol, 94%). ¹H NMR (400 MHz, DMSO-d₆) δ 10.26 (s, 1H), 7.84 – 7.69 (m, 2H), 7.64 – 7.57 (m, 1H), 7.57 – 7.50 (m, 2H), 7.26 – 7.17 (m, 2H), 7.12 – 7.05 (m, 2H), 7.05 – 6.97 (m, 1H). ¹³C NMR (101 MHz, DMSO-d₆) δ 139.49, 137.63, 132.82, 129.19, 129.10, 126.59, 124.05, 120.04. LC-MS (ESI): m/z 232.4 [M-1]⁻, t_R = 2.16 min, purity > 95% (UV).

N-(4-Aminophenyl)benzenesulfonamide (1n). The compound was synthesized in two steps. For step 1, the general procedure A was followed starting from 4-nitroaniline (1.38 g, 9.99 mmol) and benzenesulfonyl chloride (1.40 mL, 11.0 mmol). Complete conversion was seen after 24 h, and workup afforded *N*-(4-nitrophenyl)benzenesulfonamide (**1n-11**) as a yellow solid (0.28 g, 9.94 mmol, quantitative). ¹H NMR (400 MHz, DMSO-d₆) δ 11.28 (s, 1H), 8.17–8.09 (m, 2H), 7.91–7.85 (m, 2H), 7.69–7.57 (m, 3H), 7.36–7.28 (m, 2H). ¹³C NMR (101 MHz, DMSO-d₆) δ 144.11, 142.58, 138.96, 133.54, 129.58, 126.67, 125.34, 117.98. For step 2, a solution of

1n-11 (1.39 g, 5.00 mmol) and iron powder (1.40 g, 25.0 mmol) in EtOH (30.0 mL) heated at 55 °C was added a solution of NH₄Cl (0.13 g, 2.50 mmol) in water (15.0 mL), and the mixture stirred at 90 °C for 15 h. Upon complete conversion, the mixture was filtered hot, and the filtrate concentrated in vacuo. The residue was diluted with water (15 mL), basified with saturated aqueous NaHCO₃ to pH 7 and extracted with EtOAc (3 x 20 mL). The combined organic phases were dried over MgSO₄, filtered and concentrated in vacuo. Purification by flash chromatography afforded **1n** as a white solid (0.37 g, 1.50 mmol, 30%). ¹H NMR (400 MHz, DMSO-d₆) δ 9.45 (s, 1H), 7.65–7.62 (m, 2H), 7.54–7.49 (m, 2H), 6.66 (m, 2H), 6.40–6.35(m, 2H), 4.94 (s, 2H). ¹³C NMR (101 MHz, DMSO-d₆) δ 146.52, 139.72, 132.36, 128.87, 126.69, 125.20, 124.64, 113.91.

N-(o-Tolyl)benzenesulfonamide (1o). The general procedure A was followed starting from o-toluidine (0.27 mL, 2.50 mmol) and benzenesulfonyl chloride (0.49 g, 2.75 mmol). Complete conversion was seen after 3 h, and purification afforded **1o** as a white solid (0.63 g, 2.50 mmol, quantitative). ¹H NMR (400 MHz, DMSO-d₆) δ 9.54 (s, 1H), 7.63 (m, 3H), 7.58 – 7.48 (m, 2H), 7.15 – 7.03 (m, 3H), 6.95 (dd, J = 5.3, 3.4 Hz, 1H), 1.96 (s, 3H). ¹³C NMR (101 MHz, DMSO-d₆) δ 140.55, 134.74, 134.11, 132.65, 130.67, 129.12, 126.47, 126.42, 126.40, 126.27, 17.49. LC-MS (ESI): m/z 246.8 [M-1]⁻, t_R = 4.75–4.90 min, purity > 95% (UV).

N-(2,3-Dimethylphenyl)benzenesulfonamide (1p). The general procedure A was followed starting from 2,3-dimethylaniline (0.31 mL, 2.50 mmol) and benzenesulfonyl chloride (0.49 g, 2.75 mmol). Complete conversion was seen after 21 h, and purification afforded **1p** as a white solid (0.57 g, 2.20 mmol, 87 %). ¹H NMR (400 MHz, DMSO-d₆) δ 9.51 (s, 1H), 7.63 (m, 3H), 7.54 (m, 2H), 7.05 – 6.98 (m, 1H), 6.94 (t, J = 7.7 Hz, 1H), 6.69 (dd, J = 7.9, 1.4 Hz, 1H), 2.16 (s, 3H), 1.92 (s, 3H). ¹³C NMR (101 MHz, DMSO-d₆) δ 140.46, 137.50, 134.51, 133.65, 132.56,

129.04, 128.07, 126.56, 125.35, 124.70, 20.10, 13.93. LC-MS (ESI): m/z 261.0 [M-1], t_R = 5.09 min, purity > 95% (UV).

4-Methoxy-*N*-phenylbenzenesulfonamide (1q). A solution of 4-methoxybenzenesulfonyl chloride (1.65 g, 4.0 mmol) in dry DCM (25 mL) was added dropwise to a solution of aniline (0.80 mL, 4.40 mmol) and pyridine (1.0 mL) in dry DCM (15 mL) and the mixture stirred at RT overnight. Upon reaction completion, the mixture was poured into water (500 mL) and extracted with DCM (150 mL). The organic phase was washed with 2 M HCl (2 x 30 mL), saturated aqueous Na₂CO₃ (30 mL) and sat. brine (30 mL), dried over MgSO₄, filtered and concentrated in vacuo. Recrystallization from methanol afforded **1q** as an off-white solid (0.20 g, 0.76 mmol, 19 %). ¹H NMR (400 MHz, Chloroform-d) δ 7.71–7.66 (m, 2H), 7.24 (dd, J = 7.0, 1.5 Hz, 2H), 7.14–7.09 (m, 1H), 7.06–7.02 (m, 2H), 6.90–6.86 (m, 2H), 6.37 (s, 1H), 3.83 (s, 3H). ¹³C NMR (101 MHz, Chloroform-d) δ 163.12, 136.51, 130.68, 129.41, 129.33, 125.45, 121.81, 114.15, 55.57.

4-Methoxy-*N*-(*o*-tolyl)benzenesulfonamide (1r). The general procedure A was followed starting from *o*-toluidine (0.27 mL, 2.50 mmol) and 4-methoxybenzenesulfonyl chloride (0.57 g, 2.75 mmol). Complete conversion was seen after 14 h, and purification afforded **1r** as an off-white solid (0.61 g, 2.20 mmol, 89 %). ¹H NMR (400 MHz, DMSO-d₆) δ 9.38 (s, 1H), 7.62 – 7.53 (m, 2H), 7.18 – 7.03 (m, 5H), 7.01 – 6.94 (m, 1H), 3.82 (s, 3H), 2.01 (s, 3H). ¹³C NMR (101 MHz, DMSO-d₆) δ 162.26, 134.97, 133.94, 132.26, 130.64, 128.69, 126.24, 126.22, 114.21, 55.60, 17.58. LC-MS (ESI): m/z 277.0 [M-1], t_R = 4.90 min, purity > 95% (UV).

***N*-(4-Aminonaphthalen-1-yl)methanesulfonamide (1t)**. The compound was synthesized in two steps. For step 1, the general procedure C was followed starting from 4-nitronaphthalen-1-amine (0.75 g, 4.00 mmol) in THF (50 mL). Complete conversion was seen after 24 h, and workup afforded naphthalene-1,4-diamine (**1t-I1**) as a dark-green solid (0.63 g, 4.00 mmol, quantitative). ¹H NMR (400 MHz, DMSO-d₆) δ 7.95–7.89 (m, 2H), 7.36–7.30 (m, 2H), 6.53 (s, 2H), 4.75 (s, 4H). For step 2, a solution of **1t-I1** (0.34 g, 2.15 mmol) in THF (10 mL) cooled to 0 °C was added mesyl chloride (0.15 mL, 1.94 mmol) and Na₂CO₃ (0.33 g, 3.07 mmol), and the mixture stirred under nitrogen at 0 °C for 19 h. Upon reaction completion, the mixture was diluted with petroleum ether (20 mL), filtered, and the filter cake washed with 2 M HCl. Recrystallization from MeCN afforded **1t** as a brown powder (0.045 g, 0.19 mmol, 10 %). ¹H NMR (400 MHz, DMSO-d₆) δ 9.09 (s, 1H), 8.13–7.95 (m, 2H), 7.48 (ddd, J = 8.4, 6.7, 1.3 Hz, 1H), 7.40 (ddd, J = 8.1, 6.7, 1.4 Hz, 1H), 7.20 (d, J = 8.0 Hz, 1H), 6.64 (d, J = 8.0 Hz, 1H), 5.85 (s, 2H), 2.91 (s, 3H). ¹³C NMR (101 MHz, DMSO-d₆) δ 142.93, 131.44, 127.35, 127.02, 125.60, 124.11, 122.80, 121.89, 121.73, 108.97, 39.82.

***N,N'*-(Naphthalene-1,4-diyl)dimethanesulfonamide (1u)**. The compound is synthesized in two steps. 4-Nitronaphthalen-1-amine (250.0 mg, 1.33 mmol) was dissolved in THF (15 mL) and placed under nitrogen. Pd/C (5% w/w; 84.8 mg, 0.80 mmol) was added and the atmosphere was replaced with hydrogen. The resulting mixture was stirred at under an atmosphere of hydrogen for 21 h. After 21 h the reaction mixture was purged with nitrogen. The reaction mixture was filtered through celite and the filter washed with DCM. The filtrate was concentrated in vacuo to afford **1u-I1** as yellow crystals (217 mg, quantitative). LC-MS (ESI): m/z 159.2 [M+1]⁺, purity > 95% (UV). To a solution of naphthalene-1,4-diamine **1u-I1** (217.0 mg, 1.37 mmol) in dry toluene (20 mL) was added methylsulfonyl chloride (0.24 mL, 3.15 mmol) and pyridine (0.33 mL, 4.12 mmol). The flask was mounted with a condenser which was closed with a rubber septum. The flask was evacuated and backfilled

with nitrogen; this was repeated two more times. The reaction mixture was then stirred at 100 °C under nitrogen for 3 hours and then stirred at RT for an additional 3 days. The reaction was monitored by TLC and LC-MS. The cooled reaction mixture was then evaporated in vacuo. The solid residue was added additional toluene (20 mL) and evaporated in vacuo. This procedure was repeated once more. The solid residue was redissolved in EtOAc (20 mL) and washed with water (2 x 20 mL) and 2 M HCl (2 x 20 mL). The organic phase was dried over Na₂SO₄ and concentrated in vacuo. Purification by flash chromatography and two times preparative HPLC afforded **1u** as a white solid (yield not determined). LC-MS: MS (ESI) m/z 313.0 [M-1]⁻. ¹H NMR (600 MHz, DMSO-d₆) δ 8.26 (s, 2H), 7.58 (s, 2H), 7.44 (s, 2H), 3.00 (s, 6H).

***N*-(4-Aminonaphthalen-1-yl)benzenesulfonamide (1v)**. A solution of **1t-I1** (0.34 g, 2.15 mmol) in THF (10 mL) cooled to 0 °C was added benzenesulfonyl chloride (0.25 mL, 1.94 mmol) and Na₂CO₃ (0.33 g, 3.07 mmol), and the mixture stirred under nitrogen at 0 °C for 19 h. Upon reaction completion, the mixture was diluted with petroleum ether (20 mL), filtered, and the filter cake washed with 2 M HCl. Recrystallization from MeCN afforded **1v** as a dark brown solid (0.21 g, 0.69 mmol, 32%). ¹H NMR (600 MHz, DMSO-d₆) δ 9.57 (s, 1H), 8.02–7.96 (m, 1H), 7.85–7.79 (m, 1H), 7.65–7.60 (m, 2H), 7.60–7.55 (m, 1H), 7.51–7.46 (m, 2H), 7.35–7.26 (m, 2H), 6.69 (d, J = 8.0 Hz, 1H), 6.46 (d, J = 8.0 Hz, 1H), 5.79 (s, 2H). ¹³C NMR (101 MHz, DMSO-d₆) δ 142.81, 138.78, 130.70, 130.01, 127.25, 125.15, 124.86, 123.88, 122.08, 121.79, 121.08, 126.69, 118.09, 104.62.

***N*-(4-Aminonaphthalen-1-yl)-4-methoxybenzenesulfonamide (1w)**. In a round-bottomed flask, 4-nitronaphthalen-1-amine (100.0 mg, 0.53 mmol) and 4-methoxybenzenesulfonyl chloride (131.8 mg, 0.64 mmol) was dissolved in THF (6 mL) and pyridine (2.0 mL). The stirring mixture was brought to reflux and stirred for five days. Upon reaction completion, the reaction mixture was concentrated under vacuum, taken up in

EtOAc (6 mL), and washed with HCl (2 M, 6 mL) and water (2 x 6 mL). The organic fraction was dried over Na₂SO₄, filtered, and dried under vacuo. The resulting solid was washed with ether (2 x 3 mL) and recrystallized from toluene to yield 4-methoxy-*N*-(4-nitronaphthalen-1-yl)benzenesulfonamide **1w-I1** as a white solid (109.0 mg, 57%). LC-MS: MS (ESI) *m/z* 359.1 [M+1]⁺. *N*-(4-aminonaphthalen-1-yl)-4-methoxybenzenesulfonamide **1w-I1** (50.0 mg, 0.14 mmol) was dissolved in EtOH (25 mL) and AcOH (5 mL) and filtrated. The compound was reduced by H-Cube (50 bar, 1 mL/min and RT, 10% Pd/C). The reaction mixture was evaporated and dried. Purification by two times preparative HPLC afforded **1w** as a white solid (22 mg, 48%). LC-MS: MS (ESI) *m/z* 329.1 [M+1]⁺. ¹H NMR (600 MHz, DMSO-*d*₆) δ 9.46 (s, 1H), 8.02 – 7.97 (m, 1H), 7.94 – 7.86 (m, 1H), 7.59 – 7.51 (m, 2H), 7.40 – 7.32 (m, 2H), 7.06 – 6.96 (m, 2H), 6.72 (d, *J* = 8.0 Hz, 1H), 6.53 (s, 1H), 3.79 (s, 4H).

***N*-(4-Aminonaphthalen-1-yl)-*N*-(phenylsulfonyl)glycine (1x).** The compound was synthesized in 4 steps. For step 1, a solution of 4-nitronaphthalen-1-amine (0.25 g, 1.40 mmol), benzenesulfonyl chloride (0.41 mL, 1.20 mmol) and pyridine (1.0 mL) in THF (3.0 mL) was stirred at reflux for 12 h. Upon reaction completion, the mixture was concentrated in vacuo, retaken in EtOAc (5 mL), and the solution washed with 2 M HCl (5 mL) and water (2 x 5 mL). The organic phase was concentrated in vacuo. Purification by flash chromatography afforded *N*-(4-nitronaphthalen-1-yl)benzenesulfonamide (**1x-I1**) as a yellow solid (0.26 g, 0.79 mmol, 57%). ¹H NMR (400 MHz, DMSO-*d*₆) δ 10.93 (s, 1H), 8.38 (d, *J* = 8.7 Hz, 1H), 8.25 (dd, *J* = 10.1, 8.3 Hz, 2H), 7.83 – 7.73 (m, 3H), 7.69 – 7.58 (m, 2H), 7.54 (dd, *J* = 8.4, 6.9 Hz, 2H), 7.42 (d, *J* = 8.4 Hz, 1H). For step 2, a solution of **1x-I1** (0.25 g, 0.76 mmol) and K₂CO₃ (0.32 g, 2.28 mmol) in NMP (2.0 mL) was stirred at 85 °C for 30 min, before ethyl bromoacetate (0.15 mL, 1.37 mmol) was added. The mixture was stirred at 85 °C for an additional 30 min. Upon reaction completion, the mixture was poured into ice water (20 mL), extracted with EtOAc (3 x 15 mL), and the combined organic phases washed with 2 M HCl (10 mL), water (2 x 15 mL) and sat. brine (15 mL). The

organic phase was dried over Na₂SO₄, filtered and concentrated in vacuo to afford ethyl *N*-(4-nitronaphthalen-1-yl)-*N*-(phenylsulfonyl)glycinate (**1x-I2**) as an orange oil (0.31 g, 0.76 mmol, quantitative). ¹H NMR (400 MHz, DMSO-d₆) δ 8.33 – 8.21 (m, 3H), 7.82 (ddd, J = 8.4, 6.8, 1.3 Hz, 1H), 7.78 – 7.69 (m, 5H), 7.65 – 7.57 (m, 2H), 7.39 (d, J = 8.2 Hz, 1H), 4.72 – 4.54 (m, 2H), 4.21 – 4.11 (m, 2H), 4.10 – 3.97 (m, 3H), 1.20 (q, J = 7.3 Hz, 2H), 1.09 (t, J = 7.1 Hz, 3H). For step 3, a solution of **1x-I2** (0.31 g, 0.76 mmol) and SnCl₂·2H₂O (1.37 g, 6.09 mmol) in EtOH (9 mL) was stirred at reflux for 1 h. Upon reaction completion the mixture was concentrated in vacuo, and the residue basified with sat. Na₂CO₃ to pH 9 and extracted with EtOAc (50 mL). The organic phase was washed with water (3 x 25 mL) and saturated brine (25 mL), dried over Na₂SO₄, filtered and concentrated in vacuo to afford ethyl *N*-(4-aminonaphthalen-1-yl)-*N*-(phenylsulfonyl)glycinate (**1x-I3**) as a white to grey solid (0.11 g, 0.29 mmol, 40 %). ¹H NMR (400 MHz, DMSO-d₆) δ 8.09 – 8.01 (m, 1H), 7.99 – 7.91 (m, 1H), 7.75 – 7.63 (m, 3H), 7.56 (dd, J = 8.3, 7.1 Hz, 2H), 7.47 – 7.37 (m, 2H), 6.85 (d, J = 8.1 Hz, 1H), 6.61 (d, J = 8.1 Hz, 1H), 4.53 (d, J = 17.5 Hz, 1H), 4.38 (d, J = 17.5 Hz, 1H), 4.07 – 3.95 (m, 3H), 1.08 (t, J = 7.1 Hz, 3H). For step 4, a solution of **1x-I3** (0.038 g, 0.10 mmol) and NaOH (0.40 g, 10.0 mmol) in 1:1 MeOH:water (7 mL) was stirred at reflux for 2 h. Upon reaction completion, the mixture was concentrated in vacuo. Purification by preparative HPLC afforded **1x** as a light pink solid (yield not determined). LC-MS (ESI): m/z 355.1 [M-1]⁻, t_R = 3.07 min, purity > 95% (UV). ¹H NMR (400 MHz, DMSO-d₆) δ 8.09 (dd, J = 7.9, 1.8 Hz, 1H), 8.02 – 7.96 (m, 1H), 7.81 – 7.74 (m, 2H), 7.63 – 7.56 (m, 1H), 7.49 (t, J = 7.7 Hz, 2H), 7.40 – 7.28 (m, 2H), 6.90 (d, J = 8.1 Hz, 1H), 6.39 (d, J = 8.2 Hz, 1H), 5.79 (s, 2H), 4.07 (d, J = 16.2 Hz, 1H), 3.76 (d, J = 16.3 Hz, 1H). ¹³C NMR (101 MHz, DMSO-d₆) δ 170.76, 144.84, 140.14, 132.84, 132.07, 128.43, 127.73, 124.84, 123.46, 122.88, 122.08, 105.93, 39.20, 38.98.

1-(Piperidin-1-yl)ethan-1-one (2d). To a solution of piperidine (0.58 mL, 5.87 mmol) in DCM (3 mL) at 0°C was added anhydride acetic (0.28 mL, 2.94 mmol). The reaction mixture was allowed to warm up to RT and was

stirred for 24 h. The solution was transferred to a separation funnel and was washed with 1M HCl. The organic layer was dried with Na₂SO₄, filtered, and concentrated under reduced pressure to afford **2d** as colorless oil (397 mg, 52%). ¹H NMR (600 MHz, DMSO-d₆) δ 3.40 – 3.36 (m, 2H), 3.35 (m, 2H), 1.96 (s, 3H), 1.56 (dddd, J = 9.1, 5.3, 4.2, 2.1 Hz, 2H), 1.50 – 1.45 (m, 2H), 1.42 – 1.36 (m, 2H). ¹³C NMR (151 MHz, DMSO-d₆) δ 167.81, 46.68, 41.64, 26.01, 25.27, 24.01, 21.29.

N,N-Dimethylcyclohexanecarboxamide (2f). Dimethylamine (0.76 mL, 15.0 mmol) was added to a solution of cyclohexanecarbonyl chloride (0.67 mL, 5.0 mmol) with triethylamine (2.2 mL, 15.0 mmol) in DCM (25 mL). The mixture reaction was left stirring at RT for 2 h. The reaction mixture was quenched by addition of water. The desired amide was extracted DCM (3 x 10 mL). Successively, the combined organic layers were washed with water (2 x 15 mL), saturated sodium carbonate solution (2 x 15 mL), brine (2 x 15 mL). Then, it was dried over MgSO₄, filtered, and concentrated in vacuo. The crude was purified by flash chromatography (heptane:EtOAc) to afford **2f** (615 mg, 79%). LC-MS: MS (ESI) m/z 156.3 (M+H)⁺. ¹H NMR (400 MHz, CDCl₃): δ 3.03 (s, 1H), 2.92 (s, 1H), 2.48 (tt, J = 11.6 Hz and J = 3.4 Hz, 1H), 1.64–1.85 (m, 5H), 1.33–1.45 (m, 2H), 1.17–1.33 (m, 3H). ¹³C NMR (100 MHz, CDCl₃): δ 176.1, 40.7, 37.1, 35.5, 29.2, 25.9, 25.8.

1-(2-(Dimethylamino)ethyl)pyrrolidine-2,5-dione (2h). Succinic anhydride (200 mg, 2.0 mmol) and 2-dimethylaminoethylamine (0.22 mL, 2.0 mmol) were taken together and heated at 125 °C with stirring for 15 min and cooled to RT. The obtained blue mixture was washed with ETOH and concentrated in vacuo. The crude was purified by preparative HPLC to afford **2h** (186 mg, 53%). LC-MS: MS (ESI) m/z 171.2 (M+H)⁺. ¹H NMR (400 MHz, CDCl₃): δ 3.87 (t, J = 5.4 Hz, 2H), 3.30 (t, J = 5.6 Hz, 2H), 2.88 (s, 6H), 2.79 (s, 4H). ¹³C NMR (100 MHz, CDCl₃): δ 178.1, 54.5, 43.0, 33.6, 28.4.

2-(2-(Dimethylamino)ethyl)isoindoline-1,3-dione (2i). Phthalic anhydride (741 mg, 5 mmol) and 2-dimethylaminoethylamine (0.27 mL, 2.5 mmol) were mixed and heated at 135 °C for 60 min and cooled to RT. The crude was purified by flash chromatography (DCM:MeOH) to afford **2i** (18 mg, 3.3%). LC-MS: MS (ESI) m/z 219.2 (M+H)⁺. ¹H NMR (400 MHz, CDCl₃): δ 7.86–7.80 (m, 2H), 7.73–7.67 (m, 2H), 3.81 (t, J = 6.56 Hz, 2H), 2.60 (t, J = 6.64 Hz, 2H), 2.29 (s, 6H). ¹³C NMR (100 MHz, CDCl₃): δ 167.4, 132.8, 131.2, 122.2, 56.1, 44.5, 34.9.

2-(Piperidin-2-ylmethyl)isoindoline-1,3-dione (2l). *N*-Boc protected methylamino-1,2,3,4-tetrahydroisoquinoline (214 mg, 1.0 mmol) was dissolved in toluene (3 mL) and phthalic anhydride (296 mg, 2.0 mmol) was added and stirred at 50 °C for 3 h, then heated at 80 °C up to 24 h. Then pure TFA (2.5 mL) was added dropwise. The mixture was left stirring for 2 h. The mixture reaction was concentrated under pressure. The mixture was diluted with DCM and the pH was neutralized by potassium bicarbonate, extracted with DCM (3 x 10 mL), dried over MgSO₄, and concentrated in vacuo. The crude was purified by preparative HPLC to afford **2l** (not determined). LC-MS: MS (ESI) m/z 245.3 (M+H)⁺.

Cyclohexyl(piperidin-1-yl) methanone (2o). Cyclohexanecarbonyl chloride (0.41 mL, 3.41 mmol) was added in one portion to a solution of the piperidine (0.58 mL, 3.75 mmol), TEA (0.60 mL, 4.26 mmol) and DCM (7 mL) at RT, resulting in a rapidly boiling solution. The reaction mixture was stirred for 30 min at RT and was then diluted with DCM (10 mL). The solution was transferred to a separation funnel and was washed with 1 M HCl. The organic layer was dried with Na₂SO₄, filtered, and concentrated under reduced pressure to afford **2o** as colorless oil (132.0 mg, 20%). ¹H NMR (600 MHz, Chloroform-d) δ 3.62 – 3.31 (m, 4H), 2.45 (tt, J = 11.6, 3.4 Hz,

1H), 1.82 – 1.73 (m, 2H), 1.73 – 1.65 (m, 2H), 1.62 (qd, J = 6.0, 4.8, 2.4 Hz, 2H), 1.59 – 1.45 (m, 6H), 1.30 – 1.16 (m, 3H).

Cyclohexyl(3,4-dihydroisoquinolin-2(1H)-yl)methanone (2q). 1,2,3,4-Tetrahydroisoquinoline (0.25 mL, 2.0 mmol) was added to a solution of cyclohexanecarbonyl chloride (0.27 mL, 2.0 mmol) in DCM (10 mL). Then, triethylamine (0.328 mL, 2.0 mmol) was added. The mixture was stirred for 4 h at RT, concentrated in vacuo, dissolved in water (25 mL) and extracted with DCM (3 x 10 mL). Successively, the combined organic layers were washed with water (2 x 15 mL), saturated sodium carbonate solution (2 x 15 mL), brine (2 x 15 mL). Then, it was dried over MgSO₄, filtered, and concentrated in vacuo. The crude was purified by flash chromatography (heptane:EtOAc) to afford **2q** (212 mg, 44%). LC-MS: MS (ESI+) m/z 244.2 (M+H)⁺. ¹H NMR (400 MHz, CDCl₃): δ 7.23–7.08 (m, 4H), 4.72 (s, 1H), 4.66 (s, 1H), 3.82 (t, J = 5.9 Hz, 1H), , 3.72 (t, J = 5.9 Hz, 1H), 2.91 (t, J = 5.7 Hz, 1H), , 2.84 (t, J = 5.7 Hz, 1H), 2.61–2.51 (m, 1H), 1.86–1.66 (m, 5H), 1.63–1.48 (m, 2H), 1.37–1.19 (m, 3H). ¹³C NMR (100 MHz, CDCl₃): δ 175.3, 175.1, 135.5, 134.3, 134.0, 133.2, 129.2, 128.4, 127.1, 126.9, 126.7, 126.6, 126.5, 126.2, 47.5, 44.6, 43.2, 41.3, 41.2, 40.0, 30.1, 29.6, 29.5, 28.7, 26.1, 26.1.

(S)-2-((1,2,3,4-Tetrahydroisoquinolin-1-yl)methyl)isoindoline-1,3-dione (2r). Compound **2r** was synthesized in ten steps. Step 1: To a stirred solution of (S)-2-amino-2-phenylethan-1-ol (4.80 g, 35.0 mmol) and TEA (14.6 mL, 105.0 mmol) in DCM (90 mL) was added triphosgene (4.15 g, 14.0 mmol) portionwise at 0°C. The reaction mixture was stirred for 30 min at 0 °C and was then allowed to warm to RT. Water (90 mL) was added to the stirred reaction mixture and the phases were separated. The organic phase was washed with 2M HCl (2 x 90 mL), saturated NaHCO₃ solution (90 mL), brine (90 mL), dried with Na₂SO₄, and concentrated in vacuo. Purification by flash column chromatography (Hep:EtOAc) afforded (S)-4-phenyloxazolidin-2-one **2r-I1** as white

48

solid (4.84 g, 85%). ^1H NMR (400 MHz, Chloroform- d) δ 7.46 – 7.32 (m, 5H), 5.37 (s, 1H), 4.95 (ddd, J = 8.2, 7.0, 0.9 Hz, 1H), 4.74 (t, J = 8.6 Hz, 1H), 4.20 (dd, J = 8.6, 6.9 Hz, 1H). ^{13}C NMR: (101 MHz, Chloroform- d) δ 159.43, 139.41, 129.25, 128.91, 126.05, 72.54, 56.39. LC-MS (ESI): m/z 164.1 $[\text{M}+1]^+$, purity > 95% (UV). Step 2: To a solution of **2r-I1** (4.84 g, 29.6 mmol) and ethyl 2-bromoacetate (3.6 mL, 32.6 mmol) in DMF (60 mL) was added K_2CO_3 (12.29 g, 88.9 mmol) and the mixture was stirred at RT for 18 h. The mixture was partitioned between EtOAc (200 mL) and water (160 mL). The organic phase was separated, washed with water (2 x 80 mL) and brine (40 mL), dried (Na_2SO_4) and concentrated in vacuo. Purification by flash column chromatography (Hep:EtOAc) afforded ethyl (*S*)-2-(2-oxo-4-phenyloxazolidin-3-yl)acetate **2r-I2** as colorless oil (3.93 g, 89%). ^1H NMR (400 MHz, Chloroform- d) δ 7.46 – 7.27 (m, 5H), 5.07 (t, J = 8.3 Hz, 1H), 4.71 (t, J = 8.8 Hz, 1H), 4.29 (d, J = 18.0 Hz, 1H), 4.23 – 4.10 (m, 3H), 3.37 (d, J = 18.0 Hz, 1H), 1.25 (t, J = 7.1 Hz, 3H). ^{13}C NMR: (101 MHz, Chloroform- d) δ 168.39, 158.42, 136.81, 129.43, 129.35, 127.21, 70.23, 61.48, 60.02, 43.14, 14.11. LC-MS (ESI): m/z 250.1 $[\text{M}+1]^+$, purity > 95% (UV). Step 3: To a solution of **2r-I2** (6.56 g, 26.3 mmol) in THF (100 mL) was added 2M NaOH (40.0 mL). The resulting biphasic mixture was stirred vigorously at RT for 3 h. The mixture was concentrated in vacuo to a volume of approx. 70 mL, the resulting mixture was acidified with 2M HCl (70 mL) and EtOAc (150 mL). The organic phase was separated and the aq. phase was extracted with EtOAc (2 x 100 mL). The combined organic phases were washed with brine (100 mL), dried (Na_2SO_4) and concentrated in vacuo to afford (*S*)-2-(2-oxo-4-phenyloxazolidin-3-yl)acetic acid **2r-I3** as colorless sticky oil (5.82 g, quantitative). ^1H NMR (400 MHz, Chloroform- d) δ 7.47 – 7.28 (m, 5H), 5.05 (t, J = 8.4 Hz, 1H), 4.72 (t, J = 8.8 Hz, 1H), 4.34 (d, J = 18.3 Hz, 1H), 4.22 – 4.08 (m, 1H), 3.44 (d, J = 18.3 Hz, 1H). LC-MS (ESI): m/z 222.1 $[\text{M}+1]^+$, purity > 95% (UV). Step 4: To a solution of **2r-I3** (5.82 g, 26.30 mmol) in DCM (40 mL) was added thionyl chloride (7.67 mL, 105.20 mmol) and DMF (8 drops). The resulting mixture was heated under reflux until gas evolution ceased (about 45–75 min at 50 °C). The volatiles (DCM and excess thionyl chloride) were removed in vacuo to afford (10bS)-5,10b-dihydro-1H-oxazolo[4,3-*a*]isoquinoline-3,6-dione **2r-I4**, which was used without further purification. The

residue was dissolved in DCM (80 mL) and added dropwise to a suspension of aluminium trichloride (17.53 g, 131.50 mmol) in DCM (160 mL) at 0 °C and the mixture was stirred at RT for 1 h. The rxn was poured into crushed ice (~ 400 mL) and the organic phase was separated. The aq. phase was extracted with DCM (2 x 20 mL). The combined organic phases were washed with saturated NaHCO₃ solution (80 mL), brine (60 mL), dried (Na₂SO₄) and concentrated in vacuo. ¹H NMR (400 MHz, Chloroform-d) δ 8.22 – 8.10 (m, 1H), 7.76 – 7.65 (m, 1H), 7.52 (dd, J = 9.2, 6.2 Hz, 1H), 7.21 (d, J = 7.8 Hz, 1H), 5.28 – 5.17 (m, 1H), 4.94 (td, J = 8.4, 3.8 Hz, 1H), 4.73 (dd, J = 18.5, 2.9 Hz, 1H), 4.58 – 4.44 (m, 1H), 4.08 – 3.93 (m, 1H). UPLC-MS (ESI): m/z 204.1 [M+1]⁺, purity > 95% (UV). Step5: A solution of **2r-14** (1.00 g, 4.90 mmol) in THF (200 ml) was hydrogenated in the H-Cube apparatus at 25 bar and 50 °C with a flowrate of 1.0 mL/min with Pd/C as catalyst. The crude was concentrated in vacuo and purified by flash column chromatography (Hep:EtOAc) to afford (*S*)-1,5,6,10b-tetrahydro-3H-oxazolo[4,3-a]isoquinolin-3-one **2r-15** as white crystals (0.53 g, 57%). ¹H NMR (400 MHz, Chloroform-d) δ 7.29 – 7.26 (m, 1H), 7.25 – 7.24 (m, 1H), 7.20 – 7.15 (m, 1H), 7.03 – 6.98 (m, 1H), 5.06 – 4.99 (m, 1H), 4.82 (t, J = 8.5 Hz, 1H), 4.21 (dd, J = 8.3, 6.7 Hz, 1H), 4.10 (ddd, J = 13.3, 6.4, 1.9 Hz, 1H), 3.25 (ddd, J = 13.3, 11.7, 4.3 Hz, 1H), 3.12 – 3.02 (m, 1H), 2.78 – 2.71 (m, 1H). UPLC-MS (ESI): m/z 190.1 [M+1]⁺, purity > 95% (UV). Step 6: To a solution of **2r-15** (1.00 g, 6.03 mmol) in EtOH (25 ml) was added 5M NaOH (4.5 mL) and the mixture was heated under reflux (100 °C) for 1 h. After cooling, the mixture was concentrated in vacuo. The residue was diluted with brine (25 mL) and extracted with DCM (3 x 45 mL). The organic phase was dried (Na₂SO₄) and concentrated in vacuo to afford (*S*)-(1,2,3,4-tetrahydroisoquinolin-1-yl)methanol **2r-16** as yellowish oil (0.91 g, 93%). ¹H NMR (400 MHz, Chloroform-d) δ 8.00 – 7.94 (m, 1H), 7.78 (td, J = 7.6, 1.5 Hz, 1H), 7.55 (tdd, J = 7.6, 1.9, 0.9 Hz, 2H), 5.38 (ddd, J = 8.4, 4.7, 0.9 Hz, 1H), 4.90 (dd, J = 8.9, 8.3 Hz, 1H), 4.52 (dd, J = 8.9, 4.7 Hz, 1H), 4.36 – 4.22 (m, 2H). ¹³C NMR (101 MHz, Chloroform-d) δ 190.20, 156.64, 140.79, 134.96, 130.18, 128.93, 128.11, 124.05, 68.28, 53.12, 49.48. Step 7: To a solution of **2r-16** (0.90 g, 5.51 mmol) and DIPEA (0.59 mL, 6.62 mmol) in THF (15 mL) was added benzyl bromide (0.72 mL, 6.07 mmol) and the resulting solution was stirred

at RT for 18 h (a white precipitate was formed after 15 min). The mixture was concentrated in vacuo. The residue was diluted with EtOAc (60 mL), washed with 1 M K₂CO₃ (15 mL), water (15 mL) and brine (15 mL). The resulting organic phase was concentrated in vacuo to afford (*S*)-(2-benzyl-1,2,3,4-tetrahydroisoquinolin-1-yl)methanol **2r-17** as yellow oil (1.16 g, 83%). ¹H NMR (400 MHz, DMSO-d₆) δ 7.43 – 7.37 (m, 2H), 7.36 – 7.29 (m, 2H), 7.28 – 7.22 (m, 1H), 7.20 – 7.07 (m, 4H), 4.40 (dd, J = 6.7, 3.9 Hz, 1H), 3.80 (d, J = 3.7 Hz, 2H), 3.71 – 3.62 (m, 2H), 3.59 – 3.48 (m, 1H), 3.12 (ddd, J = 12.7, 9.8, 4.6 Hz, 1H), 2.86 (ddd, J = 15.7, 9.8, 5.4 Hz, 1H), 2.68 (ddd, J = 12.7, 5.4, 4.0 Hz, 1H), 2.56 (t, J = 4.3 Hz, 1H). LC-MS (ESI): m/z 254.1 [M+1]⁺, purity > 95% (UV). Step 8: A flask was charged with triphenyl phosphine (1.79 g, 6.83 mmol) under a nitrogen atmosphere, and dissolved in anhydrous THF (45 mL). The reaction mixture was cool to 0 °C and DIAD (1.32 mL, 6.83 mmol) was added. The reaction mixture was stirred at 0 °C for 30 min before addition of phthalimide (0.67 g, 4.55 mmol) followed by a solution of **2r-17** (1.15 g, 4.55 mmol) in anhydrous THF (15 mL). The resulting solution was allowed to warm to RT and stirring was continued for 22 h. The reaction mixture was concentrated in vacuo. The residue was diluted with EtOAc (60 mL) and heptane (15 mL), washed with water (45 mL) and brine (30 mL). The resulting organic phase was concentrated in vacuo and purified by flash column chromatography (Hep:EtOAc) to afford (*S*)-2-((2-Benzyl-1,2,3,4-tetrahydroisoquinolin-1-yl)methyl)isoindoline-1,3-dione **2r-18** as colorless oil (1.27 g, 73%). ¹H NMR (600 MHz, Chloroform-d) δ 7.81 (dd, J = 5.4, 3.0 Hz, 2H), 7.76 – 7.71 (m, 2H), 7.25 (s, 1H), 7.23 – 7.18 (m, 2H), 7.18 – 7.14 (m, 1H), 6.98 (tt, J = 7.3, 1.4 Hz, 1H), 6.95 – 6.90 (m, 2H), 6.84 – 6.78 (m, 2H), 4.07 (dd, J = 13.9, 11.2 Hz, 1H), 3.95 (dd, J = 11.2, 4.0 Hz, 1H), 3.70 (d, J = 13.2 Hz, 1H), 3.64 – 3.56 (m, 2H), 3.53 (d, J = 13.2 Hz, 1H), 3.10 – 2.96 (m, 2H), 2.54 (dd, J = 16.6, 4.5 Hz, 1H). LC-MS (ESI): m/z 383.2 [M+1]⁺, purity > 95% (UV). Step 9: **2r-18** (0.11 g, 0.29 mmol) was dissolved in EtOH (29 mL). The H-Cube apparatus was applied and the following parameters were used: 100 bar and 100 °C with a flowrate of 1.0 mL/min with 20% Pd(OH)₂/C as catalyst. After a completed run the solution was concentrated in vacuo and purified by flash

column chromatography (Hep:EtOAc) to afford **2r** as white solid (0.23 g, 27%). LC-MS (ESI): m/z 393.1 $[M+1]^+$, purity > 95% (UV).

***N,N*-Dimethylbenzenesulfonamide (3e)**. THF (10 mL) was added to dimethyl amine 40% aqueous solution (2.8 mL, 22.0 mmol). The solution was cooled down to 0 °C and benzenesulfonyl chloride was slowly added (2.6 mL, 20.0 mmol) while the solution was vigorously stirred. The solution was allowed to warm to RT and stirred for 22 h. Then EtOAc (10 mL) and water (10 mL) were added. The organic phase was washed with water (3 x 5 mL) and dried with $MgSO_4$ and concentrated in vacuo. the residue was purified by flash chromatography (Hep:EtOAc) to afford **3e** as a white solid (1.074 mg, 29%). LC-MS (ESI): m/z 186.0 $[M+1]^+$, purity > 95% (UV). 1H NMR: (400 MHz, Chloroform- d) δ 7.82–7.76 (m, 2H), 7.64–7.51 (m, 3H), 2.71 (s, 6H). ^{13}C NMR: (101 MHz, Chloroform- d) δ 135.74, 132.81, 129.14, 127.88, 38.08.

3,4-Dihydro-2H-benzo[*b*][1,4]oxathiepine-5,5-dioxide (3f). The compound was synthesized in two steps. Cesium carbonate (1.00 g, 3.07 mmol) was suspended in DMF (10 mL). Then 2-mercaptophenol (1.00 g, 7.93 mmol) and 3-bromopropanol (0.80 mL, 8.84 mmol) were added and the solution was stirred for 50 minutes at RT. The mixture was added into water (10 mL) and extracted with EtOAc (15 mL). The aqueous was washed with EtOAc (3 x 10 mL). The combined phases were dried over $MgSO_4$ and concentrated in vacuo. The residue was purified by flash chromatography (Hep:EtOAc) to afford 2-((3-hydroxypropyl)thio)phenol **3f-I1** as a clear yellow oil (964.3 mg, 66%). LC-MS (ESI): m/z 183.2 $[M-1]^-$, purity > 95% (UV). 1H NMR: (400 MHz, Chloroform- d) δ 6.99 (dd, J = 8.2, 1.3 Hz, 1H), 6.87 (td, J = 7.5, 1.3 Hz, 1H), 3.76 (t, J = 6.0 Hz, 2H), 2.83 (t, J = 7.2 Hz, 2H), 1.81 (dt, J = 7.2, 6.0 Hz, 2H). **3f-I1** (0.966 g, 5.24 mmol) was dissolved in THF (20 mL). Triphenylphosphine (1.733 g, 6.61 mmol) was added and the solution was cooled down to -40 °C by using a cooling bath of dried ice in

52

acetonitrile. DIBAD (1.243 g, 5.40 mmol) was dissolved in THF (5 mL) and the solution was added slowly to the reaction mixture. The reaction mixture was warmed to RT and stirred for 17 h. TFA (4 mL) was added and the mixture was stirred for 90 minutes. The reaction mixture was then evaporated and taken up in DCM (30 mL). The obtained solution was washed with water (30 mL) and the aqueous layer was extracted with DCM (3 x 30 mL). The combined organic phases were dried over MgSO_4 , concentrated in vacuo, dissolved in DCM (10 mL) and purified by flash chromatography (Hep:EtOAc) to afford **3f** as a colorless oil (36.0 mg, 7%). LC-MS (ESI): m/z 198.3 $[\text{M}-1]^-$, purity > 95% (UV). ^1H NMR: (400 MHz, $\text{DMSO}-d_6$) δ 7.37 (dd, $J = 7.6, 1.7$ Hz, 1H), 7.19 (ddd, $J = 8.0, 7.2, 1.7$ Hz, 1H), 7.02–6.96 (m, 2H), 4.14–4.10 (m, 2H), 2.92–2.87 (m, 2H), 2.19–2.12 (m, 2H). ^{13}C NMR: (101 MHz, $\text{DMSO}-d_6$) δ 160.52, 133.31, 131.94, 128.39, 123.45, 122.09, 72.04, 32.57, 30.58.

3,4-Dihydro-2H-benzo[b][1,4,5]oxathiazepine-1,1-dioxide (3g). The compound was synthesized in two steps. To the solution of ethanolamine (0.16 mL, 2.57 mmol) in THF (10 mL) and water (2.5 mL) was added potassium carbonate (0.710 g, 5.14 mmol) and then 2-fluorobenzenesulfonyl chloride (0.34 mL, 2.57) was added slowly. The resulting reaction mixture was stirred at RT for 21 h. The reaction mixture was diluted with water (20 mL) and extracted with EtOAc (40 mL). The aqueous layer was washed with EtOAc (2 x 20 mL). The combined organic layers were washed with brine (30 mL), dried over MgSO_4 , filtered and concentrated in vacuo to afford 2-fluoro-*N*-(2-hydroxyethyl)benzenesulfonamide **3g-I1** (321 mg, 57%). LC-MS (ESI): m/z 241 $[\text{M}+\text{Na}]^+$, purity > 95% (UV). ^1H NMR: (400 MHz, $\text{DMSO}-d_6$) δ 7.84 (s, 1H), 7.80 (td, $J = 7.6, 1.8$ Hz, 1H), 7.70 (tdd, $J = 7.3, 5.0, 1.7$ Hz, 1H), 7.47–7.35 (m, 2H), 4.67 (s, 1H), 3.37 (t, $J = 6.6$ Hz, 2H), 2.91 (t, $J = 6.5$ Hz, 2H). ^{13}C NMR: (101 MHz, $\text{DMSO}-d_6$) δ 158.16 (d, $J = 253.2$ Hz), 135.05 (d, $J = 8.5$ Hz), 129.55, 128.58 (d, $J = 14.2$ Hz), 124.79 (d, $J = 3.7$ Hz), 117.18 (d, $J = 21.3$ Hz), 59.87, 44.88. To a solution of **3g-I1** (0.648 g, 2.96 mmol) in DMSO was added KOTu (0.996 g; 8.88 mmol) and the resulting mixture was stirred at 80 °C for 24 h. The reaction mixture was then

diluted with water (15 mL), adjusted to pH 6 with 2 M HCl, and extracted with EtOAc (40 mL + 2 x 20 mL) and the combined organic layer was dried over MgSO₄, filtrated and concentrated in vacuo. The crude product was purified by flash chromatography (Hep:EtOAc) to afford **3g** as white solid (100.2 mg, 14%). LC-MS (ESI): m/z 198.5 [M-1]⁻, purity > 95% (UV). ¹H NMR: (400 MHz, DMSO-d₆) δ 7.74 (dd, J = 7.8, 1.7 Hz, 1H), 7.55 (td, J = 7.8, 18.0 Hz, 1H), 7.27 (td, J = 7.6, 1.2 Hz, 1H), 7.21 (dd, J = 8.1, 1.1 Hz, 1H), 4.12–4.06 (m, 2H); 3.47–3.40 (m, 2H). ¹³C NMR: (101 MHz, DMSO-d₆) δ 155.21, 137.33 133.83, 127.15, 123.97, 123.11, 72.66, 44.49.

(R)-4-Methyl-3,4-dihydro-2H-benzo[b][1,4,5]oxathiazepine 1,1-dioxide (3h). The compound was synthesized in two steps according to previously described procedure²⁰ with minor deviations. To a solution of (*R*)-1-aminopropan-2-ol (0.2 g, 2.7 mmol, 1.0 equiv) in THF/water (1:1, 15 mL) was slowly added K₂CO₃ (0.1 g, 2.7 mmol, 1.0 equiv) and then 2-fluorobenzenesulfonyl chloride (0.88 mL, 2.7 mmol, 1.0 equiv). The reaction mixture was stirred at RT for 66 h. The reaction mixture was then diluted with water (15 mL), extracted with EtOAc (3 x 15 mL), and the combined organic layers washed with brine (20 mL), dried over Na₂SO₄, filtered, and concentrated in vacuo. The crude was purified by flash chromatography (heptane:EtOAc, 0–100% gradient) to furnish **3h-11** as a red oil (0.66 g, 2.8 mmol, quantitative). ¹H NMR (600 MHz, Chloroform-d) δ 7.91 (td, J = 7.5, 1.8 Hz, 1H), 7.63–7.55 (m, 1H), 7.29 (td, J = 7.7, 1.1 Hz, 1H), 7.22 (ddd, J = 10.3, 8.3, 1.1 Hz, 1H), 5.19 (s, 1H), 3.94 (d, J = 8.0 Hz, 1H), 3.13 (d, J = 12.9 Hz, 1H), 2.88–2.80 (m, 1H), 1.89 (s, 1H), 1.18 (d, J = 6.3 Hz, 3H). The compound was synthesized according to previously described procedure²⁰ with no deviations. Starting from **3h-11** (0.66 g, 2.8 mmol), **3h** was obtained as a white solid (0.59 g, 2.8 mmol, quantitative). LC-MS: MS (ESI) m/z 236.0 [M+1]⁺. ¹H NMR (400 MHz, Chloroform-d) δ 7.84 (dd, J = 7.8, 1.7 Hz, 1H), 7.46 (td, J = 7.8, 1.7 Hz, 1H), 7.23–7.12 (m, 2H), 4.68 (s, 1H), 4.22–4.10 (m, 1H), 3.63 (dt, J = 15.0, 9.2 Hz, 1H), 3.42 (ddd, J = 15.1, 5.2, 2.2 Hz, 1H), 1.40 (d, J = 6.4 Hz, 3H).

1,4-dimethyl-1H-benzo[d][1,2,3]triazole (3k). The compound was synthesized in three steps. To a solution of 3-methyl-2-nitroaniline (1.00 g, 6.57 mmol) in DMF (15 mL), sodium hydride (0.172 g, 7.16 mmol) was added at RT. The reaction mixture was stirred at RT for 30 minutes and then methyl iodide (0.43 mL, 6.83 mmol) was added. The reaction mixture was stirred for 21 h at RT and then was poured into water (200 mL). The formed precipitate was collected by filtration, dissolved in DCM (15 mL) and purified by flash chromatography (heptane:EtOAc) to afford N,3-dimethyl-2-nitroaniline **3k-I1** brown solid (393.0 mg, 36%). LC-MS: MS (ESI) m/z 164.9 [M-1]⁻. ¹H NMR: (400 MHz, Chloroform-d) δ 7.24 (d, J = 7.8 Hz, 1H); 6.66 (d, J = 8.5 Hz, 1H); 6.53 (d, J = 7.4 Hz, 1H), 2.93 (s, 3H), 2.48 (s, 3H). ¹³C NMR: (101 MHz, Chloroform-d) δ 135.86, 133.44, 119.35, 110.84, 30.28, 21.63 (two carbon signals missing). To a solution of **3k-I1** (0.390 g, 2.35 mmol) in EtOH (20 mL) tin(II) chloride was added (2.120 g, 9.40 mmol). The reaction mixture was stirred at 75 °C for 23 h. The solvent was adjusted to pH = 14 using aq. NaOH. Then it was extracted with EtOAc (3 x 20 mL) and the combined organic layer was dried over MgSO₄ and concentrated in vacuo to afford 1,3-dimethylbenzene-1,2-diamine **3k-I2** as red oil (390 mg, quantitative). LC-MS: MS (ESI) m/z 136.8 [M+1]⁺. ¹H NMR: (400 MHz, Chloroform-d) δ 6.78 (t, J = 7.7 Hz, 1H), 6.64 (d, J = 7.5, 1H), 6.59 (d, J = 7.7 Hz, 1H), 3.26 (br s, 3H), 2.87 (s, 3H), 2.22 (s, 3H). ¹³C NMR: (101 MHz, Chloroform-d) δ 138.42, 132.81, 122.84, 120.84, 119.77, 109.54, 31.43, 17.62. To **3k-I2** (0.390 g, 2.65 mmol) in H₂SO₄ 10% (10.0 mL) at 0 °C sodium nitrite (0.258 g; 3.71 mmol) was added in small portion over 20 minutes. After the reaction was stirred for 2 hours and 40 minutes further. Then water (200 mL) was added. The solution was extracted with ethyl acetate (3 x 15 mL) and the combined organic layers were washed with water (2 x 10 mL) and with brine (1 x 9 mL), dried over MgSO₄, filtrated, and concentrated in vacuo to afford **3k** (50.7 mg, 13%) as a brown solid. LC-MS: MS (ESI) m/z 148.1 [M+1]⁺. ¹H NMR: (600 MHz, Chloroform-d) δ 7.39 (dd, J = 8.3, 6.9 Hz, 1H), 7.33 (d, J = 8.3 Hz, 1H), 7.14 (dt, J = 6.9, 1.1 Hz, 1H), 4.29 (s,3H), 2.80 (s,3H). ¹³C NMR: (101 MHz, Chloroform-d) δ 146.05, 133.55, 131.02, 127.47, 123.82, 106.51, 34.39, 16.88.

7-Methoxy-1H-benzo[d][1,2,3]triazole (3I). The compound is synthesized in three steps. Procedure D was used with **(3I-I1)** (1.0 g, 6.49 mmol). After 18 h the mixture was poured into water. The resulting precipitate was collected by filtration and the solid was washed with water and dried to give the 2-methoxy-6-nitroaniline **3I-I2** as yellow crystals (1.09 g, 91%). ¹H NMR (600 MHz, Chloroform-d) δ 7.73 (dd, J = 8.9, 1.3 Hz, 1H), 6.88 (dd, J = 7.7, 1.2 Hz, 1H), 6.61 (dd, J = 8.9, 7.8 Hz, 1H), 6.43 (s, 2H), 3.93 (s, 3H). General procedure E was used with **3I-I2** (1.09 g, 6.49 mmol) to afford 3-methoxybenzene-1,2-diamine **3I-I3** as an orange solid (0.77 g, 86%). ¹H NMR (400 MHz, Chloroform-d) δ 6.68 (t, J = 8.0 Hz, 1H), 6.41 (td, J = 8.0, 1.2 Hz, 2H), 3.84 (s, 3H), 3.49 (d, J = 3.4 Hz, 4H). LC-MS: MS (ESI) m/z 139.2 [M+1]⁺, purity > 95% (UV). General procedure F was used with **3I-I3** (2.00 g, 14.47 mmol) to afford **3I** as light brown solid (2.02 g, 94%). ¹H NMR (400 MHz, DMSO-d₆) δ 15.62 (s, 1H), 7.36 (s, 2H), 6.85 (s, 1H), 4.01 (s, 3H). LC-MS: MS (ESI) m/z 148.1 [M-1]⁻, purity > 95% (UV).

2-Benzyl-3,4-dihydro-2H-benzo[b][1,4,5]oxathiazepine 1,1-dioxide (3n). A suspension of **3g** (20.0 mg, 0.1 mmol) and K₂CO₃ (59.7 mg, 0.43 mmol) in acetone (1 mL) was thoroughly mixed under vigorous stirring for 5 min, and then benzyl bromide (0.05 mL, 0.43 mmol) was added. The reaction mixture was stirred at 40°C for 2 h. The reaction mixture was poured into water (10 mL) and extracted with EtOAc (2 x 5 mL). The resulting organic phase was concentrated in vacuo. Purification by flash column chromatography (hep:EtOAc) afforded **3n** as a colorless oil (0.029 g, quantitative). LC-MS (ESI): m/z 290.1 [M+1]⁺, purity > 95% (UV). ¹H NMR (400 MHz, Chloroform-d) δ 7.91 (dd, J = 7.8, 1.8 Hz, 1H), 7.52 (td, J = 7.8, 1.8 Hz, 1H), 7.38 – 7.30 (m, 4H), 7.28 (d, J = 1.2 Hz, 1H), 7.24 (d, J = 1.2 Hz, 1H), 7.20 (dd, J = 8.1, 1.2 Hz, 1H), 4.26 – 4.16 (m, 4H), 3.64 – 3.57 (m, 2H).

3-(7-methoxy-1-methyl-1H-benzo[d][1,2,3]triazol-5-yl)propanoic acid (3m). The compound was synthesized in eight steps. For step 1, a previously described procedure²⁰ was employed with no deviations. Starting from 2-amino-3-nitrophenol (10.0 g, 64.9 mmol), 2-methoxy-6-nitroaniline (**3m-I1**) was obtained as an orange solid (9.73 g, 57.8 mmol, 89%). ¹H NMR (600 MHz, Chloroform-d) δ 7.73 (dd, J = 8.9, 1.3 Hz, 1H), 6.88 (dd, J = 7.7, 1.2 Hz, 1H), 6.61 (dd, J = 8.9, 7.8 Hz, 1H), 6.43 (s, 2H), 3.92 (s, 3H). ¹³C NMR (151 MHz, Chloroform-d) δ 148.30, 137.20, 131.83, 117.52, 114.72, 113.44, 56.40. For step 2, a previously described procedure²⁰ was employed with no deviations. Starting from **3m-I1** (9.73 g, 57.8 mmol), 4-bromo-2-methoxy-6-nitroaniline (**3m-I2**) was obtained as an orange solid (12.64 g, 51.2 mmol, 88%). ¹H NMR (600 MHz, DMSO-d₆) δ 7.71 (d, J = 2.1 Hz, 1H), 7.24 (s, 2H), 7.20 (d, J = 2.1 Hz, 1H), 3.91 (s, 3H). For step 3, a previously described procedure²⁰ was employed with no deviations. Starting from **3m-I2** (12.64 g, 51.2 mmol), 4-bromo-2-methoxy-N-methyl-6-nitroaniline (**3m-I3**) was obtained as an orange solid (8.67 g, 33.2 mmol, 65%). ¹H NMR (400 MHz, DMSO-d₆) δ 7.59 (d, J = 2.2 Hz, 1H), 7.23 (s, 3H), 7.18 (d, J = 2.3 Hz, 1H), 3.91 (s, 2H), 3.87 (s, 3H), 2.86 (d, J = 5.4 Hz, 3H). For step 4, a previously described procedure²⁰ was employed with minor deviations. To a solution of **3m-I3** (1.30 g, 5.0 mmol, 1.0 equiv) in EtOH (25 mL) was added SnCl₂·2H₂O (4.49 g, 19.9 mmol, 4.0 equiv) and the reaction mixture was stirred at 75 °C for 2 h. Then the mixture was adjusted to pH 14 using 40% aq. NaOH, followed by addition of water (150 mL), and extraction with EtOAc (3 x 100 mL). The combined organic layers were dried over Na₂SO₄ and concentrated in vacuo. The crude was purified by flash chromatography (heptane:EtOAc, 0–100% gradient) to furnish 4-bromo-6-methoxy-N1-methylbenzene-1,2-diamine (**3m-I4**) as a yellow solid (1.03 g, 4.6 mmol, 90%). ¹H NMR (400 MHz, Chloroform-d) δ 6.54 (d, J = 2.0 Hz, 1H), 6.45 (d, J = 2.0 Hz, 1H), 4.11 (d, J = 67.7 Hz, 2H), 3.81 (s, 3H), 2.70 (s, 3H), 0.07 (s, 3H). For step 5, a previously described procedure²⁰ was followed with no deviations. Starting from **3m-I4** (1.03 g, 4.5 mmol), 5-bromo-7-methoxy-1-methyl-1H-benzo[d][1,2,3]triazole (**3m-I5**) was obtained as a brown solid (0.89 g, 3.7 mmol, 83%). ¹H NMR (600 MHz, Chloroform-d) δ 7.76 (d, J = 1.3 Hz, 1H), 6.85 (d, J = 1.3 Hz, 1H), 4.44 (s, 3H), 3.99 (s, 3H). To a solution of **3m-I5** (0.89 g, 3.7 mmol) in dry

DMF (5 mL), methyl acrylate (1.66 mL, 18.4 mmol), DIPEA (1.59 mL, 9.2 mmol), and tri-*o*-phosphine (0.22 g, 0.74 mmol) were added. Then Pd(OAc)₂ (0.08 g, 0.37 mmol, 0.1 equiv) was added. The reaction mixture was stirred at 95 °C for 4 h under an atmosphere of nitrogen. The reaction mixture was then poured into water (10 mL) and extracted with EtOAc (2 x 15 mL). The resulting organic phase was concentrated in vacuo. The crude was purified by flash chromatography (heptane:EtOAc, 0–100% gradient) to furnish methyl (E)-3-(7-methoxy-1-methyl-1H-benzo[d][1,2,3]triazol-5-yl)acrylate (**3m-I6**) as a brown solid (0.31 g, 1.25 mmol, 32%). ¹H NMR (400 MHz, Chloroform-*d*) δ 7.84–7.68 (m, 2H), 6.91 (d, *J* = 1.1 Hz, 1H), 6.45 (d, *J* = 15.9 Hz, 1H), 4.46 (s, 3H), 4.02 (s, 3H), 3.83 (s, 3H). **3m-I6** (27.9 mg, 0.11 mmol) was dissolved in EtOH (3 mL) and placed under nitrogen. Pd/C (5% w/w; 2.0 mg, 0.02 mmol) was added and the atmosphere was replaced with hydrogen. The resulting mixture was stirred at under an atmosphere of hydrogen for 24 h. The reaction mixture was poured into water (5 mL) and extracted with EtOAc (5 mL). The resulting organic phase was concentrated in vacuo. The crude was purified by flash chromatography (heptane:EtOAc, 0–100% gradient) to furnish methyl 3-(7-methoxy-1-methyl-1H-benzo[d][1,2,3]triazol-5-yl)propanoate **3m-I7** as a yellowish solid (0.005 g, 18%). To a solution of **3m-I7** (5 mg, 0.020 mmol) in MeOH (1.0 mL) was added NaOH (2 M, 0.25 mL). The reaction mixture was heated to 80 °C for 40 min. The resulting reaction mixture was acidified with HCl (1 M) to pH 3, extracted with EtOAc (3 x 5 mL), washed with brine (5 mL), and concentrated in vacuo. Purification by preparative HPLC afforded **3m** as a white solid (0.014 g, 87%). LC-MS (ESI): *m/z* 236.1 [M+1]⁺, purity > 95% (UV).

3-(7-Methoxy-1-methyl-1H-benzo[d][1,2,3]triazol-5-yl)-3-phenylpropanoic acid (3o). The compound was synthesized in eight steps. Intermediate **3m-I6** was used as starting point. Methyl 3-(7-methoxy-1-methyl-1H-benzo[d][1,2,3]triazol-5-yl)-3-phenylpropanoate **3o-I1** was synthesized according to previously described procedure²⁰ with no deviations. Starting from **3m-I6** (0.025 g, 0.10 mmol), **3o-I1** was obtained as a white solid

(0.014 g, 43%). LC-MS (ESI): m/z 326.2 $[M+1]^+$, purity > 95% (UV). To a solution of **3o-I1** (14 mg, 0.043 mmol) in MeOH (2.0 mL) was added NaOH (2 M, 0.35 mL). The reaction mixture was heated to 80 °C for 40 min. The resulting reaction mixture was acidified with HCl (1 M) to pH 3, extracted with EtOAc (3 x 5 mL), washed with brine (5 mL), and concentrated in vacuo. Purification by preparative HPLC afforded **3o** as a white solid (0.010 g, 75%). LC-MS (ESI): m/z 312.2 $[M+1]^+$, purity > 95% (UV). ^1H NMR (600 MHz, Chloroform- d) δ 7.52 (s, 1H), 7.22 (t, J = 7.5 Hz, 2H), 7.18 – 7.13 (m, 3H), 6.55 (s, 1H), 4.59 (t, J = 7.7 Hz, 1H), 4.38 (s, 3H), 3.84 (s, 3H), 3.19 – 3.02 (m, 2H). ^{13}C NMR (151 MHz, Chloroform- d) δ 174.83, 146.29, 145.58, 142.83, 142.54, 128.84, 127.60, 127.02, 124.79, 108.14, 107.73, 56.02, 47.04, 40.07, 37.75.

(1-Cyclohexylethoxy)benzene (4a). To a solution of 1-cyclohexylethanol (0.54 mL, 3.9 mmol), phenol (440.4 mg, 4.7 mmol) and Ph_3P (1227 mg, 4.7 mmol) in THF (4 mL), was added dropwise a solution of DIAD (0.92 mL, 4.7 mmol) in THF (4 mL). The reaction mixture was stirred at room temperature for 32 h. The solvent was evaporated and the residue was purified by silica flash column chromatography (heptane/EtOAc) to afford **4a** as a colorless oil (423 mg, 53%). ^1H NMR (600 MHz, DMSO- d_6): δ 7.25 (td, J = 8.0, 7.3, 2.3 Hz, 2H), 6.89 (td, J = 9.0, 4.5 Hz, 3H), 4.21 (td, J = 6.1, 2.1 Hz, 1H), 1.85 (d, J = 13.0 Hz, 1H), 1.71 (q, J = 10.5, 7.7 Hz, 3H), 1.67 – 1.58 (m, 1H), 1.53 (tdq, J = 11.6, 5.8, 2.9 Hz, 1H), 1.26 – 0.97 (m, 8H). ^{13}C NMR (101 MHz, DMSO- d_6): δ 158.52, 129.93, 120.61, 116.05, 77.26, 43.00, 28.75, 28.25, 26.56, 26.13, 16.82.

5-Cyclopropyl-1-phenyl-1H-pyrazole-4-carboxylic acid (4c). The compound is synthesized in three steps. To a solution of ethyl 3-cyclopropyl-3-oxopropanoate (0.5 mL, 3.4 mmol) in 1,4-dioxane (10 mL), 1,1-dimethoxy-*N,N*-dimethylmethanamine (0.67 mL, 5.1 mmol) was added. The reaction mixture was stirred at 95 °C for 4 h. The solvent was evaporated to afford ethyl 2-(cyclopropanecarbonyl)-3-(dimethylamino)acrylate **4c-I1** as

yellow liquid (646 mg, 90%). LC-MS (ESI) m/z : 212.2 $[M+H]^+$ (3.349 min, 5.325 min) (isomers). **4c-I1** (646.0 mg, 3 mmol) was diluted in EtOH (5 mL) and treated with phenylhydrazine hydrochloride (441.9 mg, 3 mmol), followed by triethylamine (0.42 mL, 3 mmol). The mixture was stirred at RT for 24 h. Then the mixture was partitioned between EtOAc (50 mL) and water (50 mL) and the organic phase was washed further with water (2 x 20 mL), dried over $MgSO_4$ and concentrated in vacuo to afford ethyl 5-cyclopropyl-1-phenyl-1H-pyrazole-4-carboxylate **4c-I2** as brown liquid (676 mg, 88%). LC-MS (ESI) m/z : 257.1 $[M+H]^+$ (5.608 min). 1H NMR (600 MHz, Chloroform- d): δ 8.01 (s, 1H), 7.50 (m, 4H), 7.45 – 7.40 (m, 1H), 4.32 (q, J = 7.1 Hz, 2H), 2.00 – 1.93 (m, 1H), 1.38 (t, J = 7.1 Hz, 3H), 1.27 (dtd, J = 15.7, 7.1, 1.1 Hz, 2H), 0.64 (qd, J = 6.3, 5.6, 3.1 Hz, 2H). A stirred solution of **4c-I2** (676.0 mg, 2.6 mmol) in EtOH (25 mL) was treated with a solution of NaOH (432.0 mg, 10.4 mmol) in water (9 mL). After 60 h, the mixture was acidified with 1 N HCl (60 mL) and extracted into EtOAc (3 x 20 mL). The combined organic phases were dried over $MgSO_4$, filtered, and concentrated in vacuo. The residue was purified by silica flash column chromatography (DCM/MeOH) to afford **4c** as brown solid (451 mg, 76%). LC-MS (ESI) m/z : 226.9 $[M-H]^-$ (3.892 min). 1H NMR (600 MHz, DMSO- d_6): δ 12.31 (s, 1H), 7.94 (s, 1H), 7.59 (d, J = 7.4 Hz, 2H), 7.55 (t, J = 7.7 Hz, 2H), 7.51 – 7.46 (m, 1H), 2.08 (tt, J = 8.6, 5.4 Hz, 1H), 0.88 – 0.77 (m, 2H), 0.52 (dt, J = 6.5, 3.2 Hz, 2H). ^{13}C NMR (151 MHz, DMSO- d_6): δ 164.31, 147.45, 142.40, 139.76, 129.41, 128.78, 125.86, 114.54, 8.62, 7.45.

1-(3-Cyclohexylphenyl)-5-methyl-1H-pyrazole-4-carboxylic acid (4d). The compound was synthesized in seven steps. Step 1: To a solution of ethyl acetoacetate (2.0 mL, 16.3 mmol) in 1,4-dioxane (40 mL), 1,1-dimethoxy-*N,N*-dimethylmethanamine (3.2 mL, 24.4 mmol) was added. The reaction mixture was stirred at 95 °C for 5 h. The solvent was evaporated to afford ethyl 2-((dimethylamino)methylene)-3-oxobutanoate **4d-I1** as a light brown oil (2.7 g, 92%). LC-MS (ESI) m/z : 186.1 $[M+H]^+$ (2.559 min, 4.290 min)⁸⁰ (isomers). Step 2: **4d-I1** (937.5

mg, 5 mmol) was diluted in EtOH (6 mL) and treated with 3-bromophenylhydrazine hydrochloride (1117.5 mg, 5 mmol), followed by TEA (0.70 mL, 5.0 mmol) and heated at 80 °C for 3 h. The mixture was extracted with DCM and washed with water, and the organic layer was collected and dried in vacuo. The residue was purified by silica flash column chromatography (heptane/EtOAc) to afford ethyl 1-(3-bromophenyl)-5-methyl-1H-pyrazole-4-carboxylate **4d-I2** as red oil (958 mg, 62%). LC-MS (ESI) m/z: 309.1 [M+H]⁺ (6.068 min). ¹H NMR (600 MHz, Chloroform-d): δ 8.03 (s, 1H), 7.63 (dt, J = 2.4, 1.0 Hz, 1H), 7.60 – 7.55 (m, 1H), 7.40 – 7.33 (m, 2H), 4.33 (q, J = 7.1 Hz, 2H), 2.59 (s, 3H), 1.38 (t, J = 7.1 Hz, 3H). Step 3: A mixture of **4d-I2** (332.0 mg, 1.1 mmol), bis(pinacolato)diboron (300.0 mg, 1.2 mmol), KOAc (210.8 mg, 2.2 mmol) and Pd(dppf)Cl₂ (39.3 mg, 5 mol%) in dioxane (10 mL) was stirred under reflux for 5 hours. The mixture was then concentrated and partitioned between EtOAc and water. The organic phase was washed with water and then brine before it was dried (MgSO₄), filtered, and concentrated in vacuo to afford ethyl 5-methyl-1-(3-(4,4,5,5-tetramethyl-1,3,2-dioxaborolan-2-yl)) **4d-I3** as brown oil (219 mg, 56%). LC-MS (ESI) m/z: 275.1 [M+H] (3.907 min). ¹H NMR (400 MHz, Chloroform-d): δ 8.02 (s, 1H), 7.90 – 7.81 (m, 2H), 7.56 – 7.44 (m, 2H), 4.33 (q, J = 7.1 Hz, 2H), 2.55 (s, 3H), 1.38 (t, J = 7.1 Hz, 3H), 1.34 (s, 12H). Step 4: To solution of cyclohexanone (0.33 mL, 3.2 mmol) in anhydrous THF (15 mL) was added LiHMDS (3.8 mL, 1.0 M in THF, 3.8 mmol) at -78 °C. After 1 h at -78 °C under N₂ atmosphere, a solution of PhNTf₂ (1.6 g, 4.5 mmol) in anhydrous THF (17 mL) was added dropwise to the mixture solution at -78 °C. The mixture solution was allowed to warm to RT over a period of 4 h and stirred for additional 12 h. After the completion of the reaction, the resulting solution was treated with saturated aqueous NH₄Cl (5 mL) and extracted with Et₂O (3 x 50 mL). The combined organic solution was washed with saturated aqueous Na₂CO₃ (5 mL), dried over anhydrous MgSO₄, filtered and concentrated in vacuo. The residue was purified by silica flash column chromatography (heptane/EtOAc) to afford cyclohex-1-en-1-yl trifluoromethanesulfonate **4d-I4** as a yellow oil (250 mg, 34%). ¹H NMR (600 MHz, Chloroform-d): δ 5.76 (tt, J = 3.9, 1.6 Hz, 1H), 2.31 (ddq, J = 9.0, 6.6, 2.6 Hz, 2H), 2.18 (tq, J = 6.0, 2.9 Hz, 2H), 1.83 – 1.74 (m, 2H), 1.62 – 1.58

(m, 2H). Step 5: A stirred mixture of 4d-I4 (96.9 mg, 0.42 mmol), phenyl **4d-I3** (100.0 mg, 0.28 mmol), aqueous Na₂CO₃ (3 M, 0.28 mL, 0.84 mmol) and Pd(PPh₃)₄ (24.3 mg, 7.5 mol%) in EtOH (0.5 mL) and toluene (1.5 mL) was heated to reflux for 18 h. After cooling, the mixture was partitioned between EtOAc (5 mL) and water (5 mL). The organic phase was washed with water (5 mL) and brine (5 mL) before it was dried (MgSO₄), filtered, and concentrated in vacuo to afford ethyl 5-methyl-1-(2',3',4',5'-tetrahydro-[1,1'-biphenyl]-3-yl)-1H-pyrazole-4-carboxylate **4d-I5** as brown oil (67 mg, 77%). LC-MS (ESI) m/z: 311.2 [M+H]⁺ (7.309 min). Step 6: A solution of **4d-I5** (15.0 mg, 0.05 mmol) in EtOH (1.5 mL) was degassed and treated with Pd/C 10% (2.6 mg, 0.025 mmol) and shaken under an atmosphere of hydrogen for 27 h. The catalyst was removed by filtration and the solution was concentrated in vacuo to afford ethyl 1-(3-cyclohexylphenyl)-5-methyl-1H-pyrazole-4-carboxylate **4d-I6** as brown oil (8 mg, 53%). LC-MS (ESI) m/z: 313.3 [M+H]⁺ (7.508 min). Step 7: A stirred solution of **4d-I6** (3.1 mg, 0.01 mmol) in EtOH (0.5 mL) was treated with a solution of NaOH (2.0 mg, 0.05 mmol) in water (0.1 mL). After 14 hours, the reaction was stopped and the mixture was acidified with 1 M HCl (0.5 mL) and extracted into EtOAc (3 x 1 mL). The combined organic phases were dried (Na₂SO₄), filtered, and concentrated in vacuo. The residue was purified by preparative HPLC to afford **4d** as brown oil (1.6 mg, 60%). LC-MS (ESI) m/z: 283.1 [M-H]⁻ (5.853 min).

1-Phenyl-1H-1,2,3-triazole (5f). A mixture of 1H-1,2,3-triazole (100.0 mg, 1.5 mmol), iodobenzene (365.0 mg, 1.75 mmol), cubic Cu₂O nanoparticles (17.0 mg, 8 mol%), 1,10-phenanthroline (40.5 mg, 15 mol%), and TBAF (4.5 mL, 4.5 mmol) was stirred at 110–115 °C for 48 h until complete consumption of the starting material was observed. EtOAc (20 mL) was poured into the mixture, which was then washed with sat. aq NaCl (3 x 8 mL), extracted with Et₂O (2 x 8 mL), dried over Na₂SO₄ and concentrated in vacuo. Purification by flash chromatography (heptane:EtOAc, 0–100% gradient) to furnish **5f** as a brown solid (0.177 g, 82%). LC-MS (ESI):

m/z 146.1 [M+1]⁺, purity > 95% (UV). ¹H NMR (400 MHz, Chloroform-d): δ 8.00 (d, J = 1.2 Hz, 1H), 7.86 (d, J = 1.2 Hz, 1H), 7.80 – 7.72 (m, 2H), 7.60 – 7.50 (m, 2H), 7.50 – 7.41 (m, 1H). ¹³C NMR (101 MHz, Chloroform-d): δ 134.40, 129.79, 128.82, 121.72, 120.72.

4-(3-Nitrophenyl)-1H-1,2,3-triazole (5g). The compound was synthesized in three steps. To a stirred solution of 1-iodo-3-nitrobenzene (249.0 mg, 6 mmol) and Et₃N (3.3 mL, 24 mmol) in dioxane (24 mL) were added trimethylsilyl acetylene (1.1 mL, 7.8 mmol), PdCl₂(PPh₃)₂ (42.1 mg, 0.06 mmol), and CuI (22.9 mg, 0.12 mmol). The reaction mixture was stirred at 45 °C for 5 h under N₂. After consumption of 1-nitro-3-[2-(trimethylsilyl)ethynyl]benzene **5g-I1**, Et₂O (20 mL) and 0.1 M HCl (10 mL) were added, and the organic layer was separated, neutralized with a saturated NaHCO₃ (2 x 6 mL), washed with brine (6 mL), dried over Na₂SO₄ and concentrated in vacuo. Purification by flash chromatography (heptane:EtOAc, 0–100% gradient) to furnish **5g-I1** as a brown solid (0.83 g, 63%). ¹H NMR (400 MHz, Chloroform-d): δ 8.30 (t, J = 2.1 Hz, 1H), 8.15 (ddd, J = 8.0, 2.1, 1.2 Hz, 1H), 7.74 (dt, J = 8.0, 1.2 Hz, 1H), 7.48 (t, J = 8.0 Hz, 1H), 0.27 (s, 9H). **5g-I1** (830.0 mg, 3.8 mmol) was added to KF (791.6, 13.6 mmol) dissolved in MeOH (19 mL), and the reaction mixture was stirred for 3.5 h at RT. After consumption of **5g-I1**, the reaction mixture was concentrated, and DCM (15 mL) and water (12 mL) were added. The organic layer was collected, dried (Na₂SO₄), and filtered through a short silica plug (70 mL of DCM). The resulting product was concentrated in vacuo to afford 1-ethynyl-3-nitrobenzene **5g-I2** as brown oil (513 mg, 92%). ¹H NMR (400 MHz, Chloroform-d): δ 8.34 (t, J = 2.1 Hz, 1H), 8.21 (ddd, J = 8.0, 2.1, 1.2 Hz, 1H), 7.79 (dt, J = 8.0, 1.2 Hz, 1H), 7.52 (t, J = 8.0 Hz, 1H), 3.22 (s, 1H). Trimethylsilyl azide (0.69 mL, 5.23 mmol) was added to a DMF and MeOH solution (7 mL, 9:1) of CuI (33.2 mg, 0.17 mmol) and **5g-I2** (513 mg, 3.49 mmol), under N₂ in a pressure vial. The reaction mixture was stirred at 100 °C for 5 h. The mixture was cooled to RT, filtered and concentrated in vacuo to afford **5g** as brown solid (135 mg, 12%). LC-MS (ESI): m/z 191.1 [M+1]⁺,

purity > 95% (UV). ¹H NMR (400 MHz, Chloroform-d): δ 8.68 (s, 1H), 8.26 – 8.16 (m, 2H), 8.08 (s, 1H), 7.65 (t, J = 8.0 Hz, 1H). ¹³C NMR (151 MHz, Chloroform-d): δ 130.97, 129.37, 129.01, 123.28, 122.31, 120.20, 119.98, 118.62.

(1-(3-Iodophenyl)-1H-1,2,3-triazole) (5h). The compound was synthesized in two steps. 3-iodoaniline (500 mg, 2.28 mmol) was suspended in water (2 mL). Concentrated aqueous HCl (2 mL) was added and the solution was cooled at 0 °C. A solution of NaNO₂ (189.0, 2.74 mmol) in water (3 mL) was added dropwise at 0 °C and the mixture was further stirred for 20 min. A solution of NaN₃ (223 mg, 3.42 mmol) in water (3 mL) was added dropwise at 0 °C and the obtained suspension was stirred for 2 h. The solution was extracted with of Et₂O (8 mL); the organic phase was washed with brine (8 mL), dried over MgSO₄, filtered, and concentrated in vacuo to afford 1-azido-3-iodobenzene **5h-I1** as yellow oil (561 mg, quantitative). ¹H NMR (400 MHz, Chloroform-d): δ 7.47 (dt, J = 7.9, 1.2 Hz, 1H), 7.38 (t, J = 2.1 Hz, 1H), 7.07 (t, J = 7.9 Hz, 1H), 6.99 (ddd, J = 7.9, 2.1, 1.2 Hz, 1H). A solution of **5t-I1** (561 mg, 2.29 mmol), propiolic acid (0.21 mL, 3.43 mmol), CuI (87.2 mg, 0.46 mmol), sodium ascorbate (181.4 mg, 0.92 mmol), and DBU (0.17 mL, 1.14 mmol) in DMF (20 mL) in a sealed tube was stirred under N₂ at 60 °C for 7 h. After consumption of 5h, the mixture was diluted with water (60 mL), extracted with DCM (3 × 40 mL), washed with water, dried over Na₂SO₄ and concentrated in vacuo. Purification by flash chromatography (heptane:EtOAc, 0–100% gradient) to furnish **5t** as a yellowish solid (0.120 g, 19%). LC-MS (ESI): m/z 271.9 [M+1]⁺, purity > 95% (UV). ¹H NMR (400 MHz, DMSO-d₆): δ 8.89 (d, J = 1.2 Hz, 1H), 8.31 (t, J = 1.9 Hz, 1H), 8.00 – 7.95 (m, 2H), 7.87 (dt, J = 8.0, 1.2 Hz, 1H), 7.40 (t, J = 8.0 Hz, 1H). ¹³C NMR (101 MHz, DMSO-d₆): δ 138.04, 137.69, 135.01, 132.21, 128.65, 123.82, 119.99, 95.86.

1-(3-Fluorophenyl)-1,2,3-triazole (5i). The compound was synthesized in two steps. 3-fluoroaniline (0.87 mL, 9.0 mmol) was suspended in water (4 mL). Concentrated aqueous HCl (4 mL) was added and the solution was cooled at 0 °C. A solution of NaNO₂ (745.8 mg, 10.8 mmol) in water (11 mL) was added dropwise at 0 °C and the mixture was further stirred for 20 min. A solution of NaN₃ (877.1 mg, 13.5 mmol) in water (11 mL) was added dropwise at 0 °C and the obtained suspension was stirred for 3 h. The solution was extracted with Et₂O (15 mL); the organic phase was washed with brine (10 mL), dried over MgSO₄, filtered and concentrated in vacuo to afford 1-azido-3-fluorobenzene **5i-I1** as a yellow oil (632 mg, 51% yield). ¹H NMR (400 MHz, Chloroform-d): δ 7.35 – 7.27 (m, 1H), 6.89 – 6.80 (m, 2H), 6.74 (dt, J = 9.6, 2.3 Hz, 1H). A solution of **5i-I1** (632.0 mg, 4.61 mmol), propiolic acid (0.43 mL, 6.91 mmol), CuI (175.6 mg, 0.92 mmol), sodium ascorbate (365.3 mg, 1.84 mmol), and DBU (0.34 mL, 2.30 mmol) in DMF (22 mL) in a sealed tube was stirred under N₂ at 60 °C for 7 h. Then the mixture was diluted with brine (100 mL) and extracted with EtOAc (3 x 50 mL). The organic layers were washed with brine, dried over MgSO₄ and concentrated in vacuo. The residue was purified by silica flash column chromatography (heptane/EtOAc) and freeze-dried to afford **5i** as a yellow powder (166 mg, 22%). LC-MS (ESI) m/z: 164.0 [M+H]⁺ (3.524 min). ¹H NMR (400 MHz, Chloroform-d): δ 8.00 (d, J = 1.2 Hz, 1H), 7.87 (d, J = 1.2 Hz, 1H), 7.58 – 7.44 (m, 3H), 7.20 – 7.11 (m, 1H). ¹³C NMR (101 MHz, Chloroform-d): δ 134.69, 131.23 (d, J = 8.9 Hz), 121.65, 115.96 (d, J = 3.4 Hz), 115.70 (d, J = 21.0 Hz), 108.48 (d, J = 26.0 Hz).

3-(1,2,3-Triazol-1-yl)benzoic acid (5j). The compound was synthesized in three steps. Ethyl-3-aminobenzoate (0.45 mL, 3.0 mmol) was suspended in water (3 mL). Concentrated aqueous HCl (3 mL) was added and the solution was cooled at 0 °C. A solution of NaNO₂ (251.1 mg, 3.6 mmol) in water (3.5 mL) was added dropwise at 0 °C and the mixture was further stirred for 20 min. A solution of NaN₃ (292.5 mg, 4.5 mmol) in water (4.5 mL) was added dropwise at 0 °C and the obtained suspension was stirred for 3 h. The solution was extracted with

Et₂O (10 mL); the organic phase was washed with brine (8 mL), dried over MgSO₄, filtered and concentrated in vacuo to afford ethyl-3-azidobenzoate **5j-I1** as a brown oil (453 mg, 79%). ¹H NMR (400 MHz, Chloroform-d): δ 7.81 (dt, J = 7.9, 1.1 Hz, 1H), 7.70 (t, J = 2.2 Hz, 1H), 7.41 (t, J = 7.9 Hz, 1H), 7.18 (ddd, J = 7.9, 2.2, 1.1 Hz, 1H), 4.38 (q, J = 7.1 Hz, 2H), 1.40 (t, J = 7.1 Hz, 3H). A solution of **5j-I1** (100.0 mg, 0.52 mmol), propiolic acid (0.05 mL, 0.79 mmol), CuI (20.0 mg, 0.11 mmol), sodium ascorbate (41.4 mg, 0.21 mmol), and DBU (0.04 mL, 0.26 mmol) in DMF (4 mL) in a sealed tube was stirred under N₂ at 60 °C for 3 h. Then, the mixture was diluted with water (15 mL), extracted with DCM (3 x 10 mL), washed with water, dried over MgSO₄ and concentrated in vacuo to afford ethyl 3-(1,2,3-triazol-1-yl) benzoate **5j-I2** as a brown oil (76 mg, 67%). ¹H NMR (400 MHz, Chloroform-d): δ 8.36 (t, J = 1.9 Hz, 1H), 8.12 (dt, J = 7.8, 1.3 Hz, 1H), 8.09 (s, 1H), 8.04 (dd, J = 2.4, 1.1 Hz, 1H), 7.89 (s, 1H), 7.63 (t, J = 7.9 Hz, 1H), 4.43 (q, J = 7.1 Hz, 2H), 1.42 (t, J = 7.1 Hz, 3H). **5j-I2** (76.0 mg, 0.35 mmol) was dissolved in MeOH (1 mL) and treated with a solution of potassium hydroxide (39.3 mg, 0.7 mmol), then stirred for 2.5 h. A solution of 1 M HCl (2 mL) was added to acidify the reaction mixture and the carboxylic acid was extracted with EtOAc (3 mL). The organic phase was collected, dried over MgSO₄, filtered and concentrated in vacuo. The brown residue was purified by silica flash column chromatography (DCM/MeOH) to afford **5j** yellow solid (32 mg, 49%). LC-MS (ESI) m/z: 190.1 [M+H]⁺ (2.590 min). ¹H NMR (600 MHz, DMSO-d₆): δ 13.42 (s, 1H), 8.97 (d, J = 1.2 Hz, 1H), 8.43 (t, J = 2.2 Hz, 1H), 8.18 (ddd, J = 7.9, 2.2, 1.2 Hz, 1H), 8.04 (dt, J = 7.9, 1.2 Hz, 1H), 8.01 (d, J = 1.2 Hz, 1H), 7.75 (t, J = 7.9 Hz, 1H). ¹³C NMR (101 MHz, DMSO-d₆): δ 135.09, 130.80, 129.59, 124.64, 123.88, 120.98.

5-(2-Furanyl)-1,3,4-oxadiazole-2-amine (6e). To a stirred solution of semicarbazide hydrochloride (348.2 mg, 3.12 mmol) and sodium acetate (256.1 mg, 3.12 mmol) in water (6 mL), was added a solution of furfural (0.26 mL, 3.12 mmol) in MeOH (6 mL). After being stirred at RT for 10 min, the solvent was evaporated under

reduced pressure, and the resulting residue was redissolved in 1,4-dioxane (31 mL), followed by addition of potassium carbonate (1.3 g, 9.3 mmol) and iodine (951 mg, 3.7 mmol) in sequence. The reaction mixture was stirred at 80 °C for 3 h. After being cooled to RT, the mixture was treated with 5% Na₂S₂O₃ (120 mL) and extracted with DCM/MeOH (10:1, 60 mL x 4). The combined organic layers were dried over anhydrous MgSO₄ and concentrated in vacuo. The residue was purified by silica flash column chromatography (heptane/EtOAc) to afford **6e** as white solid (259 mg, 55%). LC-MS (ESI) m/z: 152.0 [M+H]⁺ (1.824 min). ¹H NMR (400 MHz, DMSO-d₆): δ 7.92 (d, J = 1.8 Hz, 1H), 7.30 (s, 2H), 7.00 (dd, J = 3.5, 0.7 Hz, 1H), 6.71 (dd, J = 3.5, 1.8 Hz, 1H). ¹³C NMR (101 MHz, DMSO): δ 163.74, 151.10, 145.77, 139.86, 112.56, 111.59.

Synthesis of compounds 8 and 8a-ai (Schemes S1-7)

General procedure A: Pyrazole synthesis.³² A MW vial was charged with the β -keto ester (1.4 equiv.) and DMF-dimethyl acetal (1.6 equiv.). The vial was capped and subjected to MW irradiation at 130 °C for 15 min. Upon cooling, the mixture was transferred to a round-bottomed flask, dissolved in EtOH (X-X mL) and then phenylhydrazine hydrochloride (1.0 equiv.) and Et₃N (3.6 equiv.) were added. The mixture was stirred at RT for 16-22 h until complete conversion as seen by TLC or LC-MS. The mixture was then diluted with EtOAc (10-25 mL), washed with water (10-25 mL), 0.5 M HCl (5-15 mL), sat. brine (5-15 mL), dried over Na₂SO₄ and concentrated in vacuo. Purification by flash column chromatography (hep:EtOAc).

General procedure B1: Ullmann-type coupling of sulfonamide to aryl bromides. An Ullmann-type coupling procedure reported by Deng et al. was followed.⁸¹ A dry MW vial was charged with benzenesulfonamide (0.19 g, 1.20 mmol, 1.2 equiv.), CuI (0.038 g, 0.20 mmol, 0.2 equiv.), dimethylglycine (0.021 g, 0.20 mmol, 0.2 equiv.) and K₃PO₄ (0.53 g, 2.50 mmol, 2.5 equiv.). The vial was capped and subjected to three vacuum-N₂ cycles. Under N₂ was then added a degassed solution of the aryl bromide (1.00 mmol, 1.0 equiv.) in dry DMF (2.0 mL) via a syringe. The mixture was stirred at 160 °C for 20–67 h until complete conversion. The mixture was then cooled to RT, diluted with EtOAc (20 mL), filtered through a bed of celite and the filtrate concentrated in vacuo. Purification by flash column chromatography (hep:EtOAc) afforded the pure products.

General procedure B2: Ullmann-type coupling of pyrazole to aryl sulfonamide. A dry MW vial was charged with aryl aryl halide (1.0 equiv.), ethyl 1H-pyrazole-4-carboxylate (2.0-2.2 equiv.), CuI (0.4-0.8 equiv.), K₂CO₃ (3.0 equiv.), dimethylglycine (0.1 equiv.) and dry degassed DMF. The vial was capped and subjected to three

vacuum-Ar cycles. The mixture was subjected to MW irradiation at 165 °C for 2-3 h until complete conversion as seen by TLC (hep:EtOAc 1:1). The mixture was then diluted with EtOAc (10 mL), filtered through a bed of celite, and the filtrate concentrated in vacuo.

General procedure C: Basic ester hydrolysis. A vial was charged with the ester (1.0 equiv., 0.5–1.0 mmol), either MeOH (if methyl ester, 0.1 M) or EtOH (if ethyl ester, 0.1 M) and then aq. 1 M NaOH (4.0–7.0 equiv.). The mixture was stirred at RT for 15–48 h until complete conversion. Unless otherwise stated, the mixture was then added water (10 mL/mmol), pH adjusted to 1–2 with 1 M HCl, extracted with EtOAc (3 x 20 mL/mmol), and the combined organic phases dried over Na₂SO₄ and concentrated in vacuo. Purification were carried out as specified.

General procedure D: MW-assisted *N*-sulfonylation. A microwave vial was charged with the aryl amine (1.0 equiv., 1.0–5.0 mmol), pyridine (2.0 equiv.), DCM (0.2–1.0 M) and then the benzenesulfonyl chloride (1.0–2.0 equiv.). The vial was capped and subjected to microwave irradiation at 50 °C for 5–20 min until complete conversion (as determined by TLC). The mixture was then added 2 M HCl (10 mL/mmol), extracted with DCM (2–3 times with 10 mL/mmol), and the combined organic phases dried over Na₂SO₄ and concentrated in vacuo. Purification by flash column chromatography (hep:EtOAc) afforded the pure sulfonamides.

General procedure E: Sulfonamide *N*-alkylation with alkyl bromides. NaH (2.0-8.0 equiv.) was added to a solution of the sulfonamide cmpd (1.0 equiv.) in THF (5-20 mL) at 0 °C. After stirring for 1 h, the alkylating agent (3.0-8.0 equiv.) was added. The mixture was stirred for 16 h at RT and then quenched with sat. NaHCO₃ (5-20

mL). The two phases were separated. The aq. phase was extracted with EtOAc (2 x 5-20 mL). The combined organic phases were washed with NaHCO₃ (2 x 5-20 mL), dried with Na₂SO₄, and concentrated in vacuo. Purification were carried out as specified.

General procedure F: Preparation of benzenesulfonamides. The benzenesulfonyl chloride (1.0 eq.) was dissolved in the minimum amount of acetone, and the solution was added to concentrated aqueous ammonia (5 mL) under stirring at RT. The reaction mixture was stirred for 10 min - 2 h, followed by separation of the solid by filtration. In case of no separation, the mixture was neutralized with 2 M HCl to obtain precipitation of the product. The compounds were used without any further purification.

General procedure G1: Primary amidation of carboxylic acids. In a round bottom flask were dissolved HATU (1.3 eq.) and the acid (1.0 eq.) in DMF (X mL), then DIPEA (3.0 eq.) was added. The reaction was stirred at RT for 15 min, followed by addition of ammonium chloride (2.0 eq.). The reaction was stirred for 2 h at RT and quenched with saturated ammonium chloride. The mixture was extracted with ethyl acetate and the organic layer dried over Na₂SO₄, filtered, and concentrated in vacuo. The crude product was purified by preparative HPLC.

General procedure G2: Primary amidation of carboxylic acids. The amide (1.0 eq.), EDC hydrochloride (1.6 eq.), HOBt (1.6 eq.) were dissolved in DMF (X ml) at 0°C, followed by addition of DIPEA (4.0 eq.). The mixture was stirred at 0°C for 1.5 h, then ammonium chloride (2.0 eq.) was added and reaction stirred at RT for 22 h. The reaction was quenched with 2 M HCl, and mixture extracted with ethyl acetate. Organic layer washed with

brine and dried over sodium sulphate, filtered, and concentrated in vacuo. The compounds were used without any further purification.

Compound 8 (Scheme 1)

5-Cyclopropyl-1-(3-(phenylsulfonamido)phenyl)-1H-pyrazole-4-carboxylic acid (8). General procedure C was followed starting from the ester **12** (0.41 g, 1.00 mmol). Complete conversion was seen after 28 h by LC-MS. Workup was omitted, and the mixture was concentrated in vacuo. Purification by preparative HPLC afforded **8** as a white solid (0.063 g, 0.16 mmol, 17%). ¹H NMR (400 MHz, DMSO-d₆) δ 12.32 (s, 1H), 10.60 (s, 1H), 7.90 (s, 1H), 7.84 – 7.74 (m, 2H), 7.66 – 7.58 (m, 1H), 7.59 – 7.51 (m, 2H), 7.45 – 7.34 (m, 1H), 7.29 – 7.23 (m, 2H), 7.21 (ddd, J = 8.1, 2.1, 1.1 Hz, 1H), 1.85 (tt, J = 8.6, 5.5 Hz, 1H), 0.77 – 0.55 (m, 2H), 0.48 – 0.27 (m, 2H). ¹³C NMR (101 MHz, DMSO-d₆) δ 163.69, 146.86, 142.01, 139.70, 139.17, 138.21, 133.07, 129.74, 129.32, 126.63, 120.90, 119.50, 116.50, 114.24, 8.01, 6.89. LC-MS (ESI): m/z 384.1 [M+1]⁺, t_R = 2.67 min, purity > 95% (UV).

Ethyl 5-cyclopropyl-1-(3-(phenylsulfonamido)phenyl)-1H-pyrazole-4-carboxylate (12). General procedure B1 was followed with aryl bromide **10** (0.34 g, 1.00 mmol). Complete conversion was seen after 20 h by LC-MS, and purification afforded ethyl 5-cyclopropyl-1-(3-(phenylsulfonamido)-phenyl)-1H-pyrazole-4-carboxylate (**12**) as a white solid (0.41 g, 1.00 mmol, quantitative). LC-MS (ESI): m/z 412.2 [M+1]⁺, t_R = 3.44 min, purity ≈ 82% (UV).

Ethyl 1-(3-bromophenyl)-5-cyclopropyl-1H-pyrazole-4-carboxylate (10). General procedure A was followed with ethyl 3-cyclopropyl-3-oxopropanoate (1.47 mL, 10.0 mmol). Purification by flash column chromatography (hep:EtOAc) afforded ethyl 1-(3-bromophenyl)-5-cyclopropyl-1H-pyrazole-4-carboxylate (**10**) as a golden-brown oil (1.99 g, 5.94 mmol, 85%). ¹H NMR (400 MHz, Chloroform-d) δ 8.00 (s, 1H), 7.73 (t, J = 2.0 Hz, 1H), 7.55 (ddd, J = 8.0, 1.9, 1.1 Hz, 1H), 7.49 (ddd, J = 8.0, 2.0, 1.0 Hz, 1H), 7.35 (t, J = 8.0 Hz, 1H), 4.32 (q, J = 7.1 Hz, 2H), 2.00 – 1.90 (m, 1H), 1.37 (t, J = 7.1 Hz, 3H), 1.02 – 0.92 (m, 2H), 0.68 – 0.54 (m, 2H). LC-MS (ESI): m/z 335.1+337.1 [M+1]⁺ (Br isotope pattern), t_R = 3.91 min, purity > 95% (UV).

Compound 8a-e (Scheme S1)

1-(3-(phenylsulfonamido)phenyl)-1H-pyrazole-4-carboxylic acid (8a). General procedure C was followed starting from the ester **13-I1** (0.050 g, 0.13 mmol). Complete conversion was seen after 30 h by LC-MS, and purification by preparative HPLC afforded **8a** as a white solid (0.027 g, 0.079 mmol, 60%). ¹H NMR (400 MHz, DMSO-d₆) δ 12.63 (s, 1H), 10.58 (s, 1H), 8.89 (s, 1H), 8.07 (s, 1H), 7.86 – 7.75 (m, 2H), 7.71 (t, J = 2.1 Hz, 1H), 7.66 – 7.49 (m, 4H), 7.35 (t, J = 8.1 Hz, 1H), 7.08 (ddd, J = 8.1, 2.2, 0.8 Hz, 1H). ¹³C NMR (101 MHz, DMSO-d₆) δ 163.40, 142.11, 139.54, 139.25, 138.93, 133.07, 131.06, 130.38, 129.34, 126.60, 118.08, 117.25, 114.11, 110.50. LC-MS (ESI): m/z 344.1 [M+1]⁺, t_R = 2.62 min, purity > 95%

Ethyl 1-(3-(phenylsulfonamido)phenyl)-1H-pyrazole-4-carboxylate (13-I1). General procedure B2 was followed with aryl iodide **13** (0.18 g, 0.50 mmol). Purification by flash column chromatography (hep:EtOAc) afforded ethyl 1-(3-(phenylsulfonamido)phenyl)-1H-pyrazole-4-carboxylate (**13-I1**) as a white solid (0.19 g, 0.22 mmol, 45%). LC-MS (ESI): m/z 372.1 [M+1]⁺, t_R = 3.28 min, purity > 95% (UV).

1-(3-Amino-5-(phenylsulfonamido)phenyl)-1H-pyrazole-4-carboxylic acid (8b). General procedure C was followed starting from the ester **18** (0.063 g, 0.15 mmol). Complete conversion was seen after 18 h by LC-MS, and purification by preparative HPLC afforded **8b** as a white solid (0.026 g, 0.079 mmol, 67%). ¹H NMR (600 MHz, DMSO-d₆) δ 12.74 (s, 1H), 11.20 (s, 1H), 9.22 (s, 1H), 8.45 (t, J = 2.0 Hz, 1H), 8.15 (s, 1H), 8.13 (t, J = 2.0 Hz, 1H), 7.89 (t, J = 2.0 Hz, 1H), 7.86 (t, J = 1.3 Hz, 1H), 7.85 (d, J = 1.5 Hz, 1H), 7.67 – 7.63 (m, 1H), 7.61 – 7.57 (m, 2H). ¹³C NMR (151 MHz, DMSO-d₆) δ 163.23, 149.11, 142.87, 140.24, 140.08, 138.75, 133.58, 132.23, 129.65, 126.64, 118.01, 114.88, 111.31, 108.65. LC-MS (ESI): m/z 387.1 [M-1]⁻, t_R = 2.83 min, purity > 95% (UV).

1-(3-Nitro-5-(phenylsulfonamido)phenyl)-1H-pyrazole-4-carboxylic acid (8c). General procedure C was followed starting from the ester **8c-I1** (0.023 g, 0.07 mmol). Complete conversion was seen after 6 h by LC-MS. The crude was concentrated in vacuo, dissolved in 6 mL buffer A and B (2:1), pH adjusted to 4-5 and purification by preparative HPLC afforded **8c** as a white solid (0.010 g, 0.03 mmol, 40%). ¹H NMR (600 MHz, DMSO-d₆) δ 10.26 (s, 1H), 8.54 (s, 1H), 8.00 (s, 1H), 7.80 (dd, J = 7.2, 1.7 Hz, 2H), 7.63 – 7.59 (m, 1H), 7.56 (dd, J = 8.3, 6.8 Hz, 2H), 6.79 (t, J = 2.0 Hz, 1H), 6.71 (t, J = 2.0 Hz, 1H), 6.41 (t, J = 1.9 Hz, 1H). ¹³C NMR (151 MHz, DMSO-d₆) δ 163.45, 149.63, 141.71, 140.11, 139.54, 139.41, 132.90, 130.34, 129.24, 126.64, 116.82, 103.77, 100.65, 98.84. LC-MS (ESI): m/z 359.1 [M+1]⁺, t_R = 2.35 min, purity > 95% (UV).

Ethyl 1-(3-amino-5-(phenylsulfonamido)phenyl)-1H-pyrazole-4-carboxylate (8c-I1). *N*-(3-bromo-5-nitrophenyl)benzenesulfonamide **17** (0.10 g, 0.24 mmol) was dissolved in 40 mL EtOH, which was reduced by H-Cube (2 bar, RT, 1 mL/min) with Pd/C as catalyst to afford aniline intermediate **8c-I1** (0.045 g, 0.12 mmol,

49%). After concentration in vacuo the crude was used without further purification. LC-MS (ESI): m/z 385.1 [M-1]⁻, t_R = 2.90 min, purity > 80% (UV).

Ethyl 1-(3-nitro-5-(phenylsulfonamido)phenyl)-1H-pyrazole-4-carboxylate (18). General procedure B2 was followed with *N*-(3-bromo-5-nitrophenyl)benzenesulfonamide **17** (0.36 g, 1.0 mmol). Purification by flash column chromatography (hep:EtOAc) afforded **18** as a white solid (0.16 g, 0.37 mmol, 37%). LC-MS (ESI): m/z 415.1 [M-1]⁻, t_R = 3.45 min, purity > 95% (UV).

***N*-(3-Bromo-5-nitrophenyl)benzenesulfonamide (17).** General procedure D was followed with 3-bromo-5-nitroaniline **16** (0.75 g, 3.45 mmol). Purification by flash column chromatography (hep:EtOAc) afforded *N*-(3-bromo-5-nitrophenyl)benzenesulfonamide (**17**) as a yellowish solid (0.88 g, 2.46 mmol, 71%). ¹H NMR (600 MHz, DMSO-d₆) δ 11.18 (s, 1H), 8.02 (t, J = 1.9 Hz, 1H), 7.93 (t, J = 2.0 Hz, 1H), 7.86 – 7.81 (m, 2H), 7.70 – 7.65 (m, 1H), 7.64 – 7.58 (m, 3H). LC-MS (ESI): m/z 356.9 [M-1]⁻, t_R = 3.41 min, purity > 95% (UV).

3-Bromo-5-nitroaniline (16).⁸² The 1-bromo-3,5-dinitrobenzene **15** (2470.0 mg, 10.0 mmol) was dissolved in THF (50 mL) and PMDS (2.7 mL, 20.0 mmol) and Fe(acac)₃ (706.0 mg, 2.0 mmol) were added. The mixture was stirred at 70 °C for 48 h. Upon complete reaction, EtOAc (50 mL) was added and washed with 1 M NaOH aqueous solution (2 x 50 mL), dried over Na₂SO₄, and concentrated in vacuo. Purification by flash column chromatography (hep:EtOAc) afforded 3-bromo-5-nitroaniline **16** as a yellow solid (1.76 g, 8.1 mmol, 81%). ¹H NMR (600 MHz, Chloroform-d) δ 7.70 (t, J = 1.8 Hz, 1H), 7.41 (t, J = 2.1 Hz, 1H), 7.08 (t, J = 1.9 Hz, 1H), 4.06 (s, 2H). LC-MS (ESI): m/z 216.9.1 [M-1]⁻, t_R = 3.07 min, purity > 90% (UV).

1-Bromo-3,5-dinitrobenzene (15). 1,3-Dinitrobenzene (**14**) (8405.5 mg, 50.0 mmol) was dissolved in sulfuric acid (15.0 mL, 280.0 mmol) and NBS (10679.4 mg, 60.0 mmol) was added. The mixture was stirred at 60 °C for 48 h. The reaction was cooled to RT and the mixture was poured into ice water to form a precipitate. The product was collected by filtration, washed with water. Purification by flash column chromatography (hep:EtOAc) afforded 1-bromo-3,5-dinitrobenzene **15** as a beige solid (5.33 g, 21.6 mmol, 43%). ¹H NMR (600 MHz, DMSO-d₆) δ 8.84 (d, J = 2.0 Hz, 2H), 8.80 (t, J = 2.0 Hz, 1H).

1-(3-(Phenylsulfonamido)-5-(trifluoromethyl)phenyl)-1H-pyrazole-4-carboxylic acid (8d). General procedure C was followed starting from the ester **8d-I1** (0.11 g, 0.25 mmol). Complete conversion was seen after 20 h by LC-MS, and purification of half of the amount by preparative HPLC afforded **8d** as a white solid (0.045 g, 0.11 mmol, ~88%). ¹H NMR (600 MHz, DMSO-d₆) δ 12.72 (s, 1H), 11.03 (s, 1H), 9.17 (s, 1H), 8.12 (s, 1H), 8.04 – 7.99 (m, 2H), 7.85 – 7.79 (m, 2H), 7.67 – 7.61 (m, 1H), 7.59 (dd, J = 8.3, 6.9 Hz, 2H), 7.34 (d, J = 1.7 Hz, 1H). ¹³C NMR (151 MHz, DMSO-d₆) δ 163.30, 142.65, 140.32, 139.97, 138.77, 133.49, 132.01, 131.21 (q, J = 32.6 Hz), 129.57, 126.63, 123.22 (q, J = 273.0 Hz), 117.81, 113.44 (d, J = 4.1 Hz), 113.12, 110.59 (d, J = 4.1 Hz). LC-MS (ESI): m/z 410.1 [M-1]⁻, t_R = 3.05 min, purity > 95% (UV).

Ethyl 1-(3-(phenylsulfonamido)-5-(trifluoromethyl)phenyl)-1H-pyrazole-4-carboxylate (8d-I1). General procedure B2 was followed with *N*-(3-Bromo-5-(trifluoromethyl)phenyl)benzenesulfonamide **21** (0.11 g, 1.0 mmol). Purification by flash column chromatography (hep:EtOAc) afforded **8d-I1** as a white solid (0.16 g, 0.33 mmol, 33%). LC-MS (ESI): m/z 440.1 [M+1]⁺, t_R = 3.64 min, purity > 95% (UV).

***N*-(3-Bromo-5-(trifluoromethyl)phenyl)benzenesulfonamide (21)**. General procedure D was followed with 3-bromo-5-(trifluoromethyl)aniline **19** (1.20 g, 5.0 mmol). Purification by flash column chromatography (hep:EtOAc) afforded **21** as a white crystals (0.486 g, 1.3 mmol, 26%). ¹H NMR (600 MHz, DMSO-d₆) δ 11.01 (s, 1H), 7.85 – 7.77 (m, 2H), 7.69 – 7.64 (m, 1H), 7.63 – 7.58 (m, 3H), 7.51 (t, J = 1.9 Hz, 1H), 7.38 (t, J = 1.8 Hz, 1H). ¹³C NMR (151 MHz, DMSO-d₆) δ 140.17, 138.61, 133.58, 131.59 (q, J = 32.7 Hz), 129.62, 126.62, 125.43, 125.15, 123.61, 122.98 (q, J = 3.8 Hz), 122.82, 121.80, 119.99, 114.23 (q, J = 3.9 Hz). LC-MS (ESI): m/z 380.1 [M+0]⁺, 381.9 [M+2]⁺, t_R = 3.71 min, purity > 95% (UV).

1-(3-Chloro-5-(phenylsulfonamido)phenyl)-1H-pyrazole-4-carboxylic acid (8e). General procedure C was followed starting from the ester **8e-I1** (0.12 g, 0.30 mmol). Complete conversion was seen after 24 h by LC-MS, and purification by preparative HPLC afforded **8e** as a white solid (0.030 g, 0.11 mmol, 37%). ¹H NMR (600 MHz, DMSO-d₆) δ 12.71 (s, 1H), 10.87 (s, 1H), 9.01 (s, 1H), 8.09 (s, 1H), 7.85 – 7.79 (m, 2H), 7.76 (t, J = 1.9 Hz, 1H), 7.71 (t, J = 2.0 Hz, 1H), 7.67 – 7.61 (m, 1H), 7.59 (dd, J = 8.3, 6.8 Hz, 2H), 7.08 (t, J = 1.9 Hz, 1H). ¹³C NMR (151 MHz, DMSO-d₆) δ 163.34, 142.55, 140.54, 140.19, 138.94, 134.54, 133.44, 131.71, 129.58, 126.64, 117.68, 116.95, 113.81, 108.49. LC-MS (ESI): m/z 376.1 [M-1]⁻, t_R = 2.93 min, purity > 95% (UV).

Ethyl 1-(3-chloro-5-(phenylsulfonamido)phenyl)-1H-pyrazole-4-carboxylate (8e-I1). General procedure B2 was followed with *N*-(3-Bromo-5-chlorophenyl)benzenesulfonamide **22** (0.35 g, 1.0 mmol). Purification by 2x flash column chromatography (hep:EtOAc) afforded **8e-I1** as a white solid (0.12 g, 0.30 mmol, 30%). LC-MS (ESI): m/z 404.1 [M-1]⁻, t_R = 3.57 min, purity > 90% (UV).

***N*-(3-Bromo-5-chlorophenyl)benzenesulfonamide (22)**. General procedure D was followed with 3-bromo-5-chloroaniline **20** (1.03 g, 5.0 mmol). Purification by flash column chromatography (hep:EtOAc) afforded **22** as a beige solid (1.41 g, 4.1 mmol, 81%). ¹H NMR (600 MHz, DMSO-d₆) δ 10.85 (s, 1H), 7.83 – 7.77 (m, 2H), 7.69 – 7.64 (m, 1H), 7.63 – 7.57 (m, 2H), 7.37 (t, J = 1.8 Hz, 1H), 7.21 (t, J = 1.8 Hz, 1H), 7.12 (t, J = 1.9 Hz, 1H). ¹³C NMR (151 MHz, DMSO-d₆) δ 140.41, 138.75, 134.62, 133.49, 129.59, 126.60, 125.94, 122.55, 120.23, 117.71. LC-MS (ESI): m/z 346.0 [M-1]⁻, t_R = 3.62 min, purity > 95% (UV).

Compound 8f-i (Scheme S2)

5-Cyclopropyl-1-(3-(*N*-methylphenylsulfonamido)phenyl)-1H-pyrazole-4-carboxylic acid (8f). General procedure C was followed starting from the ester **23** (0.085 g, 0.20 mmol). Complete conversion was seen after 18 h by LC-MS, and the mixture was acidified and filtrated. The filtrate was washed with water/can (1:1) to afford **8f** as a white solid (0.052 mg, 0.13 mmol, 65%). ¹H NMR (600 MHz, DMSO-d₆) δ 12.34 (s, 1H), 7.93 (s, 1H), 7.71 (tt, J = 7.0, 1.6 Hz, 1H), 7.61 – 7.54 (m, 5H), 7.54 – 7.50 (m, 2H), 7.35 (q, J = 1.5 Hz, 1H), 7.30 – 7.23 (m, 1H), 3.22 (s, 4H), 1.97 (tt, J = 8.6, 6.3 Hz, 1H), 0.83 – 0.77 (m, 2H), 0.51 – 0.47 (m, 2H). ¹³C NMR (151 MHz, DMSO-d₆) δ 164.20, 147.62, 142.55, 141.86, 140.00, 136.30, 133.93, 129.84, 129.78, 127.80, 126.09, 124.47, 123.16, 114.72, 38.21, 8.59, 7.32. LC-MS (ESI): m/z 398.2 [M+1]⁺, t_R = 2.97 min, purity > 95% (UV).

Ethyl 5-cyclopropyl-1-(3-(*N*-methylphenylsulfonamido)phenyl)-1H-pyrazole-4-carboxylate (23). General procedure E was followed with ethyl 5-cyclopropyl-1-(3-(phenylsulfonamido)phenyl)-1H-pyrazole-4-carboxylate (**12**) (0.099 g, 0.24 mmol) and methyl iodide (0.046 mL, 0.72 mmol). Purification by flash column

chromatography (hep:EtOAc) afforded **23** as a colorless oil (0.085 g, 0.20 mmol, 83%). LC-MS (ESI): m/z 426.2 $[M+1]^+$, t_R = 3.67 min, purity > 90% (UV).

5-Cyclopropyl-1-(3-(*N*-ethylphenylsulfonamido)phenyl)-1H-pyrazole-4-carboxylic acid (8g). General procedure C was followed starting from the ester **24** (0.070 g, 0.16 mmol). Complete conversion was seen after 24 h by LC-MS, and purification by preparative HPLC afforded **8g** as a white solid (0.047 g, 0.11 mmol, 71%). ¹H NMR (600 MHz, DMSO-*d*₆) δ 7.94 (s, 1H), 7.73 – 7.67 (m, 1H), 7.65 – 7.50 (m, 7H), 7.33 (t, J = 2.0 Hz, 1H), 7.17 (dt, J = 7.8, 1.6 Hz, 1H), 3.69 (q, J = 7.1 Hz, 2H), 1.98 (tt, J = 8.6, 5.5 Hz, 1H), 1.02 (t, J = 7.1 Hz, 3H), 0.83 – 0.74 (m, 2H), 0.50 – 0.42 (m, 2H). ¹³C NMR (151 MHz, DMSO-*d*₆) δ 164.20, 147.60, 142.55, 140.15, 139.15, 138.08, 133.69, 130.00, 129.80, 128.48, 127.64, 125.86, 125.25, 114.85, 45.42, 14.26, 8.57, 7.25. LC-MS (ESI): m/z 412.2 $[M+1]^+$, t_R = 3.79 min, purity > 95% (UV).

Ethyl 5-cyclopropyl-1-(3-(*N*-ethylphenylsulfonamido)phenyl)-1H-pyrazole-4-carboxylate (24). General procedure E was followed with ethyl 5-cyclopropyl-1-(3-(phenylsulfonamido)phenyl)-1H-pyrazole-4-carboxylate (**12**) (0.099 g, 0.24 mmol) and ethyl iodide (0.058 mL, 0.72 mmol). Purification by flash column chromatography (hep:EtOAc) afforded **24** as a colorless oil (0.071 g, 0.16 mmol, 67%). LC-MS (ESI): m/z 440.2 $[M+1]^+$, t_R = 3.79 min, purity > 90% (UV).

1-(3-(*N*-(Carboxymethyl)phenylsulfonamido)phenyl)-5-cyclopropyl-1H-pyrazole-4-carboxylic acid (8h). General procedure C was followed starting from the ester **25** (0.087 g, 0.18 mmol). Complete conversion was seen after 24 h by LC-MS, and purification by preparative HPLC afforded **8h** as a white solid (0.048 g, 0.11

mmol, 60%). ¹H NMR (600 MHz, DMSO-d₆) δ 7.92 (s, 1H), 7.74 – 7.65 (m, 3H), 7.57 (t, J = 7.7 Hz, 2H), 7.52 – 7.47 (m, 2H), 7.44 (d, J = 2.2 Hz, 1H), 7.30 (dt, J = 6.3, 2.4 Hz, 1H), 4.53 (s, 2H), 1.90 (tt, J = 8.6, 5.4 Hz, 1H), 0.83 – 0.67 (m, 2H), 0.50 – 0.36 (m, 3H). ¹³C NMR (151 MHz, DMSO-d₆) δ 169.83, 163.70, 147.08, 142.09, 139.86, 139.48, 138.35, 133.35, 129.48, 129.30, 127.35, 127.17, 124.58, 124.44, 114.30, 51.93, 8.06, 6.81. LC-MS (ESI): m/z 442.1 [M+1]⁺, tR = 2.60 min, purity > 95% (UV).

Ethyl 5-cyclopropyl-1-(3-(N-(2-ethoxy-2-oxoethyl)phenylsulfonamido)phenyl)-1H-pyrazole-4-carboxylate (25). General procedure E was followed with ethyl 5-cyclopropyl-1-(3-(phenylsulfonamido)phenyl)-1H-pyrazole-4-carboxylate (**12**) (0.099 g, 0.24 mmol) and 2-ethyl bromoacetate (0.080 mL, 0.72 mmol). Purification by flash column chromatography (hep:EtOAc) afforded **24** as a colorless sticky oil (0.086 g, 0.17 mmol, 72%). LC-MS (ESI): m/z 498.2 [M+1]⁺, tR = 3.76 min, purity > 90% (UV).

1-(3-(N-(2-Amino-2-oxoethyl)phenylsulfonamido)phenyl)-5-cyclopropyl-1H-pyrazole-4-carboxylic acid (8i). General procedure C was followed starting from the ester **26** (0.087 g, 0.18 mmol). Complete conversion was seen after 22 h by LC-MS. A large amount of an impurity was observed (1-(3-aminophenyl)-5-cyclopropyl-1H-pyrazole-4-carboxylic acid). Purification by preparative HPLC afforded **8i** as a white solid (0.008 g, 0.02 mmol, 11%). ¹H NMR (600 MHz, DMSO-d₆) δ 7.92 (s, 1H), 7.72 – 7.65 (m, 3H), 7.59 – 7.53 (m, 2H), 7.52 – 7.46 (m, 2H), 7.44 (q, J = 1.6 Hz, 1H), 7.32 – 7.28 (m, 1H), 4.53 (s, 2H), 1.90 (tt, J = 8.6, 5.5 Hz, 1H), 0.78 – 0.71 (m, 2H), 0.46 – 0.40 (m, 2H). LC-MS (ESI): m/z 442.1 [M+1]⁺, tR = 2.62 min, purity > 95% (UV).

Ethyl 1-(3-(*N*-(2-amino-2-oxoethyl)phenylsulfonamido)phenyl)-5-cyclopropyl-1H-pyrazole-4-carboxylate (26).

General procedure E was followed with ethyl 5-cyclopropyl-1-(3-(phenylsulfonamido)phenyl)-1H-pyrazole-4-carboxylate (**12**) (0.099 g, 0.12 mmol) and 2-bromoacetamide (0.099 g, 0.72 mmol). Purification by flash column chromatography (hep:EtOAc) afforded **26** as a colorless oil (0.054 g, 0.17 mmol, 48%). LC-MS (ESI): m/z 469.2 $[M+1]^+$, t_R = 3.03 min, purity > 95% (UV).

Compound 8j-p (Scheme S3)

5-Phenyl-1-(3-(phenylsulfonamido)phenyl)-1H-pyrazole-4-carboxylic acid (8j). General procedure C was followed starting from the ester **8j-I1** (0.11 g, 0.25 mmol). Complete conversion was seen after 16 h by LC-MS. Purification by preparative HPLC afforded **8j** as a white solid (0.063 g, 0.15 mmol, 60%). ^1H NMR (600 MHz, DMSO- d_6) δ 10.47 (s, 1H), 8.11 (s, 1H), 7.69 – 7.65 (m, 2H), 7.65 – 7.61 (m, 1H), 7.55 (t, J = 7.8 Hz, 2H), 7.39 – 7.32 (m, 1H), 7.29 (dd, J = 8.4, 6.9 Hz, 2H), 7.18 – 7.12 (m, 3H), 7.11 (t, J = 2.1 Hz, 1H), 7.02 (dd, J = 8.4, 2.2 Hz, 1H), 6.72 (dd, J = 8.3, 2.1 Hz, 1H). ^{13}C NMR (151 MHz, DMSO- d_6) δ 163.47, 145.04, 142.26, 139.51, 139.03, 138.37, 133.07, 130.26, 129.54, 129.31, 128.94, 128.42, 127.84, 126.57, 121.12, 119.16, 117.07, 114.09. LC-MS (ESI): m/z 420.1 $[M+1]^+$, t_R = 2.85 min, purity > 95% (UV).

Ethyl 5-phenyl-1-(3-(phenylsulfonamido)phenyl)-1H-pyrazole-4-carboxylate (8j-I1). General procedure B1 was followed with aryl bromide **38** (0.62 g, 1.70 mmol). Complete conversion was seen after 20 h by LC-MS. Purification by flash column chromatography (hep:EtOAc) afforded ethyl 5-phenyl-1-(3-(phenylsulfonamido)phenyl)-1H-pyrazole-4-carboxylate (**8j-I1**) as a white solid (0.40 g, 0.90 mmol, 53%). LC-MS (ESI): m/z 448.2 $[M+1]^+$, t_R = 3.51 min, purity > 95% (UV).

Ethyl 1-(3-bromophenyl)-5-phenyl-1H-pyrazole-4-carboxylate (38). General procedure A was followed with ethyl 3-oxo-3-phenylpropanoate **27** (1.11 mL, 4.0 mmol). Purification by two times flash column chromatography (1: hep:EtOAc, 2: DCM:MeOH) afforded ethyl 1-(3-bromophenyl)-5-phenyl-1H-pyrazole-4-carboxylate (**38**) as a yellowish oil (0.62 g, 1.7 mmol, 43%). LC-MS (ESI): m/z 371.1 [M+0]⁺, 373.0 [M+2]⁺, tR = 3.97 min, purity > 90% (UV).

5-(4-Methoxyphenyl)-1-(3-(phenylsulfonamido)phenyl)-1H-pyrazole-4-carboxylic acid (8k). General procedure C was followed starting from the ester **8k-11** (0.12 g, 0.25 mmol). Complete conversion was seen after 16 h by LC-MS. Purification by preparative HPLC afforded **8k** as a white solid (0.074 g, 0.16 mmol, 82%). ¹H NMR (600 MHz, DMSO-d₆) δ 12.30 (s, 1H), 10.48 (s, 1H), 8.09 (s, 1H), 7.72 – 7.66 (m, 2H), 7.66 – 7.60 (m, 1H), 7.58 – 7.51 (m, 2H), 7.16 (t, J = 8.1 Hz, 1H), 7.12 (t, J = 2.1 Hz, 1H), 7.10 – 7.07 (m, 2H), 7.03 (ddd, J = 8.2, 2.2, 1.0 Hz, 1H), 6.87 – 6.82 (m, 2H), 6.74 (ddd, J = 8.0, 2.1, 1.0 Hz, 1H), 3.76 (s, 3H), 2.07 (s, 0H, AcN). ¹³C NMR (151 MHz, DMSO-d₆) δ 163.60, 159.53, 144.99, 142.31, 139.70, 139.09, 138.37, 133.07, 131.70, 129.58, 129.28, 126.58, 121.16, 120.30, 119.11, 117.11, 113.80, 113.36, 55.11. LC-MS (ESI): m/z 450.1 [M+1]⁺, tR = 2.87 min, purity > 95% (UV).

Ethyl 5-(4-methoxyphenyl)-1-(3-(phenylsulfonamido)phenyl)-1H-pyrazole-4-carboxylate (8k-11). General procedure B1 was followed with aryl bromide **39** (0.79 g, 2.0 mmol). Complete conversion was seen after 20 h by LC-MS. Purification by flash column chromatography (hep:EtOAc) afforded ethyl ethyl 5-phenyl-1-(3-

(phenylsulfonamido)phenyl)-1H-pyrazole-4-carboxylate (**8k-11**) as a white solid (0.58 g, 1.21 mmol, 61%). LC-MS (ESI): m/z 478.2 $[M+1]^+$, t_R = 3.47 min, purity > 95% (UV).

Ethyl 1-(3-bromophenyl)-5-(4-methoxyphenyl)-1H-pyrazole-4-carboxylate (39). General procedure A was followed with ethyl 3-(4-methoxyphenyl)-3-oxopropanoate **28** (1.16 mL, 4.0 mmol). Purification by flash column chromatography (DCM:MeOH) afforded ethyl 1-(3-bromophenyl)-5-(4-methoxyphenyl)-1H-pyrazole-4-carboxylate (**39**) as a yellowish oil (0.79 g, 2.0 mmol, 49%). LC-MS (ESI): m/z 401.1 $[M+0]^+$, 403.1 $[M+2]^+$, t_R = 3.91 min, purity > 90% (UV).

5-Benzyl-1-(3-(phenylsulfonamido)phenyl)-1H-pyrazole-4-carboxylic acid (8l). General procedure C was followed starting from the ester **8l-11** (0.046 g, 0.10 mmol). Complete conversion was seen after 16 h by LC-MS. Purification by preparative HPLC afforded **8l** as a white solid (0.044 g, 0.10 mmol, quantitative). 1H NMR (400 MHz, DMSO- d_6) δ 12.57 (s, 1H), 10.59 (s, 1H), 8.02 (s, 1H), 7.75 (dd, J = 7.2, 1.8 Hz, 2H), 7.66 – 7.58 (m, 1H), 7.54 (dd, J = 8.3, 6.7 Hz, 2H), 7.30 (t, J = 8.0 Hz, 1H), 7.22 – 7.12 (m, 2H), 7.09 (p, J = 3.8 Hz, 3H), 6.95 (dd, J = 7.9, 2.0 Hz, 1H), 6.75 – 6.62 (m, 2H), 4.29 (s, 2H). ^{13}C NMR (101 MHz, DMSO- d_6) δ 164.22, 145.11, 141.88, 139.15, 139.13, 138.54, 137.11, 133.14, 130.03, 129.38, 128.28, 127.58, 126.59, 126.26, 120.99, 119.87, 116.92, 113.41, 29.34. LC-MS (ESI): m/z 434.1 $[M+1]^+$, t_R = 2.99 min, purity > 95% (UV).

Ethyl 5-benzyl-1-(3-(phenylsulfonamido)phenyl)-1H-pyrazole-4-carboxylate (8l-11). General procedure B1 was followed with aryl bromide **40** (0.077 g, 0.20 mmol). Complete conversion was seen after 20 h by LC-MS. Purification by flash column chromatography (hep:EtOAc) afforded ethyl ethyl 5-phenyl-1-(3-

(phenylsulfonamido)phenyl)-1H-pyrazole-4-carboxylate (**8k-I1**) as a white solid (0.047 g, 0.1 mmol, 51%). LC-MS (ESI): m/z 462.2 $[M+1]^+$, t_R = 3.64 min, purity > 95% (UV).

Ethyl 5-benzyl-1-(3-bromophenyl)-1H-pyrazole-4-carboxylate (40). General procedure A was followed with ethyl 3-oxo-4-phenylbutanoate **30** (0.21 mg, 1.0 mmol). Purification by flash column chromatography (hep:EtOAc) afforded ethyl 5-benzyl-1-(3-bromophenyl)-1H-pyrazole-4-carboxylate (**40**) as a yellowish oil (0.078 g, 0.20 mmol, 20%). LC-MS (ESI): m/z 385.1 $[M+0]^+$, 387.1 $[M+2]^+$, t_R = 4.08 min, purity > 90% (UV).

Ethyl 3-oxo-4-phenylbutanoate (30).⁸³ *n*-Butyllithium (8.0 ml 2.5 M in hexane, 20.0 mmol) was added slowly to a -78 °C solution of monoethyl malonate **29** (1.18 mL, 10.0 mmol) in 25 ml anhydrous THF, while allowing the temperature to rise to 0 °C near the end of the addition. After 10 min at 0 °C, the mixture was cooled to -78 °C and phenylacetyl chloride (1.32 mL, 10.0 mmol) was added dropwise. Cooling was removed and after 10 min the reaction was quenched with 1 M HCl (aq) (20 ml). The mixture was extracted with diethyl ether (40 ml). The organic extract was washed with sat. NaHCO₃ (aq) (2 x 15 ml), H₂O (15 ml) and brine (15 ml), then dried with Na₂SO₄ and concentrated in vacuo. Evaporation of the solvent yielded the product, as a colourless oil. Purification by flash column chromatography (hep:EtOAc) afforded ethyl 1-(3-bromophenyl)-5-(4-methoxyphenyl)-1H-pyrazole-4-carboxylate (**30**) as a yellowish oil (0.67 g, 2.8 mmol, 57%), which was used without further characterization. LC-MS (ESI): m/z 207.0 $[M+1]^+$, t_R = 3.89 min, purity > 70% (UV).

5-(4-Methoxybenzyl)-1-(3-(phenylsulfonamido)phenyl)-1H-pyrazole-4-carboxylic acid (8m). General procedure C was followed starting from the ester **8m-I1** (0.036 g, 0.07 mmol). Complete conversion was seen

after 16 h by LC-MS. Purification by preparative HPLC afforded **8m** as a white solid (0.033 g, 0.07 mmol, quantitative). ¹H NMR (600 MHz, DMSO-d₆) δ 12.56 (s, 1H), 10.60 (s, 1H), 8.00 (s, 1H), 7.79 – 7.73 (m, 2H), 7.65 – 7.58 (m, 1H), 7.55 (dd, J = 8.5, 7.1 Hz, 2H), 7.32 (t, J = 8.1 Hz, 1H), 7.18 (dd, J = 8.4, 2.1 Hz, 1H), 7.13 (t, J = 2.1 Hz, 1H), 6.95 (dd, J = 7.9, 2.0 Hz, 1H), 6.69 – 6.63 (m, 2H), 6.59 (d, J = 8.7 Hz, 2H), 4.20 (s, 2H), 3.65 (s, 3H). ¹³C NMR (151 MHz, DMSO-d₆) δ 164.26, 157.62, 145.59, 141.87, 139.17, 138.55, 133.17, 130.08, 129.40, 129.01, 128.63, 126.62, 121.05, 119.88, 116.95, 113.74, 113.21, 54.95, 28.47. UPLC-MS (ESI): m/z 464.1 [M+1]⁺, tR = 2.24 min, purity > 95% (UV).

Ethyl 5-(4-methoxybenzyl)-1-(3-(phenylsulfonamido)phenyl)-1H-pyrazole-4-carboxylate (8m-I1). General procedure B1 was followed with aryl bromide **41** (0.083 g, 0.20 mmol). Complete conversion was seen after 24 h by LC-MS. Purification by flash column chromatography (hep:EtOAc) afforded ethyl 5-phenyl-1-(3-(phenylsulfonamido)phenyl)-1H-pyrazole-4-carboxylate (**8k-I1**) as a white solid (0.036 g, 0.07 mmol, 37%; 0.033 g **41** reobtained). UPLC-MS (ESI): m/z 492.1 [M+1]⁺, tR = 2.70 min, purity > 90% (UV).

Ethyl 1-(3-bromophenyl)-5-(4-methoxybenzyl)-1H-pyrazole-4-carboxylate (41). General procedure A was followed with ethyl 4-(4-methoxyphenyl)-3-oxobutanoate **31** (0.59 mg, 2.5 mmol). Purification by flash column chromatography (hep:EtOAc) afforded ethyl 5-benzyl-1-(3-bromophenyl)-1H-pyrazole-4-carboxylate (**41**) as a yellowish oil (0.20 g, 0.48 mmol, 19%). UPLC-MS (ESI): m/z 415.1 [M+0]⁺, 417.1 [M+2]⁺, tR = 2.96 min, purity > 90% (UV).

Ethyl 4-(4-methoxyphenyl)-3-oxobutanoate (31). *n*-Butyllithium (8.0 ml 2.5 M in hexane, 20.0 mmol) was added slowly to a -78 °C solution of monoethyl malonate 29 (1.18 mL, 10.0 mmol) in 25 ml anhydrous THF, while allowing the temperature to rise to 0 °C near the end of the addition. After 10 min at 0 °C, the mixture was cooled to -78 °C and 2-(4-methoxyphenyl)acetyl chloride (0.76 mL, 5.0 mmol) was added dropwise. Cooling was removed and after 10 min the reaction was quenched with 1 M HCl (aq) (20 ml). The mixture was extracted with diethyl ether (40 ml). The organic extract was washed with sat. NaHCO₃ (aq) (2 x 15 ml), H₂O (15 ml) and brine (15 ml), then dried with Na₂SO₄ and concentrated in vacuo. Evaporation of the solvent yielded the product, as a colourless oil. Purification by flash column chromatography (hep:EtOAc) afforded ethyl 4-(4-methoxyphenyl)-3-oxobutanoate (**31**) as a yellowish oil (0.64 g, 3.1 mmol, 31%). UPLC-MS (ESI): *m/z* 237.0 [M+1]⁺ and 526.1 [M+1]⁺, *t*_R = 2.12 min, purity > 95% (UV).

1-(3-(Phenylsulfonamido)phenyl)-5-((phenylthio)methyl)-1H-pyrazole-4-carboxylic acid (8n). General procedure C was followed starting from the ester **8n-I1** (0.054 g, 0.11 mmol). Complete conversion was seen after 20 h by LC-MS. Purification by preparative HPLC afforded **8n** as a white solid (0.023 g, 0.05 mmol, 45%). ¹H NMR (400 MHz, DMSO-*d*₆) δ 12.64 (s, 1H), 10.61 (s, 1H), 7.94 (s, 1H), 7.79 (dd, *J* = 7.2, 1.7 Hz, 2H), 7.64 – 7.56 (m, 1H), 7.52 (dd, *J* = 8.3, 6.6 Hz, 2H), 7.34 (t, *J* = 8.0 Hz, 1H), 7.26 – 7.10 (m, 6H), 7.09 – 6.99 (m, 2H), 4.47 (s, 2H). ¹³C NMR (101 MHz, DMSO-*d*₆) δ 163.81, 142.71, 141.68, 139.21, 139.03, 138.62, 133.88, 133.12, 130.34, 130.11, 129.36, 128.91, 127.08, 126.64, 120.64, 119.96, 116.84, 113.76, 27.00. LC-MS (ESI): *m/z* 466.1 [M+1]⁺, *t*_R = 3.07 min, purity > 95% (UV).

Ethyl 1-(3-(phenylsulfonamido)phenyl)-5-((phenylthio)methyl)-1H-pyrazole-4-carboxylate (8n-I1). General procedure B1 was followed with aryl bromide **42** (0.13 g, 0.30 mmol). Complete conversion was seen after 24 h

by LC-MS. Purification by flash column chromatography (hep:EtOAc) afforded ethyl 1-(3-(phenylsulfonamido)phenyl)-5-((phenylthio)methyl)-1H-pyrazole-4-carboxylate (**8n-I1**) as a white solid (0.058 g, 0.12 mmol, 39%). UPLC-MS (ESI): m/z 494.1 [M+1]⁺, tR = 2.77 min, purity > 90% (UV).

Ethyl 1-(3-bromophenyl)-5-((phenylthio)methyl)-1H-pyrazole-4-carboxylate (42). General procedure A was followed with ethyl 3-oxo-4-(phenylthio)butanoate **33** (0.60 mg, 2.5 mmol). Purification by flash column chromatography (hep:EtOAc) afforded ethyl 1-(3-bromophenyl)-5-((phenylthio)methyl)-1H-pyrazole-4-carboxylate (**42**) as a yellowish oil (0.13 g, 0.31 mmol, 13%). UPLC-MS (ESI): m/z 417.1 [M+0]⁺, 419.1 [M+2]⁺, tR = 3.07 min, purity > 95% (UV).

Ethyl 3-oxo-4-(phenylthio)butanoate (33).⁸⁴ To a mixture of potassium hydroxide (0.85 g, 15.1 mmol) in of DMSO (8 mL) was dropwise added a solution of thiophenol (0.77 mL, 7.6 mmol) in DMSO (1 mL). The mixture was stirred at room temperature for 30 min and then ethyl 4-chloroacetoacetate **32** (1.02 mL, 7.6 mmol) was added. The mixture was stirred at RT for 22 h and then acidified by addition of hydrochloric acid (4 M). The mixture was extracted with EtOAc and the organic layer was washed with water and then with brine, dried over Na₂SO₄, and concentrated in vacuo. Purification by flash column chromatography (hep:EtOAc) afforded ethyl 4-(4-methoxyphenyl)-3-oxobutanoate (**33**) as a yellowish liquid (0.93 g, 3.9 mmol, 51%). LC-MS (ESI): m/z 147.1 [M+1]⁺ and 239.1 [M+1]⁺, tR = 3.42 min, purity > 70% (UV).

5-(trans-2-phenylcyclopropyl)-1-(3-(phenylsulfonamido)phenyl)-1H-pyrazole-4-carboxylic acid (8o). General procedure C was followed starting from the ester **8o-I1** (0.044 g, 0.09 mmol). Complete conversion was seen

after 24 h by LC-MS. Purification by preparative HPLC afforded **8o** as a white solid (0.031 g, 0.07 mmol, 75%). ¹H NMR (600 MHz, DMSO-d₆) δ 12.38 (s, 1H), 10.58 (s, 1H), 7.95 (s, 1H), 7.82 – 7.77 (m, 2H), 7.61 – 7.56 (m, 1H), 7.56 – 7.51 (m, 2H), 7.30 (q, J = 1.5 Hz, 1H), 7.20 – 7.09 (m, 6H), 6.79 – 6.75 (m, 2H), 2.22 (ddd, J = 9.0, 6.2, 5.0 Hz, 1H), 1.93 (dt, J = 8.9, 5.6 Hz, 1H), 1.20 – 1.14 (m, 1H), 0.98 (ddd, J = 8.8, 6.2, 5.2 Hz, 1H). ¹³C NMR (151 MHz, DMSO-d₆) δ 163.70, 145.80, 142.06, 140.94, 139.68, 139.17, 138.42, 133.09, 129.73, 129.35, 127.88, 126.65, 125.72, 125.66, 120.95, 119.29, 116.55, 114.36, 25.63, 18.20, 16.95. LC-MS (ESI): m/z 460.1 [M+1]⁺, tR = 3.14 min, purity > 95% (UV).

Ethyl 5-phenethyl-1-(3-(phenylsulfonamido)phenyl)-1H-pyrazole-4-carboxylate (8o-11). General procedure B1 was followed with aryl bromide **43** (0.16 g, 0.40 mmol). Complete conversion was seen after 48 h by LC-MS. Purification by flash column chromatography (hep:EtOAc) afforded ethyl 5-phenethyl-1-(3-(phenylsulfonamido)phenyl)-1H-pyrazole-4-carboxylate (**8o-11**) as a white solid (0.047 g, 0.10 mmol, 24%). UPLC-MS (ESI): m/z 488.2 [M+1]⁺, tR = 2.87 min, purity > 90% (UV).

Ethyl 1-(3-bromophenyl)-5-(trans-2-phenylcyclopropyl)-1H-pyrazole-4-carboxylate (43). General procedure A was followed with ethyl 3-oxo-4-(phenylthio)butanoate **35** (0.35 mg, 1.5 mmol). Purification by flash column chromatography (hep:EtOAc) afforded ethyl 1-(3-bromophenyl)-5-(trans-2-phenylcyclopropyl)-1H-pyrazole-4-carboxylate (**43**) as a yellowish oil (0.17 g, 0.40 mmol, 27%). LC-MS (ESI): m/z 411.1 [M+0]⁺, 413.1 [M+2]⁺, tR = 4.17 min, purity > 95% (UV).

Ethyl 3-oxo-3-(trans-2-phenylcyclopropyl)propanoate (35).⁸⁵ The acid chloride **35-I1** (0.70 mL, 6.0 mmol) was added dropwise to a solution of Meldrum's acid (0.86 g, 6.0 mmol) and pyridine (0.97 mL, 12.0 mmol) in DCM (12 mL) at 0 °C. The solution was stirred for 30 min at 0 °C and then it was allowed to stir at RT for 24 h. The reaction mixture was washed with 10% aq. HCl (2 x 5 mL) and H₂O (5 mL). The combined organic phases were dried over Na₂SO₄, filtered and concentrated in vacuo. The crude residue was dissolved in EtOH (10 mL) and heated to reflux for 24 h. The mixture was concentrated in vacuo and purified by flash column chromatography (hep:EtOAc) afforded ethyl 3-oxo-3-(trans-2-phenylcyclopropyl)propanoate (**35**) as a yellowish oil (0.46 g, 2.0 mmol, 33%). LC-MS (ESI): m/z 233.1 [M+1]⁺, tR = 3.31 min, purity > 90% (UV).

5-Phenethyl-1-(3-(phenylsulfonamido)phenyl)-1H-pyrazole-4-carboxylic acid (8p). General procedure C was followed starting from the ester **8p-I1** (0.24 g, 0.50 mmol). Complete conversion was seen after 28 h by LC-MS. Purification by preparative HPLC afforded **8p** as a white solid (0.18 g, 0.40 mmol, 81%). ¹H NMR (600 MHz, DMSO-d₆) δ 12.50 (s, 1H), 10.64 (s, 1H), 7.94 (s, 1H), 7.80 – 7.74 (m, 2H), 7.57 – 7.52 (m, 1H), 7.49 (dd, J = 8.4, 7.0 Hz, 2H), 7.38 (t, J = 8.1 Hz, 1H), 7.27 – 7.20 (m, 1H), 7.19 – 7.13 (m, 3H), 7.11 (t, J = 2.1 Hz, 1H), 7.04 – 6.99 (m, 1H), 6.88 – 6.81 (m, 2H), 3.09 – 3.03 (m, 2H), 2.64 – 2.58 (m, 2H). ¹³C NMR (151 MHz, DMSO-d₆) δ 164.15, 146.46, 141.78, 140.07, 139.06, 138.55, 133.10, 130.16, 129.32, 128.26, 127.93, 126.60, 126.12, 121.19, 119.87, 116.94, 112.76, 34.04, 26.30. LC-MS (ESI): m/z 448.2 [M+1]⁺, tR = 3.08 min, purity > 95% (UV).

Ethyl 5-phenethyl-1-(3-(phenylsulfonamido)phenyl)-1H-pyrazole-4-carboxylate (8p-I1). General procedure B1 was followed with aryl bromide **44** (0.40 g, 1.0 mmol). Complete conversion was seen after 52 h by LC-MS. Purification by flash column chromatography (hep:EtOAc) afforded ethyl 5-phenethyl-1-(3-

(phenylsulfonamido)phenyl)-1H-pyrazole-4-carboxylate (**8p-I1**) as a white solid (0.24 g, 0.51 mmol, 51%). UPLC-MS (ESI): m/z 476.1 $[M+1]^+$, t_R = 2.86 min, purity > 90% (UV).

Ethyl 1-(3-bromophenyl)-5-phenethyl-1H-pyrazole-4-carboxylate (44). General procedure A was followed with ethyl 3-oxo-5-phenylpentanoate **37** (0.55 mg, 2.5 mmol). Purification by flash column chromatography (hep:EtOAc) afforded ethyl 1-(3-bromophenyl)-5-phenethyl-1H-pyrazole-4-carboxylate (**44**) as a yellowish oil (0.40 g, 1.0 mmol, 40%). LC-MS (ESI): m/z 399.1 $[M+0]^+$, 401.1 $[M+2]^+$, t_R = 4.24 min, purity > 95% (UV).

Ethyl 3-oxo-5-phenylpentanoate (37). The acid chloride **36** (1.12 mL, 7.6 mmol) was added dropwise to a solution of Meldrum's acid (1.09 g, 7.6 mmol) and pyridine (1.2 mL, 15.1 mmol) in DCM (14 mL) at 0 °C. The solution was stirred for 30 min at 0 °C and then it was allowed to stir at RT for 24 h. The reaction mixture was washed with 10% aq. HCl (2 x 5 mL) and H₂O (5 mL). The combined organic phases were dried over Na₂SO₄, filtered and concentrated in vacuo. The crude residue was dissolved in EtOH (10 mL) and heated to reflux for 24 h. The mixture was concentrated in vacuo and purified by flash column chromatography (hep:EtOAc) afforded ethyl 3-oxo-5-phenylpentanoate (**37**) as a yellowish oil (0.73 g, 3.3 mmol, 43%). LC-MS (ESI): m/z 221.1 $[M+1]^+$, t_R = 3.94 min, purity > 90% (UV).

Compound 8q-y (Scheme S4)

5-Cyclopropyl-1-(3-((2-methoxyphenyl)sulfonamido)phenyl)-1H-pyrazole-4-carboxylic acid (8q). General procedure C was followed starting from the ester **8q-I1** (0.075 g, 0.17 mmol). Complete conversion was seen

after 50 h by LC-MS. Purification by preparative HPLC afforded **8q** as a white solid (0.036 g, 0.09 mmol, 51%). ¹H NMR (400 MHz, DMSO-d₆) δ 12.32 (s, 1H), 10.31 (s, 1H), 7.89 (s, 1H), 7.79 (dd, J = 7.8, 1.7 Hz, 1H), 7.57 (ddd, J = 8.9, 7.4, 1.7 Hz, 1H), 7.35 (t, J = 8.0 Hz, 1H), 7.24 (t, J = 2.1 Hz, 1H), 7.21 – 7.13 (m, 3H), 7.03 (td, J = 7.6, 1.0 Hz, 1H), 3.87 (s, 3H), 1.82 (tt, J = 8.5, 5.5 Hz, 1H), 0.65 – 0.57 (m, 2H), 0.38 – 0.31 (m, 2H). ¹³C NMR (101 MHz, DMSO-d₆) δ 163.74, 156.38, 146.84, 141.96, 139.60, 138.47, 135.26, 130.31, 129.52, 126.08, 120.43, 120.11, 118.89, 115.91, 114.14, 112.89, 56.15, 7.92, 6.89. LC-MS (ESI): m/z 414.1 [M+1]⁺, t_R = 2.71 min, purity > 95% (UV).

Ethyl 5-cyclopropyl-1-(3-((2-methoxyphenyl)sulfonamido)phenyl)-1H-pyrazole-4-carboxylate (8q-I1). General procedure B1 was followed with aryl bromide **10** (0.34 g, 1.0 mmol) and benzenesulfonamide **53** (0.22, 1.2 mmol). Complete conversion was seen after 48 h by LC-MS. Purification by flash column chromatography (hep:EtOAc) afforded **8q-I1** as a yellowish oil (0.078 g, 0.18 mmol, 18%). LC-MS (ESI): m/z 442.2 [M+1]⁺, t_R = 3.39 min, purity > 90% (UV).

5-Cyclopropyl-1-(3-((3-methoxyphenyl)sulfonamido)phenyl)-1H-pyrazole-4-carboxylic acid (8r). General procedure C was followed starting from the ester **8r-I1** (0.093 g, 0.21 mmol). Complete conversion was seen after 48 h by LC-MS. Purification by preparative HPLC afforded **8r** as a white solid (0.059 g, 0.14 mmol, 68%). ¹H NMR (400 MHz, DMSO-d₆) δ 12.34 (s, 1H), 10.56 (s, 1H), 7.91 (s, 1H), 7.47 (t, J = 8.0 Hz, 1H), 7.44 – 7.37 (m, 1H), 7.34 (dt, J = 7.8, 1.2 Hz, 1H), 7.26 (p, J = 2.3, 1.9 Hz, 3H), 7.20 (ddd, J = 11.1, 7.9, 2.3 Hz, 2H), 3.76 (s, 3H), 1.86 (tt, J = 8.6, 5.5 Hz, 1H), 0.73 – 0.65 (m, 2H), 0.43 – 0.37 (m, 2H). ¹³C NMR (101 MHz, DMSO-d₆) δ 163.73, 159.39, 146.92, 142.05, 140.36, 139.73, 138.23, 130.60, 129.79, 121.04, 119.69, 118.86, 118.74, 116.67, 114.28, 111.69, 55.59, 8.02, 6.91. LC-MS (ESI): m/z 414.2 [M+1]⁺, t_R = 2.80 min, purity > 95% (UV).

Ethyl 5-cyclopropyl-1-(3-((3-methoxyphenyl)sulfonamido)phenyl)-1H-pyrazole-4-carboxylate (8r-I1). General procedure B1 was followed with aryl bromide **10** (0.34 g, 1.0 mmol) and benzenesulfonamide **54** (0.22 g, 1.2 mmol). Complete conversion was seen after 25 h by LC-MS. Purification by flash column chromatography (hep:EtOAc) afforded **8r-I1** as a yellowish oil (0.27 g, 0.60 mmol, 60%). LC-MS (ESI): m/z 442.2 [M+1]⁺, tR = 3.47 min, purity > 90% (UV).

5-Cyclopropyl-1-(3-((4-methoxyphenyl)sulfonamido)phenyl)-1H-pyrazole-4-carboxylic acid (8s). General procedure C was followed starting from the ester **8s-I1** (0.13 g, 0.30 mmol). Complete conversion was seen after 40 h by LC-MS. Purification by preparative HPLC afforded **8s** as a white solid (0.39 g, 0.10 mmol, 33%). ¹H NMR (400 MHz, DMSO-d₆) δ 12.33 (s, 1H), 10.44 (s, 1H), 7.90 (s, 1H), 7.76 – 7.68 (m, 2H), 7.39 (t, J = 8.3 Hz, 1H), 7.26 – 7.16 (m, 3H), 7.10 – 7.02 (m, 2H), 3.78 (s, 3H), 1.86 (tt, J = 8.6, 5.5 Hz, 1H), 0.76 – 0.60 (m, 2H), 0.45 – 0.35 (m, 2H). ¹³C NMR (101 MHz, DMSO-d₆) δ 163.73, 162.60, 146.90, 142.02, 139.71, 138.49, 130.77, 129.72, 128.92, 120.76, 119.37, 116.42, 114.45, 114.23, 55.67, 8.00, 6.91. LC-MS (ESI): m/z 414.2 [M+1]⁺, tR = 2.76 min, purity > 95% (UV).

Ethyl 5-cyclopropyl-1-(3-((4-methoxyphenyl)sulfonamido)phenyl)-1H-pyrazole-4-carboxylate (8s-I1). General procedure B1 was followed with aryl bromide **10** (0.34 g, 1.0 mmol) and benzenesulfonamide **55** (0.22 g, 1.2 mmol). Complete conversion was seen after 18 h by LC-MS. Purification by two flash column chromatography separations (hep:EtOAc) afforded **8s-I1** as a yellowish oil (0.13 g, 0.29 mmol, 29%). LC-MS (ESI): m/z 442.2 [M+1]⁺, tR = 3.40 min, purity > 90% (UV).

4-Methoxybenzenesulfonamide (55). General procedure F was followed with 4-methoxybenzenesulfonyl chloride **46** (2.58 g, 12.5 mmol). Filtration afforded **55** as a white solid (1.75 g, 9.3 mmol, 75%). LC-MS (ESI): m/z 188.9 [M+1]⁺, tR = 1.99 min, purity > 95% (UV).

5-Cyclopropyl-1-(3-((3,4-dimethoxyphenyl)sulfonamido)phenyl)-1H-pyrazole-4-carboxylic acid (8t). General procedure C was followed starting from the ester **8t-I1** (0.075 g, 0.16 mmol). Complete conversion was seen after 28 h by LC-MS. Purification by preparative HPLC afforded **8t** as a white solid (0.048 g, 0.11 mmol, 68%). ¹H NMR (400 MHz, DMSO-d₆) δ 12.35 (s, 1H), 10.37 (s, 1H), 7.91 (s, 1H), 7.40 (t, J = 8.0 Hz, 1H), 7.34 (dd, J = 8.5, 2.2 Hz, 1H), 7.29 – 7.18 (m, 4H), 7.07 (d, J = 8.5 Hz, 1H), 3.78 (s, 3H), 3.74 (s, 3H), 1.88 (tt, J = 8.6, 5.5 Hz, 1H), 0.73 – 0.66 (m, 2H), 0.44 – 0.37 (m, 2H). ¹³C NMR (101 MHz, DMSO-d₆) δ 163.72, 152.34, 148.58, 146.90, 142.02, 139.68, 138.54, 130.55, 129.67, 120.84, 120.60, 119.64, 116.65, 114.21, 111.17, 109.38, 55.81, 55.70, 7.99, 6.91. UPLC-MS (ESI): m/z 444.2 [M-1]⁻, tR = 1.97 min, purity > 95% (UV).

Ethyl 5-cyclopropyl-1-(3-((3,4-dimethoxyphenyl)sulfonamido)phenyl)-1H-pyrazole-4-carboxylate (8t-I1). General procedure B1 was followed with aryl bromide **10** (0.084 g, 0.3 mmol) and benzenesulfonamide **55** (0.065 g, 0.3 mmol). Complete conversion was seen after 25 h by LC-MS. Purification by flash column chromatography (hep:EtOAc) afforded **8t-I1** as a white sticky solid (0.075 g, 0.16 mmol, 53%). LC-MS (ESI): m/z 472.2 [M+1]⁺, tR = 3.32 min, purity > 90% (UV).

3,4-Dimethoxybenzenesulfonamide (56). General procedure F was followed with 3,4-dimethoxybenzenesulfonyl chloride **47** (0.60 g, 2.5 mmol). Filtration afforded **56** as a white solid (0.53 g, 2.4 mmol, 98%). LC-MS (ESI): m/z 218.0 [M+1]⁺, t_R = 1.85 min, purity > 95% (UV).

5-Cyclopropyl-1-(3-((4-propylphenyl)sulfonamido)phenyl)-1H-pyrazole-4-carboxylic acid (8u). General procedure C was followed starting from the ester **8u-I1** (0.095 g, 0.21 mmol). Complete conversion was seen after 52 h by LC-MS. Purification by preparative HPLC afforded **8u** as a white solid (0.075 g, 0.18 mmol, 84%). ¹H NMR (400 MHz, DMSO-d₆) δ 12.23 (s, 1H), 10.52 (s, 1H), 7.90 (s, 1H), 7.72 – 7.65 (m, 2H), 7.43 – 7.33 (m, 3H), 7.28 – 7.15 (m, 3H), 2.61 – 2.53 (m, 2H), 1.85 (tt, J = 8.6, 5.5 Hz, 1H), 1.54 (h, J = 7.4 Hz, 2H), 0.83 (t, J = 7.3 Hz, 3H), 0.68 – 0.59 (m, 2H), 0.39 – 0.30 (m, 2H). ¹³C NMR (101 MHz, DMSO-d₆) δ 163.73, 147.95, 146.87, 142.02, 139.71, 138.37, 136.61, 129.75, 129.17, 126.75, 120.81, 119.49, 116.42, 114.30, 36.85, 23.57, 13.46, 8.00, 6.88. LC-MS (ESI): m/z 426.2 [M+1]⁺, t_R = 3.19 min, purity > 95% (UV).

Ethyl 5-cyclopropyl-1-(3-((4-propylphenyl)sulfonamido)phenyl)-1H-pyrazole-4-carboxylate (8u-I1). General procedure B1 was followed with aryl bromide **10** (0.34 g, 1.0 mmol) and benzenesulfonamide **57** (0.22 g, 1.2 mmol). Complete conversion was seen after 18 h by LC-MS. Purification by two flash column chromatography (hep:EtOAc) afforded **8u-I1** as a yellowish oil (0.27 g, 0.60 mmol, 60%). LC-MS (ESI): m/z 454.2 [M+1]⁺, t_R = 3.85 min, purity > 90% (UV).

1-(3-((4-Butylphenyl)sulfonamido)phenyl)-5-cyclopropyl-1H-pyrazole-4-carboxylic acid (8v). General procedure C was followed starting from the ester **8v-I1** (0.047 g, 0.10 mmol). Complete conversion was seen

after 24 h by LC-MS. Purification by preparative HPLC afforded **8v** as a white solid (0.032 g, 0.07 mmol, 73%). ¹H NMR (400 MHz, DMSO-d₆) δ 12.33 (s, 1H), 10.52 (s, 1H), 7.90 (s, 1H), 7.72 – 7.65 (m, 2H), 7.44 – 7.33 (m, 3H), 7.26 – 7.18 (m, 3H), 2.59 (t, J = 7.7 Hz, 2H), 1.85 (tt, J = 8.6, 5.5 Hz, 1H), 1.55 – 1.44 (m, 2H), 1.24 (h, J = 7.3 Hz, 2H), 0.85 (t, J = 7.3 Hz, 3H), 0.70 – 0.56 (m, 2H), 0.40 – 0.31 (m, 2H). ¹³C NMR (101 MHz, DMSO-d₆) δ 163.72, 148.16, 146.85, 142.00, 139.70, 138.37, 136.55, 129.73, 129.10, 126.76, 120.80, 119.48, 116.40, 114.30, 34.50, 32.57, 21.64, 13.66, 7.99, 6.87. UPLC-MS (ESI): m/z 440.2 [M+1]⁺, t_R = 2.56 min, purity > 95% (UV).

Ethyl 1-(3-((4-butylphenyl)sulfonamido)phenyl)-5-cyclopropyl-1H-pyrazole-4-carboxylate (8v-11). General procedure B1 was followed with aryl bromide **10** (0.084 g, 0.3 mmol) and benzenesulfonamide **58** (0.64 g, 0.3 mmol). Complete conversion was seen after 28 h by LC-MS. Purification by flash column chromatography (hep:EtOAc) afforded **8v-11** as a colorless oil (0.048 g, 0.10 mmol, 34%). LC-MS (ESI): m/z 468.2 [M+1]⁺, t_R = 3.99 min, purity > 90% (UV).

4-Butylbenzenesulfonamide (58). General procedure F was followed with 4-butylbenzenesulfonyl chloride **49** (0.48 mL, 2.5 mmol). Filtration afforded **58** as a white solid (0.51 g, 2.4 mmol, 96%). LC-MS (ESI): m/z 214.0 [M+1]⁺, t_R = 3.00 min, purity > 95% (UV).

1-(3-((4-(Tert-butyl)phenyl)sulfonamido)phenyl)-5-cyclopropyl-1H-pyrazole-4-carboxylic acid (8w). General procedure C was followed starting from the ester **8w-11** (0.094 g, 0.20 mmol). Complete conversion was seen after 30 h by LC-MS. Purification by preparative HPLC afforded **8w** as a white solid (0.076 g, 0.17 mmol, 86%). ¹H NMR (400 MHz, DMSO-d₆) δ 12.32 (s, 1H), 10.58 (s, 1H), 7.90 (s, 1H), 7.77 – 7.68 (m, 2H), 7.62 – 7.52 (m, 2H),

7.46 – 7.36 (m, 1H), 7.30 – 7.16 (m, 3H), 1.82 (tt, J = 8.6, 5.5 Hz, 1H), 1.24 (s, 9H), 0.64 – 0.51 (m, 2H), 0.38 – 0.23 (m, 2H). ¹³C NMR (101 MHz, DMSO-d₆) δ 164.18, 156.65, 147.30, 142.45, 140.20, 138.86, 136.90, 130.27, 127.09, 126.67, 121.18, 119.74, 116.57, 114.83, 35.33, 31.14, 8.41, 7.30. UPLC-MS (ESI): m/z 440.2 [M+1]⁺, t_R = 2.47 min, purity > 95% (UV).

Ethyl 1-(3-((4-(tert-butyl)phenyl)sulfonamido)phenyl)-5-cyclopropyl-1H-pyrazole-4-carboxylate (8w-I1).

General procedure B1 was followed with aryl bromide **10** (0.084 g, 0.3 mmol) and benzenesulfonamide **59** (0.64 g, 0.3 mmol). Complete conversion was seen after 28 h by LC-MS. Purification by flash column chromatography (hep:EtOAc) afforded **8w-I1** as a white solid (0.095 g, 0.20 mmol, 68%). LC-MS (ESI): m/z 468.2 [M+1]⁺, t_R = 3.94 min, purity > 95% (UV).

4-(Tert-butyl)benzenesulfonamide (59). General procedure F was followed with 4-(tert-butyl)benzenesulfonyl chloride **50** (0.58 g, 2.5 mmol). Filtration afforded **59** as a white solid (0.50 g, 2.4 mmol, 94%). LC-MS (ESI): m/z 214.0 [M+1]⁺, t_R = 3.05 min, purity > 95% (UV).

5-Cyclopropyl-1-(3-((2,4,6-trimethylphenyl)sulfonamido)phenyl)-1H-pyrazole-4-carboxylic acid (8x). General procedure C was followed starting from the ester **8x-I1** (0.075 g, 0.17 mmol). Complete conversion was seen after 48 h by LC-MS. Purification by preparative HPLC afforded **8x** as a white solid (0.069 g, 0.16 mmol, 95%). ¹H NMR (400 MHz, DMSO-d₆) δ 12.33 (s, 1H), 10.49 (s, 1H), 7.90 (s, 1H), 7.38 (t, J = 8.0 Hz, 1H), 7.21 (ddd, J = 8.0, 2.1, 1.0 Hz, 1H), 7.13 (t, J = 2.1 Hz, 1H), 7.08 (ddd, J = 8.2, 2.2, 1.0 Hz, 1H), 7.01 (s, 2H), 2.56 (s, 6H), 2.21 (s, 3H), 1.82 (tt, J = 8.5, 5.5 Hz, 1H), 0.71 – 0.62 (m, 2H), 0.41 – 0.34 (m, 2H). ¹³C NMR (101 MHz, DMSO-d₆) δ 163.72,

146.81, 142.35, 142.03, 139.73, 138.71, 138.25, 133.50, 131.80, 129.70, 120.22, 118.30, 115.41, 114.24, 22.38, 20.32, 7.99, 6.86. UPLC-MS (ESI): m/z 426.2 [M+1]⁺, t_R = 2.35 min, purity > 95% (UV).

Ethyl 5-cyclopropyl-1-(3-((2,4,6-trimethylphenyl)sulfonamido)phenyl)-1H-pyrazole-4-carboxylate (8x-I1).

General procedure B1 was followed with aryl bromide **10** (0.084 g, 0.3 mmol) and benzenesulfonamide **60** (0.60 g, 0.3 mmol). Complete conversion was seen after 28 h by LC-MS. Purification by flash column chromatography (hep:EtOAc) afforded **8x-I1** as a white sticky solid (0.075 g, 0.17 mmol, 55%). LC-MS (ESI): m/z 454.1 [M+1]⁺, t_R = 3.85 min, purity > 95% (UV).

2,4,6-Trimethylbenzenesulfonamide (60). General procedure F was followed with 2,4,6-trimethylbenzenesulfonyl chloride **51** (0.55 g, 2.5 mmol). Filtration afforded **60** as a white solid (0.47 g, 2.4 mmol, 95%). LC-MS (ESI): m/z 200.1 [M+1]⁺, t_R = 2.68 min, purity > 95% (UV).

5-Cyclopropyl-1-(3-((2,3,5,6-tetramethylphenyl)sulfonamido)phenyl)-1H-pyrazole-4-carboxylic acid (8y).

General procedure C was followed starting from the ester **8y-I1** (0.098 g, 0.21 mmol). Complete conversion was seen after 18 h by LC-MS. Purification by preparative HPLC afforded **8y** as a white solid (0.059 g, 0.13 mmol, 64%). ¹H NMR (600 MHz, DMSO-d₆) δ 10.56 (s, 1H), 7.89 (s, 1H), 7.35 (t, J = 8.1 Hz, 1H), 7.21 (s, 1H), 7.17 (ddd, J = 8.0, 2.1, 1.0 Hz, 1H), 7.06 (t, J = 2.1 Hz, 1H), 7.02 (ddd, J = 8.2, 2.2, 1.0 Hz, 1H), 2.48 (s, 6H), 2.18 (s, 6H), 1.75 (tt, J = 8.6, 5.5 Hz, 1H), 0.65 – 0.59 (m, 2H), 0.37 – 0.32 (m, 2H). ¹³C NMR (151 MHz, DMSO-d₆) δ 163.71, 146.75, 141.97, 139.66, 138.36, 137.68, 135.77, 135.58, 134.63, 129.66, 119.82, 117.88, 114.92, 114.27, 20.37, 17.50, 7.96, 6.79. LC-MS (ESI): m/z 440.2 [M+1]⁺, t_R = 3.22 min, purity > 95% (UV).

Ethyl 5-cyclopropyl-1-(3-((2,3,5,6-tetramethylphenyl)sulfonamido)phenyl)-1H-pyrazole-4-carboxylate (8y-I1).

General procedure B1 was followed with aryl bromide **10** (0.34 g, 1.0 mmol) and benzenesulfonamide **61** (0.24 g, 1.2 mmol). Complete conversion was seen after 22 h by LC-MS. Purification by flash column chromatography (hep:EtOAc) afforded **8y-I1** as a colorless oil (0.37 g, 0.78 mmol, 78%). UPLC-MS (ESI): m/z 468.2 $[M+1]^+$, t_R = 2.90 min, purity > 90% (UV).

2,3,5,6-Tetramethylbenzenesulfonamide (61). General procedure F was followed with 2,3,5,6-tetramethylbenzenesulfonyl chloride **52** (2.33 g, 10.0 mmol). Filtration afforded **61** as a white solid (1.95 g, 9.2 mmol, 92%). LC-MS (ESI): m/z 214.1 $[M+1]^+$, t_R = 2.85 min, purity > 90% (UV).

Compound 8z-ag (Scheme S5)

5-Cyclopropyl-N-methyl-1-(3-(phenylsulfonamido)phenyl)-1H-pyrazole-4-carboxamide (8z). General procedure G1 was followed with **8** (0.055 g, 0.14 mmol). Complete conversion was seen after 12 h. The crude product was purified by preparative HPLC to afford **8z** as white solid (0.014 g, 0.04 mmol, 25%). ^1H NMR (600 MHz, DMSO- d_6) δ 10.59 (s, 1H), 7.86 (q, J = 4.6 Hz, 1H), 7.84 (s, 1H), 7.81 – 7.75 (m, 2H), 7.67 – 7.59 (m, 1H), 7.55 (dd, J = 8.4, 7.0 Hz, 2H), 7.39 (t, J = 8.1 Hz, 1H), 7.26 (t, J = 2.1 Hz, 1H), 7.23 (dd, J = 7.7, 2.0 Hz, 1H), 7.18 (dd, J = 8.1, 2.1 Hz, 1H), 2.73 (d, J = 4.5 Hz, 3H), 1.85 (tt, J = 8.5, 5.4 Hz, 1H), 0.69 – 0.59 (m, 2H), 0.38 – 0.28 (m, 2H). ^{13}C NMR (151 MHz, DMSO- d_6) δ 162.68, 143.79, 139.90, 139.52, 139.22, 138.18, 133.08, 129.78, 129.34, 126.62, 120.53, 119.16, 118.19, 116.18, 25.77, 7.89, 6.89. LC-MS (ESI): m/z 395.2 $[M-1]^-$, t_R = 2.54 min, purity > 95% (UV).

5-Cyclopropyl-*N,N*-dimethyl-1-(3-(phenylsulfonamido)phenyl)-1H-pyrazole-4-carboxamide (8aa). General procedure G1 was followed with **8** (0.10 g, 0.26 mmol). Complete conversion was seen after 2 h. The crude product was purified by preparative HPLC to afford **8aa** as white solid (0.010 g, 0.024 mmol, 14%). ¹H NMR (600MHz, DMSO d6): δ 10.57 (s, 1H), 7.79 (d, J = 7.4 Hz, 2H), 7.69 – 7.60 (m, 2H), 7.56 (t, J = 7.6 Hz, 2H), 7.40 (t, J = 8.0 Hz, 1H), 7.36 – 7.27 (m, 2H), 7.18 (d, J = 8.0 Hz, 1H), 2.99 (d, J = 10.9 Hz, 6H), 1.76 (ddd, J = 13.7, 8.4, 5.4 Hz, 1H), 0.68 (dt, J = 6.1, 4.4 Hz, 2H), 0.36 (q, J = 6.0 Hz, 2H). ¹³C NMR (151 MHz, DMSO-d6): δ 164.83, 142.44, 140.37, 139.72, 139.26, 138.72, 133.53, 130.27, 129.81, 127.10, 120.68, 119.53, 117.60, 116.45, 7.21. LC-MS (ESI): m/z 409.2 [M-1]⁻, t_R = 2.65 min, purity > 95% (UV).

5-Cyclopropyl-*N*-hydroxy-1-(3-(phenylsulfonamido)phenyl)-1H-pyrazole-4-carboxamide (8ab). General procedure G1 was followed with **8** (0.50 g, 1.31 mmol). Complete conversion was seen after 12 h. The crude product was purified by preparative HPLC to afford **8ab** as white solid (0.015 g, 0.04 mmol, 15%). ¹H NMR (600 MHz, DMSO-d6) δ 10.65 (s, 1H), 10.60 (s, 1H), 7.81 – 7.74 (m, 3H), 7.66 – 7.59 (m, 1H), 7.55 (dd, J = 8.4, 7.0 Hz, 2H), 7.39 (t, J = 8.1 Hz, 1H), 7.26 (t, J = 2.1 Hz, 1H), 7.26 – 7.21 (m, 1H), 7.19 (ddd, J = 8.1, 2.2, 1.0 Hz, 1H), 1.83 (tt, J = 8.5, 5.5 Hz, 1H), 0.68 – 0.61 (m, 2H), 0.40 – 0.34 (m, 2H). ¹³C NMR (151 MHz, DMSO-d6) δ 160.53, 144.05, 139.82, 139.17 (d, J = 12.1 Hz), 138.21, 133.09, 129.83, 129.34, 126.62, 120.48, 119.19, 116.11, 115.53, 7.81, 6.95. LC-MS (ESI): m/z 397.2 [M-1]⁻, t_R = 2.37 min, purity > 95% (UV).

***N*-(3-(5-Cyclopropyl-4-(1H-tetrazol-5-yl)-1H-pyrazol-1-yl)phenyl)benzenesulfonamide (8ad).** **62** (0.090 g, 0.25 mmol) and TBAF (0.040 g, 0.15 mmol) were placed in a dry bottom flask under nitrogen, then TMS-Azide (0.065 g, 0.56 mmol) was added. The neat mixture was stirred at 100 °C for 22 h and diluted with HCl (2M) and washed with EtOAc. The organic layer collected, dried over Na₂SO₄, filtered, and concentrated in vacuo. The

crude compound is purified by preparative HPLC system to afford **8ad** (0.030 g, 0.07 mmol, 29%) as white solid. ^1H NMR (600 MHz, DMSO- d_6) δ 10.63 (s, 1H), 8.07 (s, 1H), 7.83 – 7.78 (m, 2H), 7.65 – 7.60 (m, 1H), 7.59 – 7.54 (m, 2H), 7.43 (t, J = 8.0 Hz, 1H), 7.37 – 7.32 (m, 2H), 7.21 (ddd, J = 8.2, 2.1, 1.0 Hz, 1H), 2.02 (tt, J = 8.4, 5.4 Hz, 1H), 0.74 – 0.69 (m, 2H), 0.19 – 0.14 (m, 2H). ^{13}C NMR (151 MHz, DMSO- d_6) δ 143.28, 140.14 – 138.78 (m), 138.28, 133.11, 129.87, 129.35, 126.64, 120.32, 119.30, 115.93, 7.86, 6.52. LC-MS (ESI): m/z 406.2 [$M-1$] $^-$, t_R = 2.65 min, purity > 95% (UV).

***N*-(3-(4-Cyano-5-cyclopropyl-1H-pyrazol-1-yl)phenyl)benzenesulfonamide (62)**. **8ac** (0.10 g, 0.26 mmol) was dissolved in DMF (2.5 mL) at 0°C, then thionyl chloride (0.080 g, 0.67 mmol) was added dropwise. The mixture was stirred at 0°C for 30 min followed by quenching with NaHCO_3 . The mixture was extracted with EtOAc, the organic layer collected, dried over Na_2SO_4 , filtered, and concentrated in vacuo to afford **62** as yellow oil (0.090 g, 0.25 mmol, 94%). Compound used without further purification. LC-MS (ESI): m/z 365.2 [$M+1$] $^+$, t_R = 3.19 min, purity > 95% (UV).

5-Cyclopropyl-1-(3-(phenylsulfonamido)phenyl)-1H-pyrazole-4-carboxamide (8ac). General procedure G2 was followed with **8** (0.10 g, 0.26 mmol). Complete conversion was seen after 22 h. The crude product was purified by preparative HPLC to afford **8ac** as white solid (0.10 g, 0.26 mmol, quantitative). ^1H NMR (600MHz, DMSO d_6): δ 10.60 (s, 1H), 7.89 (s, 1H), 7.79 (d, J = 7.4 Hz, 2H), 7.63 (t, J = 7.4 Hz, 1H), 7.56 (t, J = 7.6 Hz, 2H), 7.40 (t, J = 8.1 Hz, 1H), 7.36 (s, 1H), 7.26 (s, 1H), 7.23 (d, J = 7.9 Hz, 1H), 7.19 (dd, J = 8.2, 1.1 Hz, 1H), 7.13 (s, 1H), 1.88 (tt, J = 8.5, 5.5 Hz, 1H), 0.70 – 0.59 (m, 2H), 0.38 – 0.30 (m, 2H). ^{13}C NMR (151 MHz, DMSO- d_6): δ 164.41, 144.69, 140.61, 140.39, 139.68, 138.64, 133.56, 130.24, 129.81, 127.11, 121.08, 119.65, 118.51, 116.7, 8.52, 7.32. LC-MS (ESI): m/z 381.2 [$M-1$] $^-$, t_R = 2.44 min, purity > 95% (UV).

***N*-(3-(5-Cyclopropyl-4-(5-hydroxy-1,3,4-oxadiazol-2-yl)-1H-pyrazol-1-yl)phenyl)-benzenesulfonamide (8ae).**

General procedure B1 was followed with aryl bromide **64** (0.080 g, 0.23 mmol). Complete conversion was seen after 24 h by LC-MS. Purification by flash column chromatography (hep:EtOAc) afforded **8ae** (0.008 g, 0.02 mmol, 7%) as white solid. ¹H NMR (600 MHz, DMSO-d₆) δ 12.40 (s, 6H), 10.77 – 10.40 (m, 5H), 7.98 (s, 1H), 7.79 (d, J = 7.4 Hz, 2H), 7.66 – 7.59 (m, 1H), 7.59 – 7.52 (m, 2H), 7.45 – 7.37 (m, 2H), 7.30 (d, J = 7.0 Hz, 2H), 7.20 (d, J = 8.7 Hz, 1H), 1.94 – 1.85 (m, 2H), 0.75 – 0.65 (m, 2H), 0.36 – 0.26 (m, 2H). ¹³C NMR (151 MHz, DMSO-d₆) δ 154.36, 149.69, 143.28, 139.47, 139.18, 138.79, 138.28, 133.09, 129.79, 129.34, 126.65, 120.46, 119.42, 116.06, 107.54, 7.89, 6.37. LC-MS (ESI): m/z 424.0 [M+1]⁺, t_R = 2.70 min, purity > 95% (UV).

5-(1-(3-Bromophenyl)-5-cyclopropyl-1H-pyrazol-4-yl)-1,3,4-oxadiazol-2-ol (64). **63** (0.10 g, 0.31 mmol) was dissolved in 3 mL of DCM at 0 °C under nitrogen, then triphosgene (0.014 g, 0.47 mmol) was dropwise added. The mixture was stirred 18 h and diluted with EtOAc, washed with HCl 1 M and brine. The organic layer was collected, dried over Na₂SO₄, filtered, and concentrated in vacuo. The organic layer was collected and dried over sodium sulphate, filtered and solvent removed. Purification by flash column chromatography (DCM:MeOH) afforded **64** as a white solid (0.060 g, 0.17 mmol, 54%). LC-MS (ESI): m/z 347.0 and 349.0 [M+1]⁺, t_R = 2.33 min, purity > 95% (UV).

1-(3-Bromophenyl)-5-cyclopropyl-1H-pyrazole-4-carbohydrazide (63). General procedure G2 was followed with **63-11** (0.20 g, 0.65 mmol). Complete conversion was seen after 16 h. After concentrated in vacuo **63** was

afforded as orange oil (0.15 g, 0.47 mmol, 72%), which was used without further purification. LC-MS (ESI): m/z 406.2 [M+1]⁺, t_R = 2.33 min, purity > 95% (UV).

1-(3-Bromophenyl)-5-cyclopropyl-1H-pyrazole-4-carboxylic acid (63-I1). General procedure C was followed starting from the ester **10** (0.12 g, 0.36 mmol). Complete conversion was seen after 16 h by LC-MS and after the extraction procedure, the white solid of **63-I1** (0.10 g, 0.36 mmol, quantitative) was used without further purification. LC-MS (ESI): m/z 305.0 and 307.0 [M-1]⁻, t_R = 2.99 min, purity > 95% (UV).

N-(3-(5-Cyclopropyl-4-(2,2,2-trifluoro-1-hydroxyethyl)-1H-pyrazol-1-yl)phenyl)benzenesulfonamide (8af).

General procedure B1 was followed with aryl bromide **64** (0.070 g, 0.19 mmol). Complete conversion was seen after 24 h by LC-MS. Purification by flash column chromatography (hep:EtOAc) afforded **8af** (0.035 g, 0.08 mmol, 42%) as white solid. ¹H NMR (600 MHz, DMSO-d₆) δ 10.55 (s, 1H), 7.78 (dd, J = 5.2, 3.4 Hz, 2H), 7.66 – 7.59 (m, 2H), 7.55 (t, J = 7.6 Hz, 2H), 7.37 (t, J = 8.0 Hz, 1H), 7.31 – 7.22 (m, 2H), 7.21 – 7.12 (m, 1H), 5.13 (q, J = 7.4 Hz, 1H), 1.76 (tt, J = 8.4, 5.5 Hz, 1H), 0.79 (tdd, J = 8.8, 6.2, 4.4 Hz, 1H), 0.64 – 0.52 (m, 1H), 0.39 (td, J = 9.9, 5.7 Hz, 1H), 0.06 (td, J = 10.0, 5.7 Hz, 1H). ¹³C NMR (151 MHz, DMSO-d₆) δ 141.84, 139.98, 139.26, 138.50, 138.15, 133.05, 129.66, 129.32, 126.61, 119.98, 118.73, 116.85, 115.74, 63.49 (q, J = 31.8 Hz), 6.33, 6.28, 5.34. LC-MS (ESI): m/z 436.2 [M-1]⁻, t_R = 3.04 min, purity > 95% (UV).

1-(1-(3-Bromophenyl)-5-cyclopropyl-1H-pyrazol-4-yl)-2,2,2-trifluoroethanol (67). **66** (0.080 g, 0.22 mmol) was dissolved in THF (1 mL + 0.4 mL EtOH) at 0 °C then NaBH₄ as added (0.030 g, 0.8 mmol). The mixture was stirred at 0 °C under nitrogen 4 h, quenched with NaHCO₃ and extracted with EtOAc. The organic layer was collected,

dried over Na₂SO₄, filtered, and concentrated in vacuo to afford **67** as colorless oil (0.070 g, 0.19 mmol, 88%). Compound used without any further purification. LC-MS (ESI): m/z 361.1 and 363.1 [M+1]⁺, t_R = 2.48 min, purity > 95% (UV).

1-(1-(3-Bromophenyl)-5-cyclopropyl-1H-pyrazol-4-yl)-2,2,2-trifluoroethanone (66). **65** (0.65 g, 1.86 mmol) was dissolved in dry THF at 0 °C with cesium fluoride (0.25 g, 1.7 mmol), then TMS-CF₃ (0.80 g, 5.6 mmol) was added dropwise under nitrogen. The mixture stirred at RT 18 h then 10 mL of HCl 2 M were added and stirred for 30 min at RT. The mixture was extracted with EtOAc, the organic layer collected, dried over Na₂SO₄, filtered, and concentrated in vacuo to afford **66** as yellow oil (0.49 g, 1.36 mmol, 73%). LC-MS (ESI): m/z 359.0 and 361.0 [M+1]⁺, t_R = 3.97 min, purity > 95% (UV).

1-(3-Bromophenyl)-5-cyclopropyl-N-methoxy-N-methyl-1H-pyrazole-4-carboxamide (65). General procedure G2 was followed with **63-I1** (0.70 g, 2.28 mmol). Complete conversion was seen after 16 h. Purification by flash column chromatography (DCM:MeOH) afforded **65** as an orange oil (0.76 g, 2.14 mmol, 94%). LC-MS (ESI): m/z 350.1 and 352.1 [M+1]⁺, t_R = 3.13 min, purity > 95% (UV).

N-(3-(5-Cyclopropyl-4-(1,1,1,3,3,3-hexafluoro-2-hydroxypropan-2-yl)-1H-pyrazol-1-yl)phenyl)benzenesulfonamide (8ag). **69** (0.080 g, 0.18 mmol) was dissolved in dry THF (1.2 mL) at 0 °C with cesium fluoride (0.060 g, 0.39 mmol), then TMS-CF₃ (0.17 g, 1.2 mmol) was added dropwise under nitrogen. Mixture stirred at RT for 24 h then 10 mL of HCl 2 M was added and stirred 1 h at RT. The mixture was extracted with EtOAc, the organic layer collected, dried over Na₂SO₄, filtered, and concentrated in vacuo.

Purification by preparative HPLC afforded **8ag** as white solid (0.038 g, 0.074 mmol, 41%). ^1H NMR (600 MHz, DMSO- d_6) δ 10.60 (s, 1H), 8.29 (s, 1H), 7.79 (d, J = 7.8 Hz, 2H), 7.67 – 7.59 (m, 2H), 7.55 (t, J = 7.5 Hz, 2H), 7.38 (t, J = 8.2 Hz, 1H), 7.20 (d, J = 13.0 Hz, 3H), 1.97 – 1.75 (m, 1H), 0.51 (d, J = 8.1 Hz, 2H), 0.19 (d, J = 5.2 Hz, 2H). ^{13}C NMR (151 MHz, DMSO- d_6) δ 143.72, 140.28, 139.21, 138.33, 138.09, 133.11, 129.73, 129.34, 126.66, 123.04 (d, J = 289.4 Hz), 121.13, 119.40, 116.83, 111.42, 75.45 (p, J = 29.9 Hz), 8.48, 6.94. LC-MS (ESI): m/z 504.2 [M-1]⁻, t_R = 3.40 min, purity > 95% (UV).

***N*-(3-(5-Cyclopropyl-4-(2,2,2-trifluoroacetyl)-1H-pyrazol-1-yl)phenyl)benzenesulfonamide (69)**. General procedure B1 was followed with aryl bromide **68** (0.20 g, 0.47 mmol). Complete conversion was seen after 4 h by LC-MS. Purification by preparative HPLC afforded **69** (0.080 g, 0.18 mmol, 39%) as white solid. LC-MS (ESI): m/z 434.2 [M-1]⁻, t_R = 3.57 min, purity > 95% (UV).

2-(1-(3-Bromophenyl)-5-cyclopropyl-1H-pyrazol-4-yl)-1,1,1,3,3,3-hexafluoropropan-2-ol (68). **66** (0.49 g, 1.36 mmol) was dissolved in dry THF (1.2 mL) at 0 °C with cesium fluoride (0.29 g, 1.9 mmol), then TMS-CF₃ (0.75 g, 5.3 mmol) was added dropwise under nitrogen. Mixture stirred at RT for 24 h then 10 mL of HCl 2 M was added and stirred 1 h at RT. The mixture was extracted with EtOAc, the organic layer collected, dried over Na₂SO₄, filtered, and concentrated in vacuo. Purification by flash column chromatography (hep:EtOAc) afforded **68** as white solid (0.35 g, 0.82 mmol, 60%). ^1H NMR (600 MHz, DMSO- d_6) δ 8.34 (s, 1H), 7.78 (t, J = 2.0 Hz, 1H), 7.68 (ddd, J = 8.1, 2.0, 0.9 Hz, 2H), 7.59 (ddd, J = 8.1, 2.1, 1.0 Hz, 1H), 7.49 (t, J = 8.0 Hz, 1H), 2.10 (tt, J = 8.5, 5.6 Hz, 1H), 0.82 – 0.73 (m, 2H), 0.43 – 0.31 (m, 2H). LC-MS (ESI): m/z 429.1 and 431.1 [M+1]⁺, t_R = 3.77 min, purity > 95% (UV).

Compound 8ah (Scheme S6)

5-Cyclopropyl-1-(3-(phenylsulfonamidomethyl)phenyl)-1H-pyrazole-4-carboxylic acid (8ah). General procedure C was followed starting from the ester **72** (0.032 g, 0.08 mmol). Complete conversion was seen after 44 h by LC-MS. Purification by preparative HPLC afforded **8ah** as a white solid (0.025 g, 0.06 mmol, 79%). ¹H NMR (600 MHz, DMSO-d₆) δ 12.32 (s, 1H), 8.28 (t, J = 6.4 Hz, 1H), 7.93 (s, 1H), 7.85 – 7.77 (m, 2H), 7.65 – 7.59 (m, 1H), 7.56 (tt, J = 6.6, 1.6 Hz, 2H), 7.48 – 7.41 (m, 3H), 7.34 (dt, J = 7.3, 1.6 Hz, 1H), 4.10 (d, J = 6.3 Hz, 2H), 2.01 (tt, J = 8.6, 5.5 Hz, 1H), 0.87 – 0.78 (m, 2H), 0.55 – 0.48 (m, 2H). ¹³C NMR (151 MHz, DMSO-d₆) δ 163.83, 146.96, 141.98, 140.76, 139.16, 139.06, 132.39, 129.20, 128.77, 127.25, 126.41, 124.29, 124.00, 114.05, 45.54, 8.22, 7.06. LC-MS (ESI): m/z 398.1 [M+1]⁺, t_R = 2.77 min, purity > 95% (UV).

Ethyl 5-cyclopropyl-1-(3-(phenylsulfonamidomethyl)phenyl)-1H-pyrazole-4-carboxylate (72). General procedure D was followed with **71** (0.050 g, 0.23 mmol). Purification by flash column chromatography (hep:EtOAc) afforded (**72**) as a colorless oil (0.031 g, 0.09 mmol, 38%). LC-MS (ESI): m/z 426.2 [M+1]⁺, t_R = 3.47 min, purity > 95% (UV).

Ethyl 1-(3-(aminomethyl)phenyl)-5-cyclopropyl-1H-pyrazole-4-carboxylate (71). The nitrile **70** (0.15 g, 0.53 mmol) was dissolved in 80 mL EtOH, and the nitrile was reduced in by H-Cube (parameters: 70 bar, 90 °C, 1 mL/min), concentrated in vacuo, and purified by two flash column chromatography (1st hep:EtOAc, 2nd DCM:MeOH) to afford **71** as a yellowish oil (0.050 g, 0.17 mmol, 33%). LC-MS (ESI): m/z 286.2 [M+1]⁺, t_R = 1.99 min, purity > 90% (UV).

Ethyl 1-(3-cyanophenyl)-5-cyclopropyl-1H-pyrazole-4-carboxylate (70). General procedure A was followed with ethyl 3-cyclopropyl-3-oxopropanoate **9** (0.59 mL, 4.0 mmol) . Purification by flash column chromatography (hep:EtOAc) afforded **70** as a colorless oil (0.42 g, 1.5 mmol, 37%). LC-MS (ESI): m/z 282.1 [M+1]⁺, tR = 3.36 min, purity > 95% (UV).

Compound 8ai (Scheme S7)

5-Cyclopropyl-1-(3-(phenylsulfonamido)phenyl)-1H-1,2,3-triazole-4-carboxylic acid (8ai). General procedure C was followed starting from the ester **76** (0.063 g, 0.15 mmol). Complete conversion was seen after 16 h by LC-MS. Purification by preparative HPLC afforded **8ai** as a white solid (0.047 g, 0.12 mmol, 82%). ¹H NMR (600 MHz, DMSO-d₆) δ 10.72 (s, 1H), 7.83 – 7.78 (m, 2H), 7.65 – 7.60 (m, 1H), 7.56 (dd, J = 8.4, 7.0 Hz, 2H), 7.48 (t, J = 7.9 Hz, 1H), 7.35 – 7.28 (m, 3H), 1.89 (ddd, J = 8.6, 5.5, 3.1 Hz, 1H), 0.75 – 0.69 (m, 2H), 0.54 – 0.46 (m, 2H). ¹³C NMR (151 MHz, DMSO-d₆) δ 162.08, 142.61, 139.06, 138.63, 137.30, 136.29, 133.20, 130.31, 129.40, 126.72, 121.17, 120.91, 116.51, 7.47, 5.01. LC-MS (ESI): m/z 383.2 [M-1]⁻, tR = 2.62 min, purity > 95% (UV).

Ethyl 5-cyclopropyl-1-(3-(phenylsulfonamido)phenyl)-1H-1,2,3-triazole-4-carboxylate (76). General procedure B1 was followed with aryl bromide **75** (0.84 g, 2.5 mmol). Complete conversion was seen after 18 h by LC-MS. Purification by flash column chromatography (hep:EtOAc) afforded **76** as a white solid (0.31 g, 0.76 mmol, 30%). ¹H NMR (600 MHz, DMSO-d₆) δ 10.72 (s, 1H), 7.83 – 7.77 (m, 2H), 7.65 – 7.60 (m, 1H), 7.59 – 7.53 (m, 2H), 7.49 (td, J = 7.8, 1.0 Hz, 1H), 7.35 – 7.28 (m, 3H), 4.33 (q, J = 7.1 Hz, 2H), 4.03 (q, J = 7.1 Hz, 0H, EtOAc),

1.90 (tt, $J = 8.6, 5.5$ Hz, 1H), 1.33 (t, $J = 7.1$ Hz, 3H), 1.17 (t, $J = 7.1$ Hz, 1H, EtOAc), 0.78 – 0.70 (m, 2H), 0.51 – 0.45 (m, 2H).

Ethyl 1-(3-bromophenyl)-5-cyclopropyl-1H-1,2,3-triazole-4-carboxylate (75). To a solution of **74** (0.79 g, 4.0 mmol), ethyl 3-cyclopropyl-3-oxopropanoate **9** (0.48 mL, 3.3 mmol), and diethylamine (0.2 mL, 1.8 mmol) were dissolved in DMSO (5 mL). Upon the completion of addition, the mixture was heated to 80 °C for 3 h, and then poured into ice water. The solution extracted with dichloromethane and the organic phase was separated, washed with brine, dried (Na_2SO_4), filtered, concentrated in vacuo, and purified by flash column chromatography (hep:EtOAc) afforded **75** as a white solid (0.93 g, 2.8 mmol, 69%). ^1H NMR (600 MHz, DMSO-d_6) δ 7.98 (t, $J = 2.0$ Hz, 1H), 7.84 (ddd, $J = 8.1, 2.1, 1.0$ Hz, 1H), 7.73 (ddd, $J = 8.0, 2.1, 1.0$ Hz, 1H), 7.60 (t, $J = 8.0$ Hz, 1H), 4.35 (q, $J = 7.1$ Hz, 2H), 2.11 (tt, $J = 8.6, 5.5$ Hz, 1H), 1.34 (t, $J = 7.1$ Hz, 3H), 0.94 – 0.85 (m, 2H), 0.63 – 0.55 (m, 2H). ^{13}C NMR (151 MHz, DMSO-d_6) δ 160.54, 143.10, 136.92, 136.80, 132.90, 131.25, 128.40, 124.91, 121.71, 60.48, 14.16, 7.53, 4.80.

1-Azido-3-bromobenzene (74). 3-bromoaniline **73** (1.9 mL, 17.44 mmol) was suspended in water (50 mL); concentrated aqueous HCl was added (10% v/v) (5 mL) and the solution was cooled at 0°C. A solution of NaNO_2 (1.44 g, 20.9 mmol, in 21 mL H_2O) was added dropwise at 0°C and the mixture was further stirred for 20 min at RT. A solution of NaN_3 (1.70 g, 26.2 mmol, in 21 mL H_2O) was added drop wise at 0°C and the obtained suspension was stirred for 3 h at RT. The solution was extracted with Et_2O ; the organic phase was washed with brine (saturated solution), dried over MgSO_4 , filtered, and concentrated in vacuo to afford **74** (3.29 g, 1.7 mmol, 87%). ^1H NMR (400 MHz, CDCl_3) δ 7.25 (dd, 1H, $J=2.1, 8.1$ Hz), 7.19 (t, 1H, $J=8.1$ Hz), 7.16 (t, 1H, $J=2.1$ Hz), 6.94 ppm (dd, 1H, $J= 2.1, 8.1$ Hz).

Synthesis of compounds 77a-d (Schemes S8 and S9)

2-(N-(3-(5-Cyclopropyl-4-(1H-tetrazol-5-yl)-1H-pyrazol-1-yl)phenyl)-2,3,5,6-tetramethylphenylsulfonamido)-acetamide (77b). General procedure G2 was followed with **77a** (0.050 g, 0.10 mmol). Complete conversion was seen after 22 h by LC-MS. Purification by preparative HPLC afforded **77b** as a white solid (0.020 g, 0.038 mmol, 38%). ¹H NMR (600 MHz, DMSO-d₆) δ 8.10 (s, 1H), 7.63 (t, J = 2.1 Hz, 1H), 7.57 (d, J = 8.0 Hz, 1H), 7.48 (t, J = 8.0 Hz, 1H), 7.35 (s, 1H), 7.32 (d, J = 8.0 Hz, 1H), 7.26 (s, 1H), 7.10 (s, 1H), 4.36 (s, 2H), 2.32 (s, 7H), 2.19 (s, 7H), 2.07 (td, J = 8.4, 4.3 Hz, 1H), 0.79 (h, J = 5.0 Hz, 2H), 0.19 (t, J = 5.6 Hz, 2H). ¹³C NMR (151 MHz, DMSO-d₆) δ 168.63, 143.45, 139.92, 139.37 (d, J = 11.7 Hz), 136.42, 136.08, 135.93, 135.71, 129.36, 127.84, 124.82, 123.88, 51.84, 20.50, 17.55, 7.88, 6.40. LC-MS (ESI): m/z 521.2 [M+1]⁺, t_R = 2.89 min, purity > 95% (UV).

2-(N-(3-(5-Cyclopropyl-4-(1H-tetrazol-5-yl)-1H-pyrazol-1-yl)phenyl)-2,3,5,6-tetramethylphenylsulfonamido)acetic acid (77a). General procedure C was followed starting from the ester **77a-11** (0.26 g, 0.47 mmol). Complete conversion was seen after 8 h by LC-MS. Purification by preparative HPLC afforded **77a** as a white solid (0.035 g, 0.17 mmol, 37%). ¹H NMR (600 MHz, DMSO-d₆) δ 8.10 (s, 1H), 7.63 (t, J = 1.9 Hz, 1H), 7.60 – 7.55 (m, 1H), 7.50 (t, J = 8.0 Hz, 1H), 7.35 (dd, J = 8.1, 1.0 Hz, 1H), 7.26 (s, 1H), 4.56 (s, 2H), 2.32 (s, 7H), 2.19 (s, 6H), 2.07 (ddd, J = 13.9, 8.4, 5.5 Hz, 1H), 0.80 – 0.72 (m, 2H), 0.22 – 0.13 (m, 2H). ¹³C NMR (151 MHz, DMSO-d₆) δ 169.81, 143.43, 139.77, 139.41 (d, J = 4.1 Hz), 136.44, 136.13, 135.89, 135.74, 129.49, 127.85, 124.64, 123.99, 51.00, 20.47, 17.48, 7.84, 6.35. LC-MS (ESI): m/z 522.2 [M+1]⁺, t_R = 3.03 min, purity > 95% (UV).

Ethyl-2-(*N*-(3-(5-cyclopropyl-4-(1H-tetrazol-5-yl)-1H-pyrazol-1-yl)phenyl)-2,3,5,6-

tetramethylphenylsulfonamido)-acetate (77a-I1). 80 (0.45 g, 0.89 mmol) and TBAF (0.140 g, 0.50 mmol) were placed in a dry bottom flask under nitrogen, then TMS-Azide (0.21 g, 1.82 mmol) was added. The neat mixture was stirred at 100 °C for 24 and diluted with HCl (2 M) and washed with EtOAc. The organic layer collected, dried over Na₂SO₄, filtered, and concentrated in vacuo. The crude compound is purified by flash column chromatography (DCM:MeOH) to afford **77a-I1** (0.26 g, 0.47 mmol, 53%) as yellowish solid. ¹H NMR (600 MHz, Chloroform-d) δ 8.20 (s, 1H), 8.06 (s, 1H), 7.73 (d, J = 2.1 Hz, 1H), 7.56 – 7.52 (m, 1H), 7.41 (t, J = 8.0 Hz, 1H), 7.30 – 7.27 (m, 1H), 7.14 (s, 1H), 4.53 (s, 2H), 4.11 (q, J = 7.1 Hz, 2H), 2.39 (s, 6H), 2.22 (d, J = 3.5 Hz, 7H), 1.20 (t, J = 7.1 Hz, 3H), 1.04 – 0.95 (m, 2H), 0.35 (dt, J = 6.5, 3.3 Hz, 2H). ¹³C NMR (151 MHz, Chloroform-d) δ 168.79, 149.48, 143.86, 140.41, 140.00, 139.85, 136.91, 136.80, 136.24, 136.16, 129.90, 129.39, 126.31, 124.76, 107.54, 61.79, 52.08, 21.18, 18.06, 14.18, 8.56, 6.70. LC-MS (ESI): m/z 550.3 [M+1]⁺, t_R = 3.53 min, purity > 95% (UV).

Ethyl-2-(*N*-(3-(4-cyano-5-cyclopropyl-1H-pyrazol-1-yl)phenyl)-2,3,5,6-tetramethylphenylsulfonamido)acetate

(80). General procedure E was followed with **79** (0.35 g, 0.83 mmol) and ethyl bromoacetate (0.42 g, 2.51 mmol). Complete conversion after 20 h. Purification by flash column chromatography (hep:EtOAc) afforded **80** as a colorless oil (0.40 g, 0.79 mmol, 95%). LC-MS (ESI): m/z 630.3 [M+1]⁺, t_R = 4.44 min, purity > 95% (UV). ¹H NMR (600 MHz, DMSO-d₆) δ 8.17 (d, J = 1.4 Hz, 1H), 7.62 – 7.50 (m, 3H), 7.42 (dt, J = 7.8, 1.7 Hz, 1H), 7.26 (s, 1H), 4.63 (s, 2H), 4.15 (t, J = 7.1 Hz, 2H), 2.29 (s, 7H), 2.18 (s, 7H), 1.82 (tt, J = 8.3, 5.3 Hz, 1H), 1.21 (t, J = 7.1 Hz, 3H), 0.89 (dt, J = 8.5, 3.2 Hz, 2H), 0.82 (dt, J = 5.6, 3.1 Hz, 2H). ¹³C NMR (151 MHz, DMSO-d₆) δ 168.38 (d, J = 3.3 Hz), 167.17, 149.90, 142.74, 139.81, 138.50, 136.18, 136.13, 135.97, 135.80, 129.89, 128.86, 125.04, 124.52,

113.69, 90.76, 61.63, 51.12, 20.44, 17.44, 13.85, 7.17, 6.78. LC-MS (ESI): m/z 507.2 $[M+1]^+$, t_R = 3.99 min, purity > 95% (UV).

***N*-(3-(4-Cyano-5-cyclopropyl-1H-pyrazol-1-yl)phenyl)-2,3,5,6-tetramethylbenzenesulfonamide (79).** General procedure B1 was followed with aryl bromide **78** (0.84 g, 2.5 mmol). Complete conversion was seen after 24 h by LC-MS. Purification by flash column chromatography (hep:EtOAc) afforded **79** as a white solid (0.75 g, 2.1 mmol, 84%). ^1H NMR (600 MHz, DMSO- d_6) δ 10.61 (s, 1H), 8.14 (s, 1H), 7.39 (t, J = 8.1 Hz, 1H), 7.26 – 7.20 (m, 2H), 7.14 (t, J = 2.2 Hz, 1H), 7.04 (dd, J = 8.3, 2.1 Hz, 1H), 2.48 (s, 6H), 2.19 (s, 6H), 1.81 (tt, J = 8.5, 5.3 Hz, 1H), 0.90 – 0.86 (m, 2H), 0.81 – 0.77 (m, 2H). ^{13}C NMR (151 MHz, DMSO- d_6) δ 149.72, 142.63, 138.67 (d, J = 5.3 Hz), 137.64, 135.78, 135.61, 134.64, 130.00, 119.43, 118.31, 114.63, 113.74, 90.74, 59.72, 20.37, 17.48, 7.17, 6.86. LC-MS (ESI): m/z 419.2 $[M-1]^-$, t_R = 3.71 min, purity > 95% (UV).

1-(3-Bromophenyl)-5-cyclopropyl-1H-pyrazole-4-carbonitrile (78). **78-I1** (0.80 g, 2.61 mmol) was dissolved in DMF (6 mL) at 0 °C then thionyl chloride (0.78 g, 6.52 mmol) was added dropwise. The mixture was stirred at 0 °C for 30 min, quenched with NaHCO₃. The mixture was extracted with EtOAc, the organic layer collected, dried over Na₂SO₄, filtered, and concentrated in vacuo to give **78** (0.70 g, 2.4 mmol, 93%) as yellow oil. Compound used without any further purification. ^1H NMR (600 MHz, Chloroform- d) δ 7.83 (s, 1H), 7.75 (d, J = 2.1 Hz, 1H), 7.60 (dd, J = 8.0, 1.9 Hz, 1H), 7.51 (dd, J = 8.0, 2.1 Hz, 1H), 7.39 (t, J = 8.0 Hz, 1H), 1.89 (tt, J = 8.6, 5.3 Hz, 1H), 1.20 – 1.07 (m, 5H). ^{13}C NMR (151 MHz, Chloroform- d) δ 150.21, 142.97, 139.70, 132.16, 130.63, 128.53, 123.87, 122.88, 113.62, 91.43, 8.42, 7.89. LC-MS (ESI): m/z 288.0 and 290.0 $[M+1]^+$, t_R = 3.56 min, purity > 80% (UV).

1-(3-Bromophenyl)-5-cyclopropyl-1H-pyrazole-4-carboxamide (78-I1). General procedure G2 was followed with **63-I1** (1.00 g, 3.26 mmol). Complete conversion was seen after 22 h. After the extraction procedure, the pale yellow solid **78-I1** (0.85 g, 2.8 mmol, 85%) was used without further purification. LC-MS (ESI): m/z 306.0 and 308.0 $[M+1]^+$, $t_R = 1.96$ min, purity > 95% (UV).

1-(3-(*N*-(2-amino-2-oxoethyl)-2,3,5,6-tetramethylphenylsulfonamido)phenyl)-5-cyclopropyl-1H-pyrazole-4-carboxylic acid (77c). To **77c-I1** (0.250 g, 0.57 mmol) in degassed DMF (2 mL) were added TBDMSCl and imidazole at 0 °C. The reaction was stirred at RT for 20 h. The reaction mixture was diluted with EtOAc and washed with water and brine, dried with Na_2SO_4 , filtered, and concentrated in vacuo. Hereafter, general procedure E was applied with 2-bromoacetamide (0.22 g, 1.59 mmol). The reaction was stirred for 3 h at 0 °C. Purification by flash column chromatography (DCM:MeOH) afforded **77c** as a yellow solid (0.050 g, 0.10 mmol, 18%). ^1H NMR (600 MHz, DMSO-d_6) δ 12.12 (s, 2H), 7.92 (d, $J = 2.6$ Hz, 1H), 7.54 – 7.43 (m, 3H), 7.33 (d, $J = 7.6$ Hz, 2H), 7.25 (s, 1H), 7.09 (s, 1H), 4.35 (d, $J = 2.0$ Hz, 2H), 2.31 (s, 6H), 2.18 (s, 7H), 1.94 – 1.84 (m, 5H), 0.80 – 0.63 (m, 2H), 0.49 – 0.31 (m, 2H). ^{13}C NMR (151 MHz, DMSO-d_6) δ 171.96, 168.59, 163.71, 147.04, 142.03, 139.83, 139.45, 136.39, 136.05, 135.90, 135.70, 129.23, 128.00, 125.14, 124.34, 114.24, 50.36 (d, $J = 424.1$ Hz), 21.03, 20.49, 17.53, 8.03, 6.79. LC-MS (ESI): m/z 497.2 $[M+1]^+$, $t_R = 2.89$ min, purity > 95% (UV).

5-Cyclopropyl-1-(3-(2,3,5,6-tetramethylphenylsulfonamido)phenyl)-1H-pyrazole-4-carboxylic acid (77c-I1). General procedure B1 was followed with aryl bromide **63-I1** (0.65 g, 2.12 mmol). Complete conversion was

seen after 24 h by LC-MS. Purification by flash column chromatography (hep:EtOAc) afforded **77c-I1** as a white solid (0.250 g, 0.57 mmol, 27%). LC-MS (ESI): 440.2 [M+1]⁺, t_R = 3.17 min, purity > 95% (UV).

1-(3-((N-(2-Amino-2-oxoethyl)-2,3,5,6-tetramethylphenyl)sulfonamido)phenyl)-5-(trans-2-phenylcyclopropyl)-1H-pyrazole-4-carboxylic acid (77d). General procedure E was followed with **77d-I1** (0.14 g, 0.23 mmol) and 2-bromoacetamide (0.095 g, 0.69 mmol). Purification by preparative HPLC afforded **77h** as a white solid (0.020 g, 0.04 mmol, 16%). LC-MS (ESI): m/z 630.3 [M+1]⁺, t_R = 4.44 min, purity > 95% (UV). ¹H NMR (600 MHz, DMSO-d₆) δ 12.38 (s, 1H), 7.97 (s, 1H), 7.59 (q, J = 1.6 Hz, 1H), 7.41 (dt, J = 6.3, 2.3 Hz, 1H), 7.34 (s, 1H), 7.29 – 7.23 (m, 2H), 7.22 (s, 1H), 7.20 – 7.15 (m, 2H), 7.14 – 7.09 (m, 2H), 6.90 – 6.85 (m, 2H), 4.31 (d, J = 1.0 Hz, 2H), 2.32 (s, 6H), 2.30 – 2.26 (m, 1H), 2.16 (s, 6H), 1.98 (dt, J = 8.9, 5.6 Hz, 1H), 1.20 (dt, J = 9.0, 5.6 Hz, 1H), 0.95 (ddd, J = 8.8, 6.2, 5.2 Hz, 1H). ¹³C NMR (151 MHz, DMSO-d₆) δ 169.17, 164.20, 146.39, 142.57, 141.52, 140.66, 139.86, 136.87, 136.63, 136.40, 136.21, 129.75, 128.41, 128.01, 126.29, 126.15, 125.41, 124.70, 114.85, 52.22, 26.19, 21.00, 18.62, 18.04, 17.45. LC-MS (ESI): m/z 573.3 [M+1]⁺, t_R = 3.33 min, purity > 95% (UV).

tert-Butyldimethylsilyl 5-(trans-2-phenylcyclopropyl)-1-(3-((2,3,5,6-tetramethylphenyl)sulfonamido)phenyl)-1H-pyrazole-4-carboxylate (77d-I1). To **77m** (0.12 g, 0.23 mmol) in degassed DMF (1-2 mL) were added TBDMSCl (0.069 g, 0.46 mmol) and imidazole (0.047 g, 0.69 mmol) at 0 °C. The reaction was stirred at 0 °C for 2 h. The reaction mixture was diluted with EtOAc and washed with water and brine, dried with Na₂SO₄, filtered, and concentrated in vacuo to afford **77d-I1** (0.15 g), which was used without further purification and characterization.

5-(trans-2-Phenylcyclopropyl)-1-(3-((2,3,5,6-tetramethylphenyl)sulfonamido)phenyl)-1H-pyrazole-4-carboxylic acid (77m). General procedure C was followed starting from the ester **81** (0.20 g, 0.38 mmol). Complete conversion was seen after 92 h. Purification by preparative HPLC afforded **77m** as a white powder (0.12 g, 61%). ¹H NMR (600 MHz, DMSO) δ 12.38 (s, 1H), 10.55 (s, 1H), 7.95 (s, 1H), 7.14 (s, 1H), 7.11 (d, *J* = 18.6 Hz, 2H), 7.07 (dt, *J* = 8.0, 1.4 Hz, 1H), 6.96 (ddd, *J* = 8.1, 2.2, 1.2 Hz, 1H), 6.73 – 6.68 (m, 2H), 2.14 (s, 7H), 1.80 (dt, *J* = 8.9, 5.6 Hz, 1H), 1.19 (dt, *J* = 9.0, 5.6 Hz, 1H), 0.97 (dt, *J* = 8.8, 5.6 Hz, 1H). LC-MS (ESI): *m/z* 516.4 [M+1]⁺, purity > 95% (UV).

Ethyl 5-(trans-2-phenylcyclopropyl)-1-(3-((2,3,5,6-tetramethylphenyl)sulfonamido)phenyl)-1H-pyrazole-4-carboxylate (81). General procedure B1 was followed with ethyl 1-(3-bromophenyl)-5-(trans-2-phenylcyclopropyl)-1H-pyrazole-4-carboxylate **43** (0.70 g, 1.7 mmol). Complete conversion was seen after 20 h by LC-MS. Purification by flash column chromatography (hep:EtOAc) afforded **81** as a white solid (0.89 g, 1.6 mmol, 96%). UPLC-MS (ESI): *m/z* 544.3 [M+1]⁺, *t*_R = 3.16 min, purity > 90% (UV).

Synthesis of compounds 77e-r (Schemes S10 and S11)

1-(3-((N-(Carboxymethyl)-3-methoxyphenyl)sulfonamido)phenyl)-5-cyclopropyl-1H-pyrazole-4-carboxylic acid (77e). General procedure C was followed starting from the ester **77e-11** (0.057 g, 0.097 mmol). Complete conversion was seen after 43 h. Purification by preparative HPLC afforded **77e** as a white powder (0.033 g, 0.070 mmol, 72%). ¹H NMR (600 MHz, DMSO-*d*₆) δ 7.93 (s, 1H), 7.53 – 7.49 (m, 2H), 7.50 – 7.43 (m, 2H), 7.34 – 7.29 (m, 1H), 7.28 – 7.21 (m, 2H), 7.15 (dd, *J* = 2.6, 1.7 Hz, 1H), 4.54 (s, 2H), 3.76 (s, 3H), 2.02 – 1.68 (m, 1H),

0.89 – 0.63 (m, 2H), 0.53 – 0.31 (m, 2H). ¹³C NMR (151 MHz, DMSO-d₆) δ 169.87, 163.71, 159.39, 147.09, 142.09, 139.90, 139.46, 130.48, 129.47, 127.31, 124.51, 124.44, 119.39, 119.31, 114.33, 111.94, 55.58, 51.88, 8.07, 6.82. LC-MS (ESI): m/z 472.2 [M+1]⁺, 943.3 [2M+1]⁺, tR = 2.80 min, purity > 95% (UV).

2-Ethoxy-2-oxoethyl 5-cyclopropyl-1-(3-((N-(2-ethoxy-2-oxoethyl)-3-methoxyphenyl)sulfonamido)phenyl)-1H-pyrazole-4-carboxylate (77e-I1). General procedure E was followed starting from **8r-I1** (0.040 g, 0.097 mmol) and ethyl bromoacetate (0.087 mL, 0.78 mmol). Workup afforded **77e-I1** as a colorless oil (yield not determined). LC-MS (ESI): m/z 586.3 [M+1]⁺, tR = 3.82 min, purity > 95% (UV).

1-(3-((N-(Carboxymethyl)-4-propylphenyl)sulfonamido)phenyl)-5-cyclopropyl-1H-pyrazole-4-carboxylic acid (77f). General procedure C was followed starting from the ester **77f-I1** (0.033 g, 0.055 mmol). Complete conversion was seen after 26 h by LC-MS. Purification by preparative HPLC afforded **77f** as a white powder (0.022 g, 0.045 mmol, 81%). ¹H NMR (600 MHz, DMSO-d₆) δ 7.91 (s, 1H), 7.62 – 7.56 (m, 2H), 7.52 – 7.47 (m, 2H), 7.39 – 7.33 (m, 3H), 7.31 (ddd, J = 5.3, 3.5, 2.1 Hz, 1H), 4.52 (s, 2H), 2.61 (dd, J = 8.3, 6.8 Hz, 2H), 1.90 (tt, J = 8.6, 5.5 Hz, 1H), 1.56 (dt, J = 14.5, 7.3 Hz, 2H), 0.84 (t, J = 7.3 Hz, 3H), 0.77 – 0.69 (m, 2H), 0.45 – 0.38 (m, 2H). ¹³C NMR (151 MHz, DMSO-d₆) δ 169.85, 163.69, 148.17, 147.02, 142.05, 139.97, 139.43, 135.70, 129.42, 129.12, 127.36, 127.25, 124.37, 124.29, 114.31, 51.88, 36.84, 23.58, 13.41, 8.07, 6.80.

2-Ethoxy-2-oxoethyl 5-cyclopropyl-1-(3-((N-(2-ethoxy-2-oxoethyl)-4-propylphenyl)sulfonamido)phenyl)-1H-pyrazole-4-carboxylate (77f-I1). General procedure E was followed with **8u-I1** (0.040 g, 0.094 mmol) and ethyl bromoacetate (0.063 mL, 0.56 mmol). Workup afforded **77f-I1** as a colorless oil (0.033 g, 0.055 mmol, 59%). LC-MS (ESI): m/z 598.3 [M+1]⁺, tR = 3.93-4.34 min, purity > 95% (UV).

1-(3-((4-Butyl-*N*-(carboxymethyl)phenyl)sulfonamido)phenyl)-5-cyclopropyl-1H-pyrazole-4-carboxylic acid (77g). General procedure C was followed starting from the ester **77g-I1** (0.034 mmol). Complete conversion was seen after 22 h by LC-MS. Purification by preparative HPLC afforded **77g** as a white powder (0.005 g, 0.010 mmol, 29%). ¹H NMR (600 MHz, DMSO-*d*₆) δ 7.91 (s, 1H), 7.60 – 7.56 (m, 2H), 7.51 – 7.47 (m, 2H), 7.38 – 7.34 (m, 3H), 7.34 – 7.30 (m, 1H), 4.51 (s, 2H), 2.67 – 2.59 (m, 2H), 1.90 (tt, *J* = 8.6, 5.5 Hz, 1H), 1.60 – 1.45 (m, 2H), 1.30 – 1.18 (m, 3H), 0.87 (t, *J* = 7.4 Hz, 3H), 0.78 – 0.70 (m, 2H), 0.46 – 0.35 (m, 2H). ¹³C NMR (151 MHz, DMSO-*d*₆) δ 169.86, 163.69, 148.42, 147.02, 142.05, 139.97, 139.43, 135.64, 129.42, 129.06, 127.39, 127.27, 124.34, 124.30, 114.31, 51.88, 42.11, 34.53, 32.60, 21.62, 13.70, 8.08, 6.80. UPLC-MS (ESI): *m/z* 498.1 [*M*+1]⁺, purity > 95% (UV).

2-Ethoxy-2-oxoethyl 1-(3-((4-butyl-*N*-(2-ethoxy-2-oxoethyl)phenyl)sulfonamido)phenyl)-5-cyclopropyl-1H-pyrazole-4-carboxylate (77g-I1). General procedure E was followed starting from **8v** (0.015 g, 0.034 mmol) and ethyl bromoacetate (0.023 mL, 0.21 mmol). Workup afforded **77g-I1** as a colorless oil (0.016 g, 77%). The intermediate was used without characterization.

1-(3-((*N*-(Carboxymethyl)-2,4,6-trimethylphenyl)sulfonamido)phenyl)-5-cyclopropyl-1H-pyrazole-4-carboxylic acid (77h). General procedure C was followed starting from the ester **77h-I1** (0.094 mmol). Complete conversion was seen after 22 h by LC-MS. Purification by preparative HPLC afforded **77h** as a white powder (0.014 g, 0.029 mmol, 31%). ¹H NMR (600 MHz, DMSO-*d*₆) δ 12.63 (s, 3H), 7.92 (s, 1H), 7.53 – 7.43 (m, 3H), 7.33 (dt, *J* = 7.7, 1.8 Hz, 1H), 7.01 (s, 2H), 4.55 (s, 2H), 2.39 (s, 6H), 2.23 (s, 3H), 1.89 (tt, *J* = 8.6, 5.5 Hz, 1H), 0.76

– 0.67 (m, 2H), 0.45 – 0.32 (m, 2H). ¹³C NMR (151 MHz, DMSO-d₆) δ 169.90, 163.69, 147.04, 142.81, 142.06, 139.67, 139.63, 139.54, 132.54, 131.79, 129.37, 128.00, 125.10, 124.55, 114.27, 51.25, 22.38, 20.38, 8.02, 6.75.

UPLC-MS (ESI): m/z 484.1 [M+1]⁺, purity > 95% (UV).

2-Ethoxy-2-oxoethyl

5-cyclopropyl-1-(3-((N-(2-ethoxy-2-oxoethyl)-2,4,6-

trimethylphenyl)sulfonamido)phenyl)-1H-pyrazole-4-carboxylate (77h-I1). General procedure E was followed starting from **8x** (0.040 g, 0.094 mmol) and ethyl bromoacetate (0.065 mL, 0.56 mmol). Workup afforded **77h-I1** as a yellowish oil (0.062 g, 110%). The intermediate was used without characterization.

1-(3-((N-(Carboxymethyl)-2,3,5,6-tetramethylphenyl)sulfonamido)phenyl)-5-cyclopropyl-1H-pyrazole-4-

carboxylic acid (77i). General procedure C was followed starting from the ester **77i-I1** (0.37 g, 0.67 mmol).

Complete conversion was seen after 16 h by LC-MS. Purification by preparative HPLC afforded **77i** as a white solid (0.30 g, 0.12 mmol, 18%). ¹H NMR (600 MHz, DMSO-d₆) δ 12.64 (s, 1H), 7.92 (d, J = 1.7 Hz, 1H), 7.56 – 7.43 (m, 3H), 7.36 (dd, J = 7.5, 1.5 Hz, 1H), 7.25 (s, 1H), 4.55 (s, 2H), 2.31 (s, 6H), 2.18 (s, 6H), 1.96 – 1.82 (m, 1H), 0.80 – 0.61 (m, 2H), 0.39 (d, J = 5.3 Hz, 2H). ¹³C NMR (151 MHz, DMSO-d₆) δ 169.81, 163.72, 147.04, 142.07, 139.71, 139.54, 136.44, 136.13, 135.90, 135.75, 129.39, 128.03, 125.06, 124.47, 114.32, 50.98, 20.48, 17.48, 8.02, 6.77. LC-MS (ESI): m/z 498.2 [M+1]⁺, t_R = 3.05 min, purity > 95% (UV).

Ethyl

5-cyclopropyl-1-(3-((N-(2-ethoxy-2-oxoethyl)-2,3,5,6-tetramethylphenyl)sulfonamido)phenyl)-1H-

pyrazole-4-carboxylate (77i-I1). General procedure E was followed with **8y-I1** (0.450 g, 0.96 mmol) and ethyl bromoacetate (0.49 g, 2.9 mmol). Purification by flash column chromatography (hep:EtOAc) afforded **77i-I1** as

a colorless oil (0.37 g, 2.0 mmol, 70%). ¹H NMR (600 MHz, DMSO-d₆) δ 7.97 (d, J = 2.2 Hz, 1H), 7.54 – 7.46 (m, 3H), 7.42 – 7.32 (m, 1H), 7.26 (s, 1H), 4.63 (d, J = 2.3 Hz, 3H), 4.24 (qd, J = 7.1, 2.2 Hz, 2H), 4.05 (qd, J = 7.2, 2.1 Hz, 3H), 2.31 (d, J = 2.4 Hz, 6H), 2.18 (d, J = 2.2 Hz, 6H), 1.94 (ttd, J = 8.4, 5.6, 2.2 Hz, 1H), 1.29 (td, J = 7.1, 2.2 Hz, 3H), 1.12 (td, J = 7.1, 2.2 Hz, 3H), 0.75 – 0.68 (m, 2H), 0.34 (dd, J = 5.6, 2.4 Hz, 2H). LC-MS (ESI): m/z 554.3 [M+1]⁺, t_R = 4.11 min, purity > 95% (UV).

1-(3-(*N*-(Carboxymethyl)phenylsulfonamido)phenyl)-5-(*trans*-2-phenylcyclopropyl)-1H-pyrazole-4-carboxylic acid (77n). General procedure C was followed starting from the ester **77n-I1** (0.033 mmol). Complete conversion was seen after 22 h. Purification by preparative HPLC afforded **77n** as a white powder (0.0024 g, 14%). ¹H NMR (600 MHz, DMSO-d₆) δ 7.97 (s, 1H), 7.68 (dq, J = 8.2, 1.5 Hz, 2H), 7.67 – 7.63 (m, 1H), 7.57 – 7.53 (m, 2H), 7.45 (dt, J = 6.3, 1.9 Hz, 2H), 7.34 – 7.31 (m, 1H), 7.26 – 7.23 (m, 1H), 7.17 (dd, J = 8.1, 6.7 Hz, 2H), 7.14 – 7.10 (m, 1H), 6.89 – 6.86 (m, 2H), 4.41 (s, 2H), 2.31 (ddd, J = 9.0, 6.2, 5.0 Hz, 1H), 2.02 (dt, J = 8.9, 5.5 Hz, 1H), 1.23 (dt, J = 9.0, 5.5 Hz, 1H), 1.01 (ddd, J = 8.8, 6.3, 5.2 Hz, 1H). ¹³C NMR (151 MHz, DMSO-d₆) δ 169.86, 163.69, 145.97, 142.12, 141.07, 140.10, 139.46, 138.38, 133.37, 129.50, 129.31, 127.95, 127.27, 127.17, 125.72, 124.76, 124.59, 114.38, 51.93, 42.11, 25.76, 18.10, 17.08. LC-MS (ESI): m/z 518.2 [M+1, purity > 95% (UV).

2-Ethoxy-2-oxoethyl **1-(3-(*N*-(2-ethoxy-2-oxoethyl)phenylsulfonamido)phenyl)-5-((1*R*,2*R*)-2-phenylcyclopropyl)-1H-pyrazole-4-carboxylate (77n-I1).** General procedure E was followed starting from **8o** (0.015 g, 0.033 mmol) and ethyl bromoacetate (0.044 mL, 0.40 mmol). Workup afforded **77n-I1** as a colorless oil (yield not determined). The intermediate was used without characterization.

1-(3-((3-Methoxyphenyl)sulfonamido)phenyl)-5-(trans-2-phenylcyclopropyl)-1H-pyrazole-4-carboxylic acid (77j). General procedure C was followed starting from the ester **82** (0.11 g, 0.22 mmol). Complete conversion was seen after 76 h. Purification by preparative HPLC afforded **77j** as a white powder (0.067 g, 62%). ¹H NMR (600 MHz, DMSO) δ 12.38 (s, 1H), 7.96 (s, 1H), 7.45 (t, *J* = 8.0 Hz, 1H), 7.36 (dt, *J* = 7.8, 1.3 Hz, 1H), 7.33 – 7.28 (m, 2H), 7.22 – 7.08 (m, 7H), 6.79 – 6.74 (m, 2H), 3.73 (s, 3H), 2.23 (ddd, *J* = 9.1, 6.2, 4.9 Hz, 1H), 1.92 (dt, *J* = 8.8, 5.6 Hz, 1H), 1.19 (dt, *J* = 9.0, 5.5 Hz, 1H), 0.98 (dt, *J* = 8.7, 5.5 Hz, 1H). ¹³C NMR (151 MHz, DMSO) δ 163.70, 159.39, 145.82, 142.08, 140.94, 140.33, 139.69, 138.42, 130.57, 129.75, 127.87, 125.69, 125.66, 121.04, 119.43, 118.90, 118.75, 116.65, 114.39, 111.69, 55.54, 25.63, 18.22, 16.94. LC-MS (ESI): *m/z* 490.2 [M+1]⁺, purity > 95% (UV).

Ethyl 1-(3-((3-methoxyphenyl)sulfonamido)phenyl)-5-(trans-2-phenylcyclopropyl)-1H-pyrazole-4-carboxylate (82). General procedure B1 was followed with **43** (1.00 g, 2.4 mmol). Complete conversion was seen after 23 h by LC-MS. Purification by flash column chromatography (hep:EtOAc) afforded **82** as a white solid (0.51 g, 42%). LC-MS (ESI): *m/z* 518.4 [M+1]⁺, *t*_R = 3.89 min, purity > 90% (UV).

1-(3-((*N*-Carboxymethyl)-3-methoxyphenyl)sulfonamido)phenyl)-5-(trans-2-phenylcyclopropyl)-1H-pyrazole-4-carboxylic acid (77o). General procedure C was followed starting from the ester **77o-I1** (0.19 g, 0.31 mmol). Complete conversion was seen after 96 h. Purification by preparative HPLC afforded **77o** as a white powder (0.12 g, 71%). ¹H NMR (600 MHz, DMSO) δ 7.97 (s, 1H), 7.49 – 7.43 (m, 3H), 7.34 (t, *J* = 7.9 Hz, 1H), 7.30 – 7.26 (m, 1H), 7.25 – 7.20 (m, 2H), 7.18 – 7.14 (m, 4H), 6.90 – 6.85 (m, 2H), 4.42 (d, *J* = 1.4 Hz, 2H), 3.74 (s, 3H), 2.32

(dt, $J = 9.1, 5.7$ Hz, 1H), 2.01 (dt, $J = 8.9, 5.6$ Hz, 1H), 1.23 (dt, $J = 9.0, 5.6$ Hz, 1H), 1.00 (dt, $J = 8.8, 5.6$ Hz, 1H). ^{13}C NMR (151 MHz, DMSO) δ 169.92, 163.72, 159.41, 145.99, 142.14, 140.16, 139.52, 139.47, 130.48, 129.52, 127.96, 127.28, 125.71 (d, $J = 2.8$ Hz), 124.67, 124.59, 119.45, 119.34, 114.41, 111.98, 55.56, 25.76, 18.14, 17.06. LC-MS (ESI): m/z 548.2 [$M+1$], purity > 95% (UV).

Ethyl 1-(3-((*N*-(2-ethoxy-2-oxoethyl)-3-methoxyphenyl)sulfonamido)phenyl)-5-(trans-2-phenylcyclopropyl)-1H-pyrazole-4-carboxylate (77o-11). General procedure E was followed starting from **82** (0.40 g, 0.77 mmol) and ethyl bromoacetate (0.26 mL, 2.3 mmol). Workup afforded **77o-11** as a colorless oil (0.37 g, 80%). LC-MS (ESI): m/z 604.3 [$M+1$]⁺, purity > 95% (UV).

5-(trans-2-Phenylcyclopropyl)-1-(3-((4-propylphenyl)sulfonamido)phenyl)-1H-pyrazole-4-carboxylic acid (77k). General procedure C was followed starting from the ester **83** (0.22 g, 0.41 mmol). Complete conversion was seen after 48 h. Purification by preparative HPLC afforded **77k** as a white powder (0.14 g, 48%). ^1H NMR (600 MHz, DMSO) δ 12.37 (s, 1H), 10.50 (s, 1H), 7.95 (s, 1H), 7.72 – 7.67 (m, 2H), 7.36 – 7.31 (m, 2H), 7.27 (d, $J = 2.2$ Hz, 1H), 7.21 – 7.08 (m, 6H), 6.78 – 6.73 (m, 2H), 2.53 – 2.51 (m, 2H), 2.23 (ddd, $J = 9.0, 6.2, 5.0$ Hz, 1H), 1.90 (dt, $J = 8.9, 5.6$ Hz, 1H), 1.47 (h, $J = 7.4$ Hz, 2H), 1.14 (dt, $J = 9.0, 5.5$ Hz, 1H), 0.93 (ddd, $J = 8.8, 6.2, 5.2$ Hz, 1H), 0.77 (t, $J = 7.3$ Hz, 3H). ^{13}C NMR (151 MHz, DMSO) δ 163.72, 147.91, 145.81, 140.93, 139.69, 138.58, 136.55, 129.73, 129.18, 127.88, 126.75, 125.71, 125.66, 120.90, 119.30, 116.49, 114.39, 36.82, 25.64, 23.45, 18.13, 16.91, 13.45. LC-MS (ESI): m/z 502.3 [$M+1$]⁺, purity > 95% (UV).

Ethyl 5-(trans-2-phenylcyclopropyl)-1-(3-((4-propylphenyl)sulfonamido)phenyl)-1H-pyrazole-4-carboxylate (83). General procedure B1 was followed with **43** (1.00 g, 2.4 mmol). Complete conversion was seen after 23 h by LC-MS. Purification by flash column chromatography (hep:EtOAc) afforded **83** as a white solid (0.64 g, 50%). LC-MS (ESI): m/z 530.4 [M+1]⁺, t_R = 4.09 min, purity > 90% (UV).

1-(3-((N-(Carboxymethyl)-4-propylphenyl)sulfonamido)phenyl)-5-(trans-2-phenylcyclopropyl)-1H-pyrazole-4-carboxylic acid (77p). General procedure C was followed starting from the ester **77p-I1** (0.17 g, 0.28 mmol). Complete conversion was seen after 100 h. Purification by preparative HPLC afforded **77p** as a white powder (0.095 g, 61%). ¹H NMR (600 MHz, DMSO) δ 12.49 (s, 2H), 7.95 (s, 1H), 7.60 – 7.56 (m, 2H), 7.47 – 7.42 (m, 1H), 7.37 (t, J = 2.1 Hz, 1H), 7.36 – 7.30 (m, 3H), 7.29 – 7.25 (m, 1H), 7.17 (dd, J = 8.2, 6.7 Hz, 2H), 7.15 – 7.09 (m, 1H), 6.90 – 6.86 (m, 2H), 4.39 (s, 2H), 2.57 (t, J = 7.6 Hz, 3H), 2.30 (dt, J = 9.0, 5.6 Hz, 1H), 2.01 (dt, J = 9.0, 5.6 Hz, 1H), 1.53 (h, J = 7.4 Hz, 2H), 1.22 (dt, J = 9.0, 5.6 Hz, 1H), 0.99 (dt, J = 8.9, 5.6 Hz, 1H), 0.82 (t, J = 7.3 Hz, 3H). ¹³C NMR (151 MHz, DMSO) δ 169.92, 163.71, 148.21, 145.94, 142.11, 141.08, 140.24, 139.44, 135.73, 129.49, 129.16, 127.97, 127.30 (d, J = 3.6 Hz), 125.73, 124.54, 124.48, 114.38, 51.88, 36.84, 25.76, 23.55, 18.10, 17.08, 13.42. LC-MS (ESI): m/z 560.2 [M+1]⁺, purity > 95% (UV).

Ethyl 1-(3-((N-(2-ethoxy-2-oxoethyl)-4-propylphenyl)sulfonamido)phenyl)-5-(trans-2-phenylcyclopropyl)-1H-pyrazole-4-carboxylate (77p-I1). General procedure E was followed starting from **83** (0.40 g, 0.76 mmol) and ethyl bromoacetate (0.25 mL, 2.3 mmol). Workup afforded **77p-I1** as a colorless oil (0.34 g, 73%). LC-MS (ESI): m/z 616.3 [M+1]⁺, purity > 95% (UV).

5-(trans-2-Phenylcyclopropyl)-1-(3-((2,4,6-trimethylphenyl)sulfonamido)phenyl)-1H-pyrazole-4-carboxylic acid (77l). General procedure C was followed starting from the ester **84** (0.18 g, 0.34 mmol). Complete conversion was seen after 52 h. Purification by preparative HPLC afforded **77l** as a white powder (0.12 g, 68%). ¹H NMR (600 MHz, DMSO) δ 12.39 (s, 1H), 10.49 (s, 1H), 7.95 (s, 1H), 7.18 – 7.08 (m, 6H), 7.02 (ddd, *J* = 8.0, 2.2, 1.2 Hz, 1H), 6.99 (s, 2H), 6.76 – 6.71 (m, 2H), 2.57 (s, 7H), 2.19 (ddd, *J* = 9.0, 6.2, 4.9 Hz, 1H), 2.14 (s, 3H), 1.86 (dt, *J* = 8.9, 5.6 Hz, 1H), 1.18 (dt, *J* = 9.0, 5.6 Hz, 1H), 0.98 (ddd, *J* = 8.8, 6.2, 5.2 Hz, 1H). ¹³C NMR (151 MHz, DMSO) δ 163.71, 145.79, 142.36, 142.08, 140.87, 139.71, 138.74, 138.49, 133.39, 131.86, 129.73, 127.86, 125.69 (d, *J* = 2.0 Hz), 120.29, 118.05, 115.40, 114.31, 25.59, 22.40, 20.31, 18.14, 16.86. LC-MS (ESI): *m/z* 502.4 [M+1]⁺, purity > 95% (UV).

Ethyl 5-(trans-2-phenylcyclopropyl)-1-(3-((2,4,6-trimethylphenyl)sulfonamido)phenyl)-1H-pyrazole-4-carboxylate (84). General procedure B1 was followed with **43** (1.00 g, 2.4 mmol). Complete conversion was seen after 22 h by LC-MS. Purification by flash column chromatography (hep:EtOAc) afforded **84** as a white solid (0.58 g, 46%). LC-MS (ESI): *m/z* 530.3 [M+1]⁺, purity > 90% (UV).

1-(3-((N-(Carboxymethyl)-2,4,6-trimethylphenyl)sulfonamido)phenyl)-5-(trans-2-phenylcyclopropyl)-1H-pyrazole-4-carboxylic acid (77q). General procedure C was followed starting from the ester **77q-I1** (0.19 g, 0.31 mmol). Complete conversion was seen after 144 h. Purification by preparative HPLC afforded **77q** as a white powder (0.064 g, 37%). ¹H NMR (600 MHz, DMSO) δ 12.43 (s, 2H), 7.97 (s, 1H), 7.57 (d, *J* = 2.1 Hz, 1H), 7.42 (pd, *J* = 4.3, 2.0 Hz, 1H), 7.31 – 7.25 (m, 2H), 7.17 (dd, *J* = 8.2, 6.7 Hz, 2H), 7.15 – 7.09 (m, 1H), 6.98 (s, 2H), 6.86 (dd, *J* = 7.1, 1.8 Hz, 2H), 4.47 (d, *J* = 5.9 Hz, 2H), 2.55 – 2.51 (m, 3H), 2.40 (s, 6H), 2.31 (ddd, *J* = 10.3, 9.0, 4.9 Hz, 1H), 2.18 (s, 3H), 1.98 (dt, *J* = 8.9, 5.5 Hz, 1H), 1.17 (dt, *J* = 9.0, 5.5 Hz, 1H), 0.95 (dt, *J* = 8.9, 5.6 Hz, 1H). ¹³C NMR (151 MHz, DMSO) δ 163.71, 145.79, 142.36, 142.08, 140.87, 139.71, 138.74, 138.49, 133.39, 131.86, 129.73, 127.86, 125.69 (d, *J* = 2.0 Hz), 120.29, 118.05, 115.40, 114.31, 25.59, 22.40, 20.31, 18.14, 16.86. LC-MS (ESI): *m/z* 502.4 [M+1]⁺, purity > 95% (UV).

MHz, DMSO) δ 169.95, 163.72, 145.93, 142.87, 142.14, 141.05, 139.99, 139.65, 139.50, 132.53, 131.87, 129.44, 127.96, 127.64, 125.71, 124.87, 124.51, 114.40, 51.22, 25.71, 22.42, 20.37, 18.10, 17.06. LC-MS (ESI): m/z 560.3 $[M+1]^+$, purity > 95% (UV).

Ethyl 1-(3-((*N*-(2-ethoxy-2-oxoethyl)-2,4,6-trimethylphenyl)sulfonamido)phenyl)-5-(trans-2-phenylcyclopropyl)-1H-pyrazole-4-carboxylate (77q-l1). General procedure E was followed starting from **84** (0.40 g, 0.76 mmol) and ethyl bromoacetate (0.25 mL, 2.3 mmol). Workup afforded **77q-l1** as a colorless oil (0.39 g, 82%). LC-MS (ESI): m/z 616.4 $[M+1]^+$, purity > 95% (UV).

5-(trans-2-Phenylcyclopropyl)-1-(3-((2,3,5,6-tetramethylphenyl)sulfonamido)phenyl)-1H-pyrazole-4-carboxylic acid (77m). General procedure C was followed starting from the ester **85** (0.10 g, 0.19 mmol). Complete conversion was seen after 92 h. Purification by preparative HPLC afforded **77m** as a white powder (0.060 g, 61%). ^1H NMR (600 MHz, DMSO) δ 12.38 (s, 1H), 10.55 (s, 1H), 7.95 (s, 1H), 7.14 (s, 1H), 7.11 (d, J = 18.6 Hz, 2H), 7.07 (dt, J = 8.0, 1.4 Hz, 1H), 6.96 (ddd, J = 8.1, 2.2, 1.2 Hz, 1H), 6.73 – 6.68 (m, 2H), 2.14 (s, 7H), 1.80 (dt, J = 8.9, 5.6 Hz, 1H), 1.19 (dt, J = 9.0, 5.6 Hz, 1H), 0.97 (dt, J = 8.8, 5.6 Hz, 1H). ^{13}C NMR (151 MHz, DMSO) δ 163.71, 145.78, 142.03, 140.83, 139.65, 138.62, 137.45, 135.74, 135.71, 134.71, 129.65, 127.83, 125.75, 125.67, 119.92, 117.68, 114.99, 114.28, 25.50, 20.42, 18.11, 17.47, 16.77. LC-MS (ESI): m/z 516.4 $[M+1]^+$, purity > 95% (UV).

Ethyl 5-(trans-2-phenylcyclopropyl)-1-(3-((2,3,5,6-tetramethylphenyl)sulfonamido)phenyl)-1H-pyrazole-4-carboxylate (85). General procedure B1 was followed with **43** (0.50 g, 1.2 mmol). Complete conversion was

seen after 25 h by LC-MS. Purification by flash column chromatography (hep:EtOAc) afforded **85** as a white solid (0.50 g, 53%). LC-MS (ESI): m/z 544.3 $[M+1]^+$, t_R = 3.16 min, purity > 90% (UV).

1-(3-((N-(Carboxymethyl)-2,3,5,6-tetramethylphenyl)sulfonamido)phenyl)-5-(trans-2-phenylcyclopropyl)-1H-pyrazole-4-carboxylic acid (77r). General procedure C was followed starting from the ester **77r-I1** (0.18 g, 0.28 mmol). Complete conversion was seen after 16 h. Purification by preparative HPLC afforded **77r** as a white powder (0.020 g, 16%). ^1H NMR (600 MHz, DMSO- d_6) δ 12.48 (s, 2H), 7.97 (s, 1H), 7.58 (t, J = 2.1 Hz, 1H), 7.41 (dt, J = 7.4, 1.8 Hz, 1H), 7.31 – 7.24 (m, 2H), 7.21 (s, 1H), 7.17 (dd, J = 8.1, 6.6 Hz, 2H), 7.14 – 7.08 (m, 1H), 6.89 – 6.80 (m, 2H), 4.43 (s, 2H), 2.31 (s, 6H), 2.15 (s, 6H), 1.96 (dt, J = 8.9, 5.6 Hz, 1H), 1.18 (dt, J = 9.0, 5.5 Hz, 1H), 0.95 (dt, J = 8.8, 5.6 Hz, 1H). ^{13}C NMR (151 MHz, DMSO- d_6) δ 170.00, 163.75, 145.88, 142.11, 141.01, 140.12, 139.44, 136.51, 136.16, 135.87, 135.72, 129.36, 127.92, 127.56, 125.78, 125.69, 124.77, 124.26, 114.44, 51.14, 25.69, 20.49, 18.08, 17.48, 16.95. LC-MS (ESI): m/z 574.3 $[M+1]^+$, purity > 95% (UV).

Ethyl 1-(3-((N-(2-ethoxy-2-oxoethyl)-2,3,5,6-tetramethylphenyl)sulfonamido)phenyl)-5-(trans-2-phenylcyclopropyl)-1H-pyrazole-4-carboxylate (77r-I1). General procedure E was followed starting from **85** (0.16 g, 0.30 mmol) and ethyl bromoacetate (0.10 mL, 0.90 mmol). Workup afforded **77r-I1** as a white solid (0.18 g, 94%). LC-MS (ESI): m/z 630.3 $[M+1]^+$, purity > 95% (UV).

Expression and purification of the human and mouse Keap1 Kelch domains

The recombinant His-tagged human Kelch domain (residue 321-609, UniProt Q14145) was cloned into a pRSET A vector and expressed in *E. coli* BL21 (DE3) pLysS followed by purification by column chromatography, as previously described.³³

The recombinant His-tagged mouse Kelch domain (residue 322-624, UniProt Q9Z2X8; 97% identical with the human sequence) was cloned into a pRSET A vector and expressed in *E. coli* BL21 (DE3) pLysS. Keap1 was grown in a pre-culture of 50 mL LB media supplemented with 1% glucose and 100 µg/mL ampicillin overnight (ON) at 37 °C to an approximate OD₆₀₀ of ~1.0. The pre-culture was transferred to 1 L LB-medium supplemented with 1% glucose and 100 µg/mL ampicillin and grown at 37 °C /180 rpm to an approximate OD₆₀₀ of ~0.5, before induction with isopropyl β-D-1-thiogalactopyranoside (IPTG) (final concentration of 0.5-1 mM) ON at 15 °C/180 rpm. Cells were harvested by centrifugation at 4,000 x *g* for 30 min. The cells were re-suspended in lysis buffer (50 mM Tris-HCl pH 7.5, cOmplete™ Protease Inhibitor Cocktail (1 tablet/50 mL of buffer), 25 µg/mL DNase, 40 mM Mg₂SO₄, 150 mM NaCl, 5 mM imidazole, 5% glycerol, 0.5% TritonX-100, 3 mM DTT, 1 mg/mL Lysozyme) and lysed using a cell disruptor at 26 KPsi in 4 °C. The cell lysate was spun down at 35,000 x *g* for 1 h at 4 °C. The supernatant was filtered on a 0.45 µm filter and loaded onto a 5 mL HisTrap HP column (GE Healthcare). The column was washed with 5 column volumes of HisTrap binding buffer (50 mM Tris-HCl pH 7.5, 150 mM NaCl, 10 mM imidazole, 3 mM DTT) followed by eluting the protein using a gradient of HisTrap elution buffer (50 mM Tris-HCl pH 7.5, 150 mM NaCl, 1 M imidazole, 3 mM DTT). The protein was eluted between 10 and 15% elution buffer. The His-tag of mouse Keap1 Kelch domain was cleaved by adding 500 µL of 1 mg/mL His-tagged Human Rhinovirus (HRV)-3C Protease to approx. 50 mg of protein and incubated overnight at 4 °C in HisTrap binding buffer. After 16 hours, the cleaved mouse Keap1 Kelch domain was purified using “reverse purification” on the HisTrap HP column and concentrated to 5 mL. The cleaved protein was

loaded onto a Superdex 75 16/600 column (GE Healthcare), equilibrated with SEC buffer (20 mM Tris-HCl pH 8.3, 20 mM DTT and 10 mM benzamidine) with a flow rate at 1 mL/min, and was eluted at 65 mL. Protein was concentrated to 18 mg/mL for crystallography and stored at -80 °C.

The proteins were analyzed on SDS page for purity, and the concentrations were measured by absorbance (Nanodrop) using molar extinction coefficients calculated based on amino acid sequence. The exact molecular weights of purified human and mouse Keap1 Kelch were confirmed by ESI-LC-MS.

Fluorescence polarization (FP) assay

Fragments and lead compounds were tested for their ability to inhibit the interaction between the human Keap1 Kelch domain and the peptide probes – Cy5-Nrf2 (Cy5-LDEETGEFL-NH₂) and FAM-Nrf2 (5(6)-FAM-LDEETGEFL-NH₂) – as described previously.³³ The 9mer Nrf2 peptide H-Nrf2-OH (H-LDEETGEFL-OH) ($K_i = 0.54 \mu\text{M}$)³³ and the short 7mer Nrf2 peptide (Ac-LDEETGE-OH) ($K_i = 3.0 \mu\text{M}$) were used as controls. The assay was performed in a 1×HBSTET assay buffer (10 mM HEPES, 150 mM NaCl, 0.005% Tween20, 3 mM EDTA, 1 mM TCEP, pH = 7.4) using black flat-bottom 384-well plates (Corning Life Sciences, NY) and a volume of 30 μL /well. Fragments were initially tested in dose response experiments (6-points, 0.25–8 mM fragment concentration, and 8% DMSO) using Cy5-Nrf2 as probe (3 nM) and Keap1 Kelch at 14 nM. Assay plates were spun-down to ascertain proper mixing and removal of potential air bubbles and incubated for 10-15 min at room temperature before measuring the FP levels on a Safire2 plate-reader (Tecan, Männedorf, Switzerland). Fragments demonstrating >5% inhibition *and* at the same time did not change total fluorescence intensity (FLINT) values by more than 30% of control wells were characterized as primary hits. This hit-threshold corresponded to a reduction of 5-10 mP out of an assay window of 80-90 mP. Hits were tested in three FP dose-response counter assays: first, by performing the assay with the FAM-Nrf2 probe; secondly, by replacing Tween20 with 0.01%

Triton-X in the assay buffer (using Cy5-Nrf2 as probe); and thirdly, by omitting the Keap1 Kelch domain (still using Cy5-Nrf2 as probe). FP values were fitted to the equation $Y = \text{Bottom} + (\text{Top} - \text{Bottom})/[1 + (10^{\text{HillSlope} \cdot (\text{LogIC}_{50} - X)})]$, where X is the logarithmic value of compound concentration. Hereby, the IC₅₀ value was obtained, which together with the K_d value and probe and Keap1 Kelch concentrations was used to calculate the theoretical competitive inhibition constant, the K_i value.⁸⁶

Thermal shift assay (TSA)

Melting curves of Keap1 with and without the presence of compounds were determined by TSA using the Sypro Orange dye (Life Technologies), a Stratagene Mx3005P RT-PCR apparatus (Agilent Technologies, Waldbronn, Germany), and clear non-skirted 96-well PCR-plates, as described previously.³³ The 77 deconstruction fragments were mixed with the human Keap1 Kelch domain (final concentration: 0.1 mg/mL; 3 μM) and Sypro Orange (final concentration: 8x) with compounds tested in 5 concentrations (0.5–8 mM) as 2-fold dilutions in the 1×HBSTET assay buffer (0.5–8% DMSO), and final sample volume of 25 μL/well. On each plate, 8 wells of DMSO blanks and 8 wells of a positive control (*N,N'*-(naphthalene-1,4-diyl)bis(4-methoxybenzenesulfonamide)²⁴; 20 μM in 4% DMSO; ΔT_{m-max}= 4.2 °C³³) were included for reference. The plates were sealed and spun-down for 2 minutes at 500 x g, and measured from 25–95 °C in 70 cycles with a 1°C temperature increase per minute and fluorescence intensities measured at each cycle. The sigmoidal plot of the normalized fluorescence intensity values versus temperature were fitted to the Boltzmann equation $Y = \text{Bottom} + (\text{Top} - \text{Bottom})/(1 + \exp((T_m - X)/\text{Slope}))$, where X is temperature in °C, whereby the melting temperature (T_m), where 50% of protein is denatured, was determined. The difference in T_m (ΔT_m) of each compound concentration compared to DMSO blanks were plotted as dose-response curves and fitted to the equation $\Delta T_m = \Delta T_{m-\text{max}} \times X/(EC_{50} + X)$, with ΔT_{m-max} being the maximal obtained T_m and X the compound concentration.

Saturation-transfer difference (STD) NMR

Fragments were screened at 1 mM by STD-NMR in 3% DMSO- d_6 . A concentrated solution of the human Keap1 Kelch domain was prepared (290 μ M, 10 v/v% D_2O) and based on 1H NMR an irradiation frequency at 0.45 ppm was chosen for the STD experiment.⁸⁷ A standard PBS buffer (0.01 M phosphate buffer, 0.0027 M KCl and 0.137 M NaCl, 1 mM TCEP, pH 7.4) was used to prepare a stock solution of Keap1 Kelch (6 μ M) in PBS buffer (10 v/v% D_2O , 2% DMSO- d_6), which was used to dilute each of the 100 mM DMSO- d_6 stock solution of the fragments to 1 mM and a final volume of 160 μ L per sample. A fully automated Gilson 215 liquid handling system was used to transfer the sample solutions to the 3 mm NMR tubes. Standard 1D and STD NMR spectra were acquired at 280 K with a Bruker 600 MHz NMR spectrometer equipped with a cryoprobe. A Bruker SampleJet sample changer was used allowing sequential measurement of all samples without user intervention. A primary hit were defined as fragments with at least one signal in the 1H NMR spectrum demonstrating an STD% > 1%. The STD% effects were measured as the ratio between the intensities of the STD signal and the 1D signal (I_{STD}/I_{1D}).

Surface plasmon resonance (SPR)

SPR measurements were performed at 25 °C using a Pioneer FE instrument (Molecular Devices, FortéBio), as described previously.³³ The Keap1 Kelch domain was covalently immobilized on biosensor chips surfaces by amine coupling up to a level between 4100–4300 RU, using a 10 mM NaOAc pH 5 immobilization buffer. The 1 \times HBSTET buffer supplemented with 4% DMSO was used as running buffer for the experiments. Microcalibration was performed for all SPR experiments to adjust for DMSO bulk effects (low limit 3.5% and high limit 4.5%). The compounds were injected in concentration series (two-fold serial dilution) or in a gradient

using the OneStep injection over immobilized Keap1. The H-Nrf2-OH peptide ($K_d = 4.2 \mu\text{M}$)³³ was used as control to evaluate assay activity. The data were analyzed using Qdat Data Analysis Tool version 2.6.3.0 (Molecular Devices, FortéBio). The sensorgrams were corrected for buffer effects and unspecific binding to the chip matrix by subtraction of blank and reference surface (a blank flow cell channel activated by injection of EDC/NHS and inactivated by injection of ethanolamine). The dissociation constants (K_d) were estimated by plotting responses at equilibrium (R_{eq}) against the injected concentration and curve fitted to a Langmuir (1:1) binding isotherm.

Crystallization, X-ray data collection, and structure determination

Mouse Keap1 Kelch domain apo initial protein crystal hits were obtained in 3–4 days using the Crystal Screen HT (Hampton Research) in a condition consisting of 0.5 M Ammonium sulfate, 0.1 M Sodium citrate tribasic dihydrate pH 5.6 and 1.0 M Lithium sulfate monohydrate at 293 K. Best apo-crystals grew within 2 days by vapor-diffusion using the hanging drop method from 0.1 M Sodium Citrate pH 5.6, 0.5 M Lithium Sulphate, 0.7–0.9 M Ammonium Sulphate. For protein–ligand complexes, crystals were soaked within 2 to 16 hrs with 1–25 mM ligand (10–25% DMSO) from 100mM DMSO stocks, in a solution containing 100 mM Bis-Tris pH 7.0, 25% PEG 4K and harvested in liquid nitrogen for X-ray diffraction. Data for mouse Keap1 Kelch domain in complex with **3l**, **8**, and **7** were collected from the ID29 beamline;⁸⁸ and in complex with **4c** from the ID30a-3 beamline⁸⁹ at the European Synchrotron Radiation Facility (ESRF; Grenoble, France). X-ray diffraction data for mouse Keap1 Kelch domain in complex with **8h**, **8u**, **77g**, **77n**, and **77e** were collected from the P13 beamline; and in complex with **8y**, **8ad**, **77i** from the P14 beamline at DESY (Hamburg, Germany).⁹⁰ Data for compound **77o** in complex with mouse Keap1 Kelch domain was collected at BioMAX beamline (MAX IV, Lund, Sweden).⁹¹ Diffraction images were integrated, scaled, merged using autoprocessed beamline tools,⁹²⁻⁹⁷ while in some

cases the data were reprocessed and scaled using XDS.⁹⁸ The structures were solved using PHASER⁹⁹ with PDB ID 5FZN²⁰ as the search model for molecular replacement. Restraints for the fragments/compounds were prepared using the AceDRG¹⁰⁰ followed by Model building and refinement using COOT¹⁰¹ and Phenix.refine¹⁰². Figures were prepared using PyMOL (The PyMOL Molecular Graphics System, Version 2.0.6 Schrödinger, LLC).¹⁰³

Molecular docking

In silico experiments were performed using Schrödinger's Maestro software (version 11.7).¹⁰⁴ Protein receptors were prepared using the Protein Preparation Wizard with default settings and with retainment of the five conserved waters at the entrance to the central channel (*vide infra*), and ligands were prepared using LigPrep with default settings. The Receptor Grid Generation tool was used for docking grid generation with default settings. Ligand docking and scoring were performed using Glide with default settings. PyMOL (version 2.1.1) was applied for visualization of docking poses.¹⁰³ A docking study was first performed using a test set of 18 X-ray crystal structures of the Keap1 Kelch domain in complex with small-molecule ligands and a single apo protein structure, obtained from the Protein Data Bank (PDB ID: 4L7B, 4L7C, 4L7D, 4N1B, 4IQK, 4XMB, 4ZY3, 5FNR, 5FNS, 5FNT, 5FNU, 4IN4, 5FZJ, 5FZN, 5FNQ, 5WIY, 5WHL, 5WHO, 1U6D).¹⁰⁵ All the structures were validated according to general guidelines, assessing their crystallographic parameters, i.e. Rfree, Rwork, coordinate error, RMSD of bond length and angle from ideal, local B factors and electron density fit with model.¹⁰⁶ First, superimposition of all of these structures revealed large clusters of conserved water molecules inside the central cavity of the Kelch domain, which formed a highly extensive network of H-bonds with the protein backbone. Crucially, five water molecules near the entrance to the channel appeared to constitute a barrier for the protrusion of ligands; they were considered structural and were thus retained in all subsequent

modeling work. Secondly, the 18 X-ray crystal structures of the Kelch domain in complex with small-molecule ligands were employed for a self-docking study (where all the ligands were extracted and docked back into their cognate protein structures) in Glide using different precision modes (SP, SP with expanded sampling, XP, and induced fit). This identified standard precision (SP) as the optimal, giving the lowest mean RMSD (1.45 Å) and highest success rate (72% of dockings gave $\text{RMSD} \leq 2.0$ Å). Finally, all 19 X-ray structures were used in a cross-docking study (where all the ligands were docked into all other protein structures than their cognate). This identified the protein from the X-ray structure with PDB ID 5FNU as the optimal, giving the lowest mean RMSD (3.43 Å) and highest success rate (56% of dockings gave $\text{RMSD} \leq 2.0$ Å). All subsequent ligand dockings were thus performed using Glide with the SP scoring function and with the protein structure from PDB ID 5FNU, prepared with retainment of the five conserved waters at the central channel entrance (Later, we observed the five waters in all of our 13 deposited X-ray structures except for the lower 2–2.6 Å resolution structures – 6ZEX, 6ZF2, and 6ZEZ – where two, three, and all five waters were missing, respectively. No direct interactions between the five waters and the compounds were seen).

Microsomal stability assay

Compounds were mixed with mouse liver microsomes (pooled from male CD-1 mice; Sigma-Aldrich) in a potassium phosphate buffer (100 mM, pH 7.4) to a final concentration of 10 μM compound (1% DMSO) and 0.5 mg/mL microsomal protein. A commercial available NADPH regenerating system (Promega) consisting of solution A (20X stock containing 26 mM NADP⁺, 66 mM glucose-6-phosphate, and 66 mM MgCl₂) and B (100X stock containing 40 U/mL glucose-6-phosphate dehydrogenase and 5 mM sodium citrate) was used as source of electrons for the oxidative cytochrome P450 reactions. Solution A and B were mixed with compound and heated to 37 °C for 5 minutes. Microsomes were added and the mixture was incubated for four hours at 37 °C,

while aliquots (25 μ L) were quenched with ice-cold MeCN (12.5 μ L) at different time points followed by vortexing and centrifugation (5 min, 10.000 g). The supernatants were analyzed by LC-MS using the selective ion mode (SIM) function to quantify amount of compound relative to time zero and determine the half-life ($t_{1/2}$) by integrating compound peaks and fitting the resulting AUC values and time points to a one phase decay equation. A negative control where NADPH and microsomes were omitted from the sample was included for each compound to discriminate general instability under the given assay conditions from microsomal metabolism. All tested compounds were found stable in these negative control samples. Imipramine and propranolol were used as positive control compounds ($t_{1/2}$ = 19 and 37 minutes, respectively) thereby confirming the activity of the microsomes.

Human blood plasma assay

Compounds were mixed with a 1:1 solution of potassium phosphate buffer (100 mM, pH 7.4) and pooled human blood plasma (3H Biomedical) to a final compound concentration of 20 μ M (2% DMSO). Samples were incubated at 37 °C for three hours, while aliquots (30 μ L) were quenched at sequential time points by addition of ice-cold MeCN (90 μ L), vortexing, and centrifugation (15 min, 10.000 g). The supernatants were analyzed by LC-MS (SIM) to quantify amount of compound relative to time zero as described for the microsomal stability assay. Compounds were also tested without presence of blood plasma to check for general stability issues, and procaine and procainamide were included as positive and negative control compounds ($t_{1/2}$ = 2 and $>>180$ minutes, respectively).

Parallel Artificial Membrane Permeability Assay (PAMPA)

The permeability of the compounds was tested using the Corning® Gentest™ Pre-coated PAMPA Plate System. Compounds were tested in duplicates at 20 μM in potassium phosphate buffer (100 mM, pH 7.4) (2% DMSO). Compound solutions (300 μL/well) were added to the receiver (donor) well and the corresponding buffer solution (200 μL/well) was added to the filter (acceptor) wells. The filter and receiver plates were assembled and incubated at room temperature for 5 hours, followed by analysis of donor and acceptor wells by LC-MS (SIM) to quantify amount of compound in the two chambers. Caffeine and antipyrine were included as positive (highly permeable) controls, and sulfasalazine and norfloxacin as negative (low permeable) controls. The effective permeability coefficient (P_e) was calculated according to manufacturer instructions.

ASSOCIATED CONTENT

Supporting Information

The Supporting Information is available free of charge:

Synthesis schemes for the SAR study of **8** (**Schemes 1–11**), structures and activities of the deconstructed fragments **1a–6f** (**Table S1–S2**), table with X-ray data collection and refinement statistics of the 13 deposited PDB structures (**Table S3**), PAMPA data (**Table S4**), supporting X-ray structures (**Figure S1–S3**), physicochemical properties of key compounds (**Figure S4**), and HPLC traces (**Figure S5**) (PDF)
Molecular formula strings (CSV)

PDB Accession Codes

Structure factors and coordinate files of mouse Keap1 Kelch domain in complex with the 13 compounds are deposited in the Protein Data Bank as follows: 6ZEW (**3l**), 6ZEX (**4c**), 6ZEY (**8**), 6Z EZ (**7**), 6ZF0 (**8y**), 6ZF1 (**8h**), 6ZF2 (**8u**), 6ZF3 (**8ad**), 6ZF4 (**77i**), 6ZF5 (**77g**), 6ZF6 (**77n**), 6ZF7 (**77e**), 6ZF8 (**77o**). Authors will release the atomic coordinates upon article publication.

AUTHOR INFORMATION

Corresponding Author

*E-mail: anders.bach@sund.ku.dk; Phone: +45 21 28 86 04

ORCID

Dilip Narayanan: 0000-0001-9164-9961

Sara M. Ø. Solbak: 0000-0003-0233-7160.

Lars J. Høj: 0000-0002-6621-6475

Federico Munafò: 0000-0001-5400-8970

Anthony D. Garcia: 0000-0003-0052-6259

Roberta Brambilla: 0000-0001-5792-7497

Tommy N. Johansen: 0000-0001-5918-0833

Grzegorz M. Popowicz: 0000-0003-2818-7498

Michael Sattler: 0000-0002-1594-0527

Michael Gajhede: 0000-0001-9864-2287

Anders Bach: 0000-0003-4305-9910

Present addresses

^VPresent address: Department of Forensic Medicine, Faculty of Health and Medical Sciences, University of Copenhagen, Teillum Building, Frederik V's Vej 11, DK-2100 Copenhagen, Denmark

^JPresent address: Molecular Modeling and Drug Discovery, Fondazione Istituto Italiano di Tecnologia, Via Morego 30, I-16163 Genova, Italy

[#]Present address: Department of Pharmaceutical, Chemical and Environmental Sciences, The University of Greenwich, Chatham Maritime, UK-ME4 4TB Kent, United Kingdom

Author Contributions

The manuscript was written by J.S.P. and A.B. with contributions from all authors. All authors have given approval to the final version of the manuscript.

Notes

The authors declare no competing financial interests.

ACKNOWLEDGEMENTS

This research was supported by the Lundbeck Foundation (grant R190-2014-3710 for A.B.); the A. P. Møller Foundation for the Advancement of Medical Science (grant 14-28 for A.B.); the Hørslev Foundation (grant 203866-MIA for A.B.); the Augustinus Foundation (grant 14-1571 for A.B.); and the Drug Research Academy/Lundbeck Foundation (scholarship for K.T.T.). We also acknowledge funding from the European Union's Framework Programme for Research and Innovation Horizon 2020 (2014-2020) under the Marie Skłodowska-Curie Grant Agreement No. 675555, Accelerated Early staGe drug discovery (AEGIS) and the Helmholtz Center Munich to M.S. and G.P.; and access to NMR measurements at the Bavarian NMR Center and at University of Copenhagen (the latter supported by grant #10-085264 from The Danish Research Council for Independent Research | Nature and Universe and grant R77-A6742 from the Lundbeck Foundation). We thank all the staff at the European beamlines (BioMAX at MAX IV, Sweden; ID29 and ID30a at ESRF, France; and P13 and P14 at DESY, Germany) for beamtime and their support and help.

ABBREVIATIONS

AREs, antioxidant response elements; BTB, broad complex, tramtrack, and bric-à-brac; COPD, chronic obstructive pulmonary disease; Cul3, cullin 3; FAM, 5(6)-carboxyfluorescein; FBDR, fragment-based deconstruction reconstruction; FLINT, total fluorescence intensity; FP, fluorescence polarization; GPx, glutathione peroxidase; GST, glutathione S-transferase; HO-1, heme oxygenase 1; IVR, intervening region; Keap1, Kelch-like ECH-associated protein 1; LE, ligand efficiency; Neh2, Nrf2-ECH homology 2; NQO1, NAD(P)H dehydrogenase (quinone) 1; Nrf2, nuclear factor erythroid 2-related factor 2; PAMPA, parallel artificial membrane permeation assay; PPI, protein-protein interaction; Ro3, rule of 3; ROS, reactive oxygen species; SIM, selective ion mode; SOD, superoxide dismutase; SPR, surface plasmon resonance; STD NMR, saturation-transfer difference NMR; TSA, thermal shift assay.

REFERENCES

1. Li, X.; Fang, P.; Mai, J.; Choi, E. T.; Wang, H.; Yang, X. F. Targeting mitochondrial reactive oxygen species as novel therapy for inflammatory diseases and cancers. *J. Hematol. Oncol.* **2013**, *6*, 19.
2. Uttara, B.; Singh, A. V.; Zamboni, P.; Mahajan, R. T. Oxidative stress and neurodegenerative diseases: a review of upstream and downstream antioxidant therapeutic options. *Curr. Neuropharmacol.* **2009**, *7*, 65-74.
3. Bach, A. Targeting Oxidative Stress in Stroke. In *Neuroprotective Therapy for Stroke and Ischemic Disease*; Lapchak, P. A.; Zhang, J. H., Eds. Springer: 2017; pp 203-250.
4. Itoh, K.; Chiba, T.; Takahashi, S.; Ishii, T.; Igarashi, K.; Katoh, Y.; Oyake, T.; Hayashi, N.; Satoh, K.; Hatayama, I.; Yamamoto, M.; Nabeshima, Y. An Nrf2/small maf heterodimer mediates the induction of phase II detoxifying enzyme genes through antioxidant response elements. *Biochem. Biophys. Res. Commun.* **1997**, *236*, 313-322.
5. Itoh, K.; Wakabayashi, N.; Katoh, Y.; Ishii, T.; Igarashi, K.; Engel, J. D.; Yamamoto, M. Keap1 represses nuclear activation of antioxidant responsive elements by Nrf2 through binding to the amino-terminal Neh2 domain. *Genes Devel.* **1999**, *13*, 76-86.
6. Tonelli, C.; Chio, I. I. C.; Tuveson, D. A. Transcriptional regulation by Nrf2. *Antioxid. Redox. Signal.* **2018**, *29*, 1727-1745.
7. Cullinan, S. B.; Gordan, J. D.; Jin, J.; Harper, J. W.; Diehl, J. A. The Keap1-BTB protein is an adaptor that bridges Nrf2 to a Cul3-based E3 ligase: oxidative stress sensing by a Cul3-Keap1 ligase. *Mol. Cell. Biol.* **2004**, *24*, 8477-8486.
8. Jiang, Z. Y.; Lu, M. C.; You, Q. D. Discovery and development of Kelch-like ECH-associated protein 1. nuclear factor erythroid 2-related factor 2 (KEAP1:NRF2) Protein-Protein Interaction Inhibitors: achievements, challenges, and future directions. *J. Med. Chem.* **2016**, *59*, 10837-10858.

9. Tong, K. I.; Katoh, Y.; Kusunoki, H.; Itoh, K.; Tanaka, T.; Yamamoto, M. Keap1 recruits Neh2 through binding to ETGE and DLG motifs: characterization of the two-site molecular recognition model. *Mol. Cell. Biol.* **2006**, *26*, 2887-2900.
10. McMahon, M.; Thomas, N.; Itoh, K.; Yamamoto, M.; Hayes, J. D. Dimerization of substrate adaptors can facilitate cullin-mediated ubiquitylation of proteins by a "tethering" mechanism: a two-site interaction model for the Nrf2-Keap1 complex. *J. Biol. Chem.* **2006**, *281*, 24756-24768.
11. Canning, P.; Cooper, C. D.; Krojer, T.; Murray, J. W.; Pike, A. C.; Chaikuad, A.; Keates, T.; Thangaratnarajah, C.; Hojzan, V.; Ayinampudi, V.; Marsden, B. D.; Gileadi, O.; Knapp, S.; von Delft, F.; Bullock, A. N. Structural basis for Cul3 protein assembly with the BTB-Kelch family of E3 ubiquitin ligases. *J. Biol. Chem.* **2013**, *288*, 7803-7814.
12. Fukutomi, T.; Takagi, K.; Mizushima, T.; Ohuchi, N.; Yamamoto, M. Kinetic, Thermodynamic, and structural characterizations of the association between Nrf2-DLGex degron and Keap1. *Mol. Cell. Biol.* **2014**, *34*, 832.
13. Baird, L.; Dinkova-Kostova, A. T. The cytoprotective role of the Keap1-Nrf2 pathway. *Arch. Toxicol.* **2011**, *85*, 241-272.
14. Pallesen, J. S.; Tran, K. T.; Bach, A. Non-covalent small-molecule Kelch-like ECH-associated protein 1-nuclear factor erythroid 2-related factor 2 (Keap1-Nrf2) inhibitors and their potential for targeting central nervous system diseases. *J. Med. Chem.* **2018**, *61*, 8088-8103.
15. Magesh, S.; Chen, Y.; Hu, L. Q. Small molecule modulators of Keap1-Nrf2-ARE pathway as potential preventive and therapeutic agents. *Med. Res. Rev.* **2012**, *32*, 687-726.
16. Baird, L.; Lleres, D.; Swift, S.; Dinkova-Kostova, A. T. Regulatory flexibility in the Nrf2-mediated stress response is conferred by conformational cycling of the Keap1-Nrf2 protein complex. *Proc. Natl. Acad. Sci. U.S.A.* **2013**, *110*, 15259-15264.
17. Adibhatla, R. M.; Hatcher, J. F. Lipid oxidation and peroxidation in CNS health and disease: from molecular mechanisms to therapeutic opportunities. *Antioxid. Redox Signal.* **2010**, *12*, 125-169.

18. Lakhan, S. E.; Kirchgessner, A.; Hofer, M. Inflammatory mechanisms in ischemic stroke: therapeutic approaches. *J. Transl. Med.* **2009**, *7*, 97.
19. Iadecola, C.; Anrather, J. Stroke research at a crossroad: asking the brain for directions. *Nat. Neurosci.* **2011**, *14*, 1363-1368.
20. Davies, T. G.; Wixted, W. E.; Coyle, J. E.; Griffiths-Jones, C.; Hearn, K.; McMEnamin, R.; Norton, D.; Rich, S. J.; Richardson, C.; Saxty, G.; Willems, H. M.; Woolford, A. J.; Cottom, J. E.; Kou, J. P.; Yonchuk, J. G.; Feldser, H. G.; Sanchez, Y.; Foley, J. P.; Bolognese, B. J.; Logan, G.; Podolin, P. L.; Yan, H.; Callahan, J. F.; Heightman, T. D.; Kerns, J. K. Monoacidic inhibitors of the Kelch-like ECH-associated protein 1: nuclear factor erythroid 2-related factor 2 (KEAP1:NRF2) protein-protein interaction with high cell potency identified by fragment-based discovery. *J. Med. Chem.* **2016**, *59*, 3991-4006.
21. Cuadrado, A.; Rojo, A. I.; Wells, G.; Hayes, J. D.; Cousin, S. P.; Rumsey, W. L.; Attucks, O. C.; Franklin, S.; Levonen, A. L.; Kensler, T. W.; Dinkova-Kostova, A. T. Therapeutic targeting of the NRF2 and KEAP1 partnership in chronic diseases. *Nat. Rev. Drug Discov.* **2019**, *18*, 295-317.
22. Lu, M. C.; Ji, J. A.; Jiang, Z. Y.; You, Q. D. The Keap1-Nrf2-ARE pathway as a potential preventive and therapeutic target: an update. *Med. Res. Rev.* **2016**, *36*, 924-963.
23. Hu, L.; Magesh, S.; Chen, L.; Wang, L.; Lewis, T. A.; Chen, Y.; Khodier, C.; Inoyama, D.; Beamer, L. J.; Emge, T. J.; Shen, J.; Kerrigan, J. E.; Kong, A. N.; Dandapani, S.; Palmer, M.; Schreiber, S. L.; Munoz, B. Discovery of a small-molecule inhibitor and cellular probe of Keap1-Nrf2 protein-protein interaction. *Bioorg. Med. Chem. Lett.* **2013**, *23*, 3039-3043.
24. Marcotte, D.; Zeng, W.; Hus, J. C.; McKenzie, A.; Hession, C.; Jin, P.; Bergeron, C.; Lugovskoy, A.; Enyedy, I.; Cuervo, H.; Wang, D.; Atmanene, C.; Roecklin, D.; Vecchi, M.; Vivat, V.; Kraemer, J.; Winkler, D.; Hong, V.; Chao, J.; Lukashev, M.; Silvan, L. Small molecules inhibit the interaction of Nrf2 and the Keap1 Kelch domain through a non-covalent mechanism. *Bioorg. Med. Chem.* **2013**, *21*, 4011-4019.

25. Jnoff, E.; Albrecht, C.; Barker, J. J.; Barker, O.; Beaumont, E.; Bromidge, S.; Brookfield, F.; Brooks, M.; Bubert, C.; Ceska, T.; Corden, V.; Dawson, G.; Duclos, S.; Fryatt, T.; Genicot, C.; Jigorel, E.; Kwong, J.; Maghames, R.; Mushi, I.; Pike, R.; Sands, Z. A.; Smith, M. A.; Stimson, C. C.; Courade, J. P. Binding mode and structure-activity relationships around direct inhibitors of the Nrf2-Keap1 complex. *ChemMedChem* **2014**, *9*, 699-705.
26. Jiang, Z. Y.; Lu, M. C.; Xu, L. L.; Yang, T. T.; Xi, M. Y.; Xu, X. L.; Guo, X. K.; Zhang, X. J.; You, Q. D.; Sun, H. P. Discovery of potent Keap1-Nrf2 protein-protein interaction inhibitor based on molecular binding determinants analysis. *J. Med. Chem.* **2014**, *57*, 2736-2745.
27. Jain, A. D.; Potteti, H.; Richardson, B. G.; Kingsley, L.; Luciano, J. P.; Ryuzoji, A. F.; Lee, H.; Kronic, A.; Mesecar, A. D.; Reddy, S. P.; Moore, T. W. Probing the structural requirements of non-electrophilic naphthalene-based Nrf2 activators. *Eur. J. Med. Chem.* **2015**, *103*, 252-268.
28. Winkel, A. F.; Engel, C. K.; Margerie, D.; Kannt, A.; Szillat, H.; Glombik, H.; Kallus, C.; Ruf, S.; Gussregen, S.; Riedel, J.; Herling, A. W.; von Knethen, A.; Weigert, A.; Brune, B.; Schmoll, D. Characterization of RA839, a noncovalent small molecule binder to Keap1 and selective activator of Nrf2 signaling. *J. Biol. Chem.* **2015**, *290*, 28446-28455.
29. Szill, H.; Ruf, S.; Glombik, H.; Kallus, C.; Engel, K.-C.; Gussregen, S.; Schmoll, D.; Kannt, A.; Dudda, A.; Monecke, P.; Elshorst, B. Naphthyl sulfonamide pyrrolidine derivatives as KEAP-1 modulators for the treatment of diabetes, obesity, dyslipidemia and related disorders. European Application no. EP143064302016.
30. Yasuda, D.; Yuasa, A.; Obata, R.; Nakajima, M.; Takahashi, K.; Ohe, T.; Ichimura, Y.; Komatsu, M.; Yamamoto, M.; Imamura, R.; Kojima, H.; Okabe, T.; Nagano, T.; Mashino, T. Discovery of benzo[g]indoles as a novel class of non-covalent Keap1-Nrf2 protein-protein interaction inhibitor. *Bioorg. Med. Chem. Lett.* **2017**, *27*, 5006-5009.
31. Callahan, J. F.; Kerns, J. K.; Li, T.; McClelland, B. W.; Nie, H.; Pero, J. E.; Davies, T. G.; Heightman, T. D.; Griffiths-Jones, C. M.; Howard, S.; Norton, D.; Verdonk, M. L.; Woolford, A. J.-A. Arylcyclohexyl pyrazoles as Nrf2 regulators. Application no. IBPCT/IB2016/0559972017.

32. Callahan, J. F.; Kerns, J. K.; Li, P.; Li, T.; Mcclelland, B. W.; Nie, H.; Pero, J. E.; Davies, T. G.; Grazia Carr, M.; Griffiths-Jones, C. M.; Heightman, T. D.; Norton, D.; Verdonk, M. L.; Woolford, A. J.-A.; Willems, H. M. G. Biaryl pyrazoles as Nrf2 regulators. Application no. IBPCT/IB2016/0559962017.
33. Tran, K. T.; Pallesen, J. S.; Solbak, S. M. Ø.; Narayanan, D.; Baig, A.; Zang, J.; Aguayo-Orozco, A.; Carmona, R. M. C.; Garcia, A. D.; Bach, A. A comparative assessment study of known small-molecule Keap1-Nrf2 protein-protein interaction inhibitors: chemical synthesis, binding properties, and cellular activity. *J. Med. Chem.* **2019**, *62*, 8028-8052.
34. Richardson, B. G.; Jain, A. D.; Potteti, H. R.; Lazzara, P. R.; David, B. P.; Tamatam, C. R.; Choma, E.; Skowron, K.; Dye, K.; Siddiqui, Z.; Wang, Y. T.; Krunic, A.; Reddy, S. P.; Moore, T. W. Replacement of a naphthalene scaffold in kelch-like ECH-associated protein 1 (KEAP1)/nuclear factor (erythroid-derived 2)-like 2 (NRF2) inhibitors. *J. Med. Chem.* **2018**, *61*, 8029-8047.
35. Lu, M. C.; Zhang, X.; Wu, F.; Tan, S. J.; Zhao, J.; You, Q. D.; Jiang, Z. Y. Discovery of a potent kelch-like ECH-associated protein 1-nuclear factor erythroid 2-related factor 2 (Keap1-Nrf2) protein-protein interaction inhibitor with natural proline structure as a cytoprotective agent against acetaminophen-induced hepatotoxicity. *J. Med. Chem.* **2019**, *62*, 6796-6813.
36. Lazzara, P. R.; David, B. P.; Ankireddy, A.; Richardson, B. G.; Dye, K.; Ratia, K. M.; Reddy, S. P.; Moore, T. W. Isoquinoline kelch-like ECH-associated protein 1-nuclear factor (erythroid-derived 2)-like 2 (KEAP1-NRF2) inhibitors with high metabolic stability. *J. Med. Chem.* **2020**, *63*, 6547-6560.
37. Lazzara, P. R.; Jain, A. D.; Maldonado, A. C.; Richardson, B.; Skowron, K. J.; David, B. P.; Siddiqui, Z.; Ratia, K. M.; Moore, T. W. Synthesis and evaluation of noncovalent naphthalene-based KEAP1-NRF2 inhibitors. *ACS Med. Chem. Lett.* **2020**, *11*, 521-527.
38. Abed, D. A.; Lee, S.; Hu, L. Discovery of disubstituted xylylene derivatives as small molecule direct inhibitors of Keap1-Nrf2 protein-protein interaction. *Bioorg. Med. Chem.* **2020**, *28*, 115343.

39. Gorgulla, C.; Boeszoermerenyi, A.; Wang, Z. F.; Fischer, P. D.; Coote, P. W.; Padmanabha Das, K. M.; Malets, Y. S.; Radchenko, D. S.; Moroz, Y. S.; Scott, D. A.; Fackeldey, K.; Hoffmann, M.; Iavniuk, I.; Wagner, G.; Arthanari, H. An open-source drug discovery platform enables ultra-large virtual screens. *Nature* **2020**, *580*, 663-668.
40. Ontoria, J. M.; Biancofiore, I.; Fezzardi, P.; Ferrigno, F.; Torrente, E.; Colarusso, S.; Bianchi, E.; Andreini, M.; Patsilidakos, A.; Kempf, G.; Augustin, M.; Steinbacher, S.; Summa, V.; Pacifici, R.; Munoz-Sanjuan, I.; Park, L.; Bresciani, A.; Dominguez, C.; Sherman, L. T.; Harper, S. Combined peptide and small-molecule approach toward nonacidic THIQ inhibitors of the KEAP1/NRF2 interaction. *ACS Med. Chem. Lett.* **2020**, *11*, 740-746.
41. Ma, B.; Lucas, B.; Capacci, A.; Lin, E. Y.; Jones, J. H.; Dechantsreiter, M.; Enyedy, I.; Marcotte, D.; Xiao, G.; Li, B.; Richter, K. Design, synthesis and identification of novel, orally bioavailable non-covalent Nrf2 activators. *Bioorg. Med. Chem. Lett.* **2020**, *30*, 126852.
42. Lu, M.; Zhang, X.; Zhao, J.; You, Q.; Jiang, Z. A hydrogen peroxide responsive prodrug of Keap1-Nrf2 inhibitor for improving oral absorption and selective activation in inflammatory conditions. *Redox Biol.* **2020**, *34*, 101565.
43. Zhou, H. S.; Hu, L. B.; Zhang, H.; Shan, W. X.; Wang, Y.; Li, X.; Liu, T.; Zhao, J.; You, Q. D.; Jiang, Z. Y. Design, synthesis, and structure-activity relationships of indoline-based kelch-like ECH-associated protein 1-nuclear factor (erythroid-derived 2)-like 2 (Keap1-Nrf2) protein-protein interaction inhibitors. *J. Med. Chem.* **2020**, *63*, 11149-11168.
44. Sun, Y.; Huang, J.; Chen, Y.; Shang, H.; Zhang, W.; Yu, J.; He, L.; Xing, C.; Zhuang, C. Direct inhibition of Keap1-Nrf2 protein-protein interaction as a potential therapeutic strategy for Alzheimer's disease. *Bioorg. Chem.* **2020**, *103*, 104172.
45. Lu, M. C.; Shao, H. L.; Liu, T.; You, Q. D.; Jiang, Z. Y. Discovery of 2-oxy-2-phenylacetic acid substituted naphthalene sulfonamide derivatives as potent KEAP1-NRF2 protein-protein interaction inhibitors for inflammatory conditions. *Eur. J. Med. Chem.* **2020**, *207*, 112734.

46. Heightman, T. D.; Callahan, J. F.; Chiarparin, E.; Coyle, J. E.; Griffiths-Jones, C.; Lakdawala, A. S.; McMenamin, R.; Mortenson, P. N.; Norton, D.; Peakman, T. M.; Rich, S. J.; Richardson, C.; Rumsey, W. L.; Sanchez, Y.; Saxty, G.; Willems, H. M. G.; Wolfe, L., 3rd; Woolford, A. J.; Wu, Z.; Yan, H.; Kerns, J. K.; Davies, T. G. Structure-activity and structure-conformation relationships of aryl propionic acid inhibitors of the kelch-like ECH-associated protein 1/nuclear factor erythroid 2-related factor 2 (KEAP1/NRF2) protein-protein interaction. *J. Med. Chem.* **2019**, *62*, 4683-4702.
47. Erlanson, D. A.; Fesik, S. W.; Hubbard, R. E.; Jahnke, W.; Jhoti, H. Twenty years on: the impact of fragments on drug discovery. *Nat. Rev. Drug. Discov.* **2016**, *15*, 605-619.
48. Scott, D. E.; Coyne, A. G.; Hudson, S. A.; Abell, C. Fragment-based approaches in drug discovery and chemical biology. *Biochemistry* **2012**, *51*, 4990-5003.
49. Hopkins, A. L.; Groom, C. R.; Alex, A. Ligand efficiency: a useful metric for lead selection. *Drug Discov. Today* **2004**, *9*, 430-431.
50. Barelier, S.; Pons, J.; Marcillat, O.; Lancelin, J. M.; Krimm, I. Fragment-based deconstruction of Bcl-xL inhibitors. *J. Med. Chem.* **2010**, *53*, 2577-2588.
51. Fry, D. C.; Wartchow, C.; Graves, B.; Janson, C.; Lukacs, C.; Kammlott, U.; Belunis, C.; Palme, S.; Klein, C.; Vu, B. Deconstruction of a nutlin: dissecting the binding determinants of a potent protein-protein interaction inhibitor. *ACS Med. Chem. Lett.* **2013**, *4*, 660-665.
52. Kavanagh, M. E.; Coyne, A. G.; McLean, K. J.; James, G. G.; Levy, C. W.; Marino, L. B.; de Carvalho, L. P. S.; Chan, D. S. H.; Hudson, S. A.; Surade, S.; Leys, D.; Munro, A. W.; Abell, C. Fragment-based approaches to the development of mycobacterium tuberculosis CYP121 inhibitors. *J. Med. Chem.* **2016**, *59*, 3272-3302.
53. Ferreira de Freitas, R.; Eram, M. S.; Smil, D.; Szewczyk, M. M.; Kennedy, S.; Brown, P. J.; Santhakumar, V.; Barsyte-Lovejoy, D.; Arrowsmith, C. H.; Vedadi, M.; Schapira, M. Discovery of a potent and selective coactivator

associated arginine methyltransferase 1 (CARM1) inhibitor by virtual screening. *J. Med. Chem.* **2016**, *59*, 6838-6347.

54. Congreve, M.; Carr, R.; Murray, C.; Jhoti, H. A 'Rule of Three' for fragment-based lead discovery? *Drug Discov. Today* **2003**, *8*, 876-877.

55. Jhoti, H.; Williams, G.; Rees, D. C.; Murray, C. W. The 'rule of three' for fragment-based drug discovery: where are we now? *Nat. Rev. Drug Discov.* **2013**, *12*, 644-645.

56. Bertrand, H. C.; Schaap, M.; Baird, L.; Georgakopoulos, N. D.; Fowkes, A.; Thiollier, C.; Kachi, H.; Dinkova-Kostova, A. T.; Wells, G. Design, Synthesis, and evaluation of triazole derivatives that induce Nrf2 dependent gene products and inhibit the Keap1-Nrf2 protein-protein interaction. *J. Med. Chem.* **2015**, *58*, 7186-7194.

57. Shimozono, R.; Asaoka, Y.; Yoshizawa, Y.; Aoki, T.; Noda, H.; Yamada, M.; Kaino, M.; Mochizuki, H. Nrf2 activators attenuate the progression of nonalcoholic steatohepatitis-related fibrosis in a dietary rat model. *Mol. Pharmacol.* **2013**, *84*, 62-70.

58. Satoh, M.; Saburi, H.; Tanaka, T.; Matsuura, Y.; Naitow, H.; Shimozono, R.; Yamamoto, N.; Inoue, H.; Nakamura, N.; Yoshizawa, Y.; Aoki, T.; Tanimura, R.; Kunishima, N. Multiple binding modes of a small molecule to human Keap1 revealed by X-ray crystallography and molecular dynamics simulation. *FEBS Open Bio* **2015**, *5*, 557-570.

59. Lagorce, D.; Oliveira, N.; Miteva, M. A.; Villoutreix, B. O. Pan-assay interference compounds (PAINS) that may not be too painful for chemical biology projects. *Drug Discov. Today* **2017**, *22*, 1131-1133.

60. Simeonov, A.; Jadhav, A.; Thomas, C. J.; Wang, Y.; Huang, R.; Southall, N. T.; Shinn, P.; Smith, J.; Austin, C. P.; Auld, D. S.; Inglese, J. Fluorescence spectroscopic profiling of compound libraries. *J. Med. Chem.* **2008**, *51*, 2363-2371.

61. Turek-Etienne, T. C.; Lei, M.; Terracciano, J. S.; Langsdorf, E. F.; Bryant, R. W.; Hart, R. F.; Horan, A. C. Use of red-shifted dyes in a fluorescence polarization AKT kinase assay for detection of biological activity in natural product extracts. *J. Biomol. Screen.* **2004**, *9*, 52-61.
62. Feng, B. Y.; Shoichet, B. K. A detergent-based assay for the detection of promiscuous inhibitors. *Nat. Protoc.* **2006**, *1*, 550-553.
63. Turek-Etienne, T. C.; Small, E. C.; Soh, S. C.; Xin, T. A.; Gaitonde, P. V.; Barrabee, E. B.; Hart, R. F.; Bryant, R. W. Evaluation of fluorescent compound interference in 4 fluorescence polarization assays: 2 kinases, 1 protease, and 1 phosphatase. *J. Biomol. Screen.* **2003**, *8*, 176-184.
64. Owicki, J. C. Fluorescence polarization and anisotropy in high throughput screening: perspectives and primer. *J. Biomol. Screen.* **2000**, *5*, 297-306.
65. Pope, A. J.; Haupts, U. M.; Moore, K. J. Homogeneous fluorescence readouts for miniaturized high-throughput screening: theory and practice. *Drug Discov. Today* **1999**, *4*, 350-362.
66. Turconi, S.; Shea, K.; Ashman, S.; Fantom, K.; Earnshaw, D. L.; Bingham, R. P.; Haupts, U. M.; Brown, M. J.; Pope, A. J. Real experiences of uHTS: a prototypic 1536-well fluorescence anisotropy-based uHTS screen and application of well-level quality control procedures. *J. Biomol. Screen.* **2001**, *6*, 275-290.
67. Vedvik, K. L.; Eliason, H. C.; Hoffman, R. L.; Gibson, J. R.; Kupcho, K. R.; Somberg, R. L.; Vogel, K. W. Overcoming compound interference in fluorescence polarization-based kinase assays using far-red tracers. *Assay Drug Dev. Technol.* **2004**, *2*, 193-203.
68. Aretz, J.; Rademacher, C. Ranking hits from saturation transfer difference nuclear magnetic resonance-based fragment screening. *Front. Chem.* **2019**, *7*, 215.
69. Quinn, J. G. Evaluation of Taylor dispersion injections: determining kinetic/affinity interaction constants and diffusion coefficients in label-free biosensing. *Anal. Biochem* **2012**, *421*, 401-410.

70. Quinn, J. G. Modeling Taylor dispersion injections: determination of kinetic/affinity interaction constants and diffusion coefficients in label-free biosensing. *Anal. Biochem.* **2012**, *421*, 391-400.
71. Davis, B. J.; Erlanson, D. A. Learning from our mistakes: the 'unknown knowns' in fragment screening. *Bioorg. Med. Chem. Lett.* **2013**, *23*, 2844-2852.
72. Giannetti, A. M.; Koch, B. D.; Browner, M. F. Surface plasmon resonance based assay for the detection and characterization of promiscuous inhibitors. *J. Med. Chem.* **2008**, *51*, 574-580.
73. Basse, N.; Kaar, J. L.; Settanni, G.; Joerger, A. C.; Rutherford, T. J.; Fersht, A. R. Toward the rational design of p53-stabilizing drugs: probing the surface of the oncogenic Y220C mutant. *Chem. Biol.* **2010**, *17*, 46-56.
74. Wielens, J.; Headey, S. J.; Rhodes, D. I.; Mulder, R. J.; Dolezal, O.; Deadman, J. J.; Newman, J.; Chalmers, D. K.; Parker, M. W.; Peat, T. S.; Scanlon, M. J. Parallel screening of low molecular weight fragment libraries: do differences in methodology affect hit identification? *J. Biomol. Screen.* **2013**, *18*, 147-159.
75. Schiebel, J.; Radeva, N.; Koster, H.; Metz, A.; Krotzky, T.; Kuhnert, M.; Diederich, W. E.; Heine, A.; Neumann, L.; Atmanene, C.; Roecklin, D.; Vivat-Hannah, V.; Renaud, J. P.; Meinecke, R.; Schlinck, N.; Sitte, A.; Popp, F.; Zeeb, M.; Klebe, G. One question, multiple answers: biochemical and biophysical screening methods retrieve deviating fragment hit lists. *ChemMedChem* **2015**, *10*, 1511-1521.
76. Zhong, M.; Lynch, A.; Muellers, S. N.; Jehle, S.; Luo, L.; Hall, D. R.; Iwase, R.; Carolan, J. P.; Egbert, M.; Wakefield, A.; Streu, K.; Harvey, C. M.; Ortet, P. C.; Kozakov, D.; Vajda, S.; Allen, K. N.; Whitty, A. Interaction energetics and druggability of the protein-protein interaction between kelch-like ECH-associated protein 1 (KEAP1) and nuclear factor erythroid 2 like 2 (Nrf2). *Biochemistry* **2020**, *59*, 563-581.
77. Kozakov, D.; Hall, D. R.; Jehle, S.; Luo, L.; Ochiana, S. O.; Jones, E. V.; Pollastri, M.; Allen, K. N.; Whitty, A.; Vajda, S. Ligand deconstruction: why some fragment binding positions are conserved and others are not. *Proc. Natl. Acad. Sci. U. S. A.* **2015**, *112*, E2585-E2594.

78. Chen, H.; Zhou, X.; Wang, A.; Zheng, Y.; Gao, Y.; Zhou, J. Evolutions in fragment-based drug design: the deconstruction-reconstruction approach. *Drug Discov. Today* **2015**, *20*, 105-113.
79. Ferrara, S. J.; Scanlan, T. S. A CNS-targeting prodrug strategy for nuclear receptor modulators. *J. Med. Chem.* **2020**, *63*, 9742-9751.
80. Bach, P.; Boström, J.; Brickmann, K.; Cheng, L.; Giordanetto, F.; Groneberg, R. D.; Harvey, D. M.; O'sullivan, M. F.; Zetterberg, F.; Österlund, K. Novel pyridine compounds. WO2006073361A1.
81. Deng, W.; Liu, L.; Zhang, C.; Liu, M.; Guo, Q.-X. Copper-catalyzed cross-coupling of sulfonamides with aryl iodides and bromides facilitated by amino acid ligands. *Tetrahedron Lett.* **2005**, *46*, 7295-7298.
82. Pehlivan, L.; Metay, E.; Laval, S.; Dayoub, W.; Demonchaux, P.; Mignani, G.; Lemaire, M. Iron-catalyzed selective reduction of nitro compounds to amines. *Tetrahedron Lett.* **2010**, *51*, 1939-1941.
83. Lager, E.; Nilsson, J.; Nielsen, E. O.; Nielsen, M.; Liljefors, T.; Sterner, O. Affinity of 3-acyl substituted 4-quinolones at the benzodiazepine site of GABA(A) receptors. *Bioorg. Med. Chem.* **2008**, *16*, 6936-6948.
84. Rashid, M. A.; Rasool, N.; Adeel, M.; Reinke, H.; Spannenberg, A.; Fischer, C.; Langer, P. Regioselective synthesis of sterically encumbered diaryl ethers based on one-pot cyclizations of 4-aryloxy-1,3-bis(trimethylsilyloxy)-1,3-dienes. *Tetrahedron* **2008**, *64*, 529-535.
85. Li, A.; Ouyang, Y. B.; Wang, Z. Y.; Cao, Y. Y.; Liu, X. Y.; Ran, L.; Li, C.; Li, L.; Zhang, L.; Qiao, K.; Xu, W. S.; Huang, Y.; Zhang, Z. L.; Tian, C.; Liu, Z. M.; Jiang, S. B.; Shao, Y. M.; Du, Y. S.; Ma, L. Y.; Wang, X. W.; Liu, J. Y. Novel pyridinone derivatives as non-nucleoside reverse transcriptase inhibitors (NNRTIs) with high potency against NNRTI-resistant HIV-1 strains. *J. Med. Chem.* **2013**, *56*, 3593-3608.
86. Nikolovska-Coleska, Z.; Wang, R.; Fang, X.; Pan, H.; Tomita, Y.; Li, P.; Roller, P. P.; Krajewski, K.; Saito, N. G.; Stuckey, J. A.; Wang, S. Development and optimization of a binding assay for the XIAP BIR3 domain using fluorescence polarization. *Anal. Biochem.* **2004**, *332*, 261-273.

87. Mayer, M.; Meyer, B. Characterization of Ligand binding by saturation transfer difference NMR spectroscopy. *Angew. Chem. Int. Ed. Engl.* **1999**, *38*, 1784-1788.
88. de Sanctis, D.; Beteva, A.; Caserotto, H.; Dobias, F.; Gabadinho, J.; Giraud, T.; Gobbo, A.; Guijarro, M.; Lentini, M.; Lavault, B.; Mairs, T.; McSweeney, S.; Petitdemange, S.; Rey-Bakaikoa, V.; Surr, J.; Theveneau, P.; Leonard, G. A.; Mueller-Dieckmann, C. ID29: a high-intensity highly automated ESRF beamline for macromolecular crystallography experiments exploiting anomalous scattering. *J. Synchrotron Radiat.* **2012**, *19*, 455-461.
89. von Stetten, D.; Carpentier, P.; Flot, D.; Beteva, A.; Caserotto, H.; Dobias, F.; Guijarro, M.; Giraud, T.; Lentini, M.; McSweeney, S.; Royant, A.; Petitdemange, S.; Sinoir, J.; Surr, J.; Svensson, O.; Theveneau, P.; Leonard, G. A.; Mueller-Dieckmann, C. ID30A-3 (MASSIF-3) - a beamline for macromolecular crystallography at the ESRF with a small intense beam. *J. Synchrotron Radiat.* **2020**, *27*, 844-851.
90. Cianci, M.; Bourenkov, G.; Pompidor, G.; Karpics, I.; Kallio, J.; Bento, I.; Roessle, M.; Cipriani, F.; Fiedler, S.; Schneider, T. R. P13, the EMBL macromolecular crystallography beamline at the low-emittance PETRA III ring for high- and low-energy phasing with variable beam focusing. *J. Synchrotron Radiat.* **2017**, *24*, 323-332.
91. Ursby, T.; Unge, J.; Appio, R.; Logan, D. T.; Fredslund, F.; Svensson, C.; Larsson, K.; Labrador, A.; Thunnissen, M. M. G. M. The macromolecular crystallography beamline I911-3 at the MAX IV laboratory. *J. Synchrotron Radiat.* **2013**, *20*, 648-653.
92. Gabadinho, J.; Beteva, A.; Guijarro, M.; Rey-Bakaikoa, V.; Spruce, D.; Bowler, M. W.; Brockhauser, S.; Flot, D.; Gordon, E. J.; Hall, D. R.; Lavault, B.; McCarthy, A. A.; McCarthy, J.; Mitchell, E.; Monaco, S.; Mueller-Dieckmann, C.; Nurizzo, D.; Ravelli, R. B. G.; Thibault, X.; Walsh, M. A.; Leonard, G. A.; McSweeney, S. M. MxCuBE: a synchrotron beamline control environment customized for macromolecular crystallography experiments. *J. Synchrotron Radiat.* **2010**, *17*, 700-707.

93. Delageniere, S.; Brenchereau, P.; Launer, L.; Ashton, A. W.; Leal, R.; Veyrier, S.; Gabadinho, J.; Gordon, E. J.; Jones, S. D.; Levik, K. E.; McSweeney, S. M.; Monaco, S.; Nanao, M.; Spruce, D.; Svensson, O.; Walsh, M. A.; Leonard, G. A. ISPyB: an information management system for synchrotron macromolecular crystallography. *Bioinformatics* **2011**, *27*, 3186-3192.
94. Bourenkov, G. P.; Popov, A. N. Optimization of data collection taking radiation damage into account. *Acta Crystallogr. D* **2010**, *66*, 409-419.
95. Incardona, M. F.; Bourenkov, G. P.; Levik, K.; Pieritz, R. A.; Popov, A. N.; Svensson, O. EDNA: a framework for plugin-based applications applied to X-ray experiment online data analysis. *J. Synchrotron Radiat.* **2009**, *16*, 872-879.
96. Winter, G.; Waterman, D. G.; Parkhurst, J. M.; Brewster, A. S.; Gildea, R. J.; Gerstel, M.; Fuentes-Montero, L.; Vollmar, M.; Michels-Clark, T.; Young, I. D.; Sauter, N. K.; Evans, G. DIALS: implementation and evaluation of a new integration package. *Acta Crystallogr. D* **2018**, *74*, 85-97.
97. Vonrhein, C.; Flensburg, C.; Keller, P.; Sharff, A.; Smart, O.; Paciorek, W.; Womack, T.; Bricogne, G. Data processing and analysis with the autoPROC toolbox. *Acta Crystallogr. D* **2011**, *67*, 293-302.
98. Kabsch, W. Xds. *Acta Crystallogr. D* **2010**, *66*, 125-132.
99. McCoy, A. J.; Grosse-Kunstleve, R. W.; Adams, P. D.; Winn, M. D.; Storoni, L. C.; Read, R. J. Phaser crystallographic software. *J. Appl. Crystallogr.* **2007**, *40*, 658-674.
100. Long, F.; Nicholls, R. A.; Emsley, P.; Grazulis, S.; Merkys, A.; Vaitkus, A.; Murshudov, G. N. AceDRG: a stereochemical description generator for ligands. *Acta Crystallogr. D* **2017**, *73*, 112-122.
101. Emsley, P.; Lohkamp, B.; Scott, W. G.; Cowtan, K. Features and development of Coot. *Acta Crystallogr. D* **2010**, *66*, 486-501.

102. Afonine, P. V.; Grosse-Kunstleve, R. W.; Echols, N.; Headd, J. J.; Moriarty, N. W.; Mustyakimov, M.; Terwilliger, T. C.; Urzhumtsev, A.; Zwart, P. H.; Adams, P. D. Towards automated crystallographic structure refinement with phenix.refine. *Acta Crystallogr. D* **2012**, *68*, 352-367.
103. Schrödinger, L. The PyMOL Molecular Graphics System, Version 2.1.1. 2018.
104. Schrödinger, L. Maestro, Version 11.7. 2019.
105. Gilliland, G.; Berman, H. M.; Weissig, H.; Shindyalov, I. N.; Westbrook, J.; Bourne, P. E.; Bhat, T. N.; Feng, Z. The protein data bank. *Nucl. Acids Res.* **2000**, *28*, 235-242.
106. Acharya, K. R.; Lloyd, M. D. The advantages and limitations of protein crystal structures. *Trends Pharmacol. Sci.* **2005**, *26*, 10-14.

Table of Contents graphic

